An Energy Recovery Filter for HVDC Systems

By

Xiao Jiang

A THESIS
Submitted to the Faculty of Graduate Studies
in partial fulfillment of the requirements for the degree of

DOCTOR OF PHILOSOPHY

Department of Electrical and Computer Engineering
The University of Manitoba
Winnipeg, Manitoba, Canada

ISBN 0-315-92231-1

Canada

Name AN ENERGY RECOVERY FILTER FOR HVDC SYSTEMS

Dissertation Abstracts International is arranged by broad, general subject categories. Please select the one subject which most nearly describes the content of your dissertation. Enter the corresponding four-digit code in the spaces provided.

ENGINEERING, ELECTRONICS AND ELECTRICAL | 0544 | U·M·I

SUBJECT TERM SUBJECT CODE

Subject Categories

THE HUMANITIES AND SOCIAL SCIENCES

COMMUNICATIONS AND THE ARTS

- Architecture 0729
- Art History 0377
- Cinema 0900
- Dance 0378
- Fine Arts 0357
- Information Science 0723
- Journalism 0391
- Library Science 0399
- Mass Communications 0708
- Music 0413
- Speech Communication 0459
- Theater 0465

EDUCATION

- General 0515
- Administration 0514
- Adult and Continuing 0516
- Agricultural 0517
- Art 0273
- Bilingual and Multicultural 0282
- Business 0688
- Community College 0275
- Curriculum and Instruction 0727
- Early Childhood 0518
- Elementary 0524
- Finance 0277
- Guidance and Counseling 0519
- Health 0680
- Higher 0745
- History of 0520
- Home Economics 0278
- Industrial 0521
- Language and Literature 0279
- Mathematics 0280
- Music 0522
- Philosophy of 0998
- Physical 0523
- Psychology 0525
- Reading 0535
- Religious 0527
- Sciences 0714
- Secondary 0533
- Social Sciences 0534
- Sociology of 0340
- Special 0529
- Teacher Training 0530
- Technology 0710
- Tests and Measurements 0288
- Vocational 0747

LANGUAGE, LITERATURE AND LINGUISTICS

- Language
  - General 0679
  - Ancient 0289
  - Linguistics 0290
  - Modern 0291
- Literature
  - General 0401
  - Classical 0294
  - Comparative 0295
  - Medieval 0297
  - Modern 0298
  - African 0316
  - American 0591
  - Asian 0305
  - Canadian (English) 0352
  - Canadian (French) 0355
  - English 0593
  - Germanic 0311
  - Latin American 0312
  - Middle Eastern 0315
  - Romance 0313
  - Slavic and East European 0314

PHILOSOPHY, RELIGION AND THEOLOGY

- Philosophy 0422
- Religion
  - General 0318
  - Biblical Studies 0321
  - Clergy 0319
  - History of 0320
  - Philosophy of 0322
- Theology 0469

SOCIAL SCIENCES

- American Studies 0323
- Anthropology
  - Archaeology 0324
  - Cultural 0326
  - Physical 0327
- Business Administration
  - General 0310
  - Accounting 0272
  - Banking 0770
  - Management 0454
  - Marketing 0338
- Canadian Studies 0385
- Economics
  - General 0501
  - Agricultural 0503
  - Commerce-Business 0505
  - Finance 0508
  - History 0509
  - Labor 0510
  - Theory 0511
- Folklore 0358
- Geography 0366
- Gerontology 0351
- History
  - General 0578
  - Ancient 0579
  - Medieval 0581
  - Modern 0582
  - Black 0328
  - African 0331
  - Asia, Australia and Oceania 0332
  - Canadian 0334
  - European 0335
  - Latin American 0336
  - Middle Eastern 0333
  - United States 0337
- History of Science 0585
- Law 0398
- Political Science
  - General 0615
  - International Law and Relations 0616
  - Public Administration 0617
- Recreation 0814
- Social Work 0452
- Sociology
  - General 0626
  - Criminology and Penology 0627
  - Demography 0938
  - Ethnic and Racial Studies 0631
  - Individual and Family Studies 0628
  - Industrial and Labor Relations 0629
  - Public and Social Welfare 0630
  - Social Structure and Development 0700
  - Theory and Methods 0344
- Transportation 0709
- Urban and Regional Planning 0999
- Women's Studies 0453

THE SCIENCES AND ENGINEERING

BIOLOGICAL SCIENCES

- Agriculture
  - General 0473
  - Agronomy 0285
  - Animal Culture and Nutrition 0475
  - Animal Pathology 0476
  - Food Science and Technology 0359
  - Forestry and Wildlife 0478
  - Plant Culture 0479
  - Plant Pathology 0480
  - Plant Physiology 0817
  - Range Management 0777
  - Wood Technology 0746
- Biology
  - General 0306
  - Anatomy 0287
  - Biostatistics 0308
  - Botany 0309
  - Cell 0379
  - Ecology 0329
  - Entomology 0353
  - Genetics 0369
  - Limnology 0793
  - Microbiology 0410
  - Molecular 0307
  - Neuroscience 0317
  - Oceanography 0416
  - Physiology 0433
  - Radiation 0821
  - Veterinary Science 0778
  - Zoology 0472
- Biophysics
  - General 0786
  - Medical 0760

EARTH SCIENCES

- Biogeochemistry 0425
- Geochemistry 0996
- Geodesy 0370
- Geology 0372
- Geophysics 0373
- Hydrology 0388
- Mineralogy 0411
- Paleobotany 0345
- Paleoecology 0426
- Paleontology 0418
- Paleozoology 0985
- Palynology 0427
- Physical Geography 0368
- Physical Oceanography 0415

HEALTH AND ENVIRONMENTAL SCIENCES

- Environmental Sciences 0768
- Health Sciences
  - General 0566
  - Audiology 0300
  - Chemotherapy 0992
  - Dentistry 0567
  - Education 0350
  - Hospital Management 0769
  - Human Development 0758
  - Immunology 0982
  - Medicine and Surgery 0564
  - Mental Health 0347
  - Nursing 0569
  - Nutrition 0570
  - Obstetrics and Gynecology 0380
  - Occupational Health and Therapy 0354
  - Ophthalmology 0381
  - Pathology 0571
  - Pharmacology 0419
  - Pharmacy 0572
  - Physical Therapy 0382
  - Public Health 0573
  - Radiology 0574
  - Recreation 0575
  - Speech Pathology 0460
  - Toxicology 0383
- Home Economics 0386

PHYSICAL SCIENCES

Pure Sciences

- Chemistry
  - General 0485
  - Agricultural 0749
  - Analytical 0486
  - Biochemistry 0487
  - Inorganic 0488
  - Nuclear 0738
  - Organic 0490
  - Pharmaceutical 0491
  - Physical 0494
  - Polymer 0495
  - Radiation 0754
- Mathematics 0405
- Physics
  - General 0605
  - Acoustics 0986
  - Astronomy and Astrophysics 0606
  - Atmospheric Science 0608
  - Atomic 0748
  - Electronics and Electricity 0607
  - Elementary Particles and High Energy 0798
  - Fluid and Plasma 0759
  - Molecular 0609
  - Nuclear 0610
  - Optics 0752
  - Radiation 0756
  - Solid State 0611
- Statistics 0463

Applied Sciences

- Applied Mechanics 0346
- Computer Science 0984
- Engineering
  - General 0537
  - Aerospace 0538
  - Agricultural 0539
  - Automotive 0540
  - Biomedical 0541
  - Chemical 0542
  - Civil 0543
  - Electronics and Electrical 0544
  - Heat and Thermodynamics 0348
  - Hydraulic 0545
  - Industrial 0546
  - Marine 0547
  - Materials Science 0794
  - Mechanical 0548
  - Metallurgy 0743
  - Mining 0551
  - Nuclear 0552
  - Packaging 0549
  - Petroleum 0765
  - Sanitary and Municipal 0554
  - System Science 0790
- Geotechnology 0428
- Operations Research 0796
- Plastics Technology 0795
- Textile Technology 0994

PSYCHOLOGY

- General 0621
- Behavioral 0384
- Clinical 0622
- Developmental 0620
- Experimental 0623
- Industrial 0624
- Personality 0625
- Physiological 0989
- Psychobiology 0349
- Psychometrics 0632
- Social 0451

Nom _____

Dissertation Abstracts International est organisé en catégories de sujets. Veuillez s.v.p. choisir le sujet qui décrit le mieux votre thèse et inscrivez le code numérique approprié dans l'espace réservé ci-dessous.

_____ ☐☐☐ U·M·I

SUJET — CODE DE SUJET

Catégories par sujets

HUMANITÉS ET SCIENCES SOCIALES

COMMUNICATIONS ET LES ARTS
Architecture 0729
Beaux-arts 0357
Bibliothéconomie 0399
Cinéma 0900
Communication verbale 0459
Communications 0708
Danse 0378
Histoire de l'art 0377
Journalisme 0391
Musique 0413
Sciences de l'information 0723
Théâtre 0465

ÉDUCATION
Généralités 515
Administration 0514
Art 0273
Collèges communautaires 0275
Commerce 0688
Économie domestique 0278
Éducation permanente 0516
Éducation préscolaire 0518
Éducation sanitaire 0680
Enseignement agricole 0517
Enseignement bilingue et multiculturel 0282
Enseignement industriel 0521
Enseignement primaire. 0524
Enseignement professionnel 0747
Enseignement religieux 0527
Enseignement secondaire 0533
Enseignement spécial 0529
Enseignement supérieur 0745
Évaluation 0288
Finances 0277
Formation des enseignants 0530
Histoire de l'éducation 0520
Langues et littérature 0279
Lecture 0535
Mathématiques 0280
Musique 0522
Orientation et consultation 0519
Philosophie de l'éducation 0998
Physique 0523
Programmes d'études et enseignement 0727
Psychologie 0525
Sciences 0714
Sciences sociales 0534
Sociologie de l'éducation 0340
Technologie 0710

LANGUE, LITTÉRATURE ET LINGUISTIQUE
Langues
- Généralités 0679
- Anciennes 0289
- Linguistique 0290
- Modernes 0291

Littérature
- Généralités 0401
- Anciennes 0294
- Comparée 0295
- Médiévale 0297
- Moderne 0298
- Africaine 0316
- Américaine 0591
- Anglaise 0593
- Asiatique 0305
- Canadienne (Anglaise) 0352
- Canadienne (Française) 0355
- Germanique 0311
- Latino-américaine 0312
- Moyen-orientale 0315
- Romane 0313
- Slave et est-européenne 0314

PHILOSOPHIE, RELIGION ET THÉOLOGIE
Philosophie 0422
Religion
- Généralités 0318
- Clergé 0319
- Études bibliques 0321
- Histoire des religions 0320
- Philosophie de la religion 0322

Théologie 0469

SCIENCES SOCIALES
Anthropologie
- Archéologie 0324
- Culturelle 0326
- Physique 0327

Droit 0398
Économie
- Généralités 0501
- Commerce-Affaires 0505
- Économie agricole 0503
- Économie du travail 0510
- Finances 0508
- Histoire 0509
- Théorie 0511

Études américaines 0323
Études canadiennes 0385
Études féministes 0453
Folklore 0358
Géographie 0366
Gérontologie 0351
Gestion des affaires
- Généralités 0310
- Administration 0454
- Banques 0770
- Comptabilité 0272
- Marketing 0338

Histoire
- Histoire générale 0578
- Ancienne 0579
- Médiévale 0581
- Moderne 0582
- Histoire des noirs 0328
- Africaine 0331
- Canadienne 0334
- États-Unis 0337
- Européenne 0335
- Moyen-orientale 0333
- Latino-américaine 0336
- Asie, Australie et Océanie 0332

Histoire des sciences 0585
Loisirs 0814
Planification urbaine et régionale 0999
Science politique
- Généralités 0615
- Administration publique 0617
- Droit et relations internationales 0616

Sociologie
- Généralités 0626
- Aide et bien-être social 0630
- Criminologie et établissements pénitentiaires 0627
- Démographie 0938
- Études de l' individu et de la famille 0628
- Études des relations interethniques et des relations raciales 0631
- Structure et développement social 0700
- Théorie et méthodes. 0344
- Travail et relations industrielles 0629

Transports 0709
Travail social 0452

SCIENCES ET INGÉNIERIE

SCIENCES BIOLOGIQUES
Agriculture
- Généralités 0473
- Agronomie. 0285
- Alimentation et technologie alimentaire 0359
- Culture 0479
- Élevage et alimentation 0475
- Exploitation des pâturages 0777
- Pathologie animale 0476
- Pathologie végétale 0480
- Physiologie végétale 0817
- Sylviculture et faune 0478
- Technologie du bois 0746

Biologie
- Généralités 0306
- Anatomie 0287
- Biologie (Statistiques) 0308
- Biologie moléculaire 0307
- Botanique 0309
- Cellule 0379
- Écologie 0329
- Entomologie 0353
- Génétique 0369
- Limnologie 0793
- Microbiologie 0410
- Neurologie 0317
- Océanographie 0416
- Physiologie 0433
- Radiation 0821
- Science vétérinaire 0778
- Zoologie 0472

Biophysique
- Généralités 0786
- Medicale 0760

SCIENCES DE LA TERRE
Biogéochimie 0425
Géochimie 0996
Géodésie 0370
Géographie physique 0368
Géologie 0372
Géophysique 0373
Hydrologie 0388
Minéralogie 0411
Océanographie physique 0415
Paléobotanique 0345
Paléoécologie 0426
Paléontologie 0418
Paléozoologie 0985
Palynologie 0427

SCIENCES DE LA SANTÉ ET DE L'ENVIRONNEMENT
Économie domestique 0386
Sciences de l'environnement 0768
Sciences de la santé
- Généralités 0566
- Administration des hôpitaux 0769
- Alimentation et nutrition 0570
- Audiologie 0300
- Chimiothérapie 0992
- Dentisterie 0567
- Développement humain 0758
- Enseignement 0350
- Immunologie 0982
- Loisirs 0575
- Médecine du travail et thérapie 0354
- Médecine et chirurgie 0564
- Obstétrique et gynécologie 0380
- Ophtalmologie 0381
- Orthophonie 0460
- Pathologie 0571
- Pharmacie 0572
- Pharmacologie 0419
- Physiothérapie 0382
- Radiologie 0574
- Santé mentale 0347
- Santé publique 0573
- Soins infirmiers 0569
- Toxicologie 0383

SCIENCES PHYSIQUES
Sciences Pures
Chimie
- Généralités 0485
- Biochimie 487
- Chimie agricole 0749
- Chimie analytique 0486
- Chimie minérale 0488
- Chimie nucléaire 0738
- Chimie organique 0490
- Chimie pharmaceutique 0491
- Physique 0494
- PolymÈres 0495
- Radiation 0754

Mathématiques 0405
Physique
- Généralités 0605
- Acoustique 0986
- Astronomie et astrophysique 0606
- Électronique et électricité 0607
- Fluides et plasma 0759
- Météorologie 0608
- Optique 0752
- Particules (Physique nucléaire) 0798
- Physique atomique 0748
- Physique de l'état solide 0611
- Physique moléculaire 0609
- Physique nucléaire 0610
- Radiation 0756

Statistiques 0463

Sciences Appliqués Et Technologie
Informatique 0984
Ingénierie
- Généralités 0537
- Agricole 0539
- Automobile 0540
- Biomédicale 0541
- Chaleur et thermodynamique 0348
- Conditionnement (Emballage) 0549
- Génie aérospatial 0538
- Génie chimique 0542
- Génie civil 0543
- Génie électronique et électrique 0544
- Génie industriel 0546
- Génie mécanique 0548
- Génie nucléaire 0552
- Ingénierie des systèmes 0790
- Mécanique navale 0547
- Métallurgie 0743
- Science des matériaux 0794
- Technique du pétrole 0765
- Technique minière 0551
- Techniques sanitaires et municipales 0554
- Technologie hydraulique 0545

Mécanique appliquée 0346
Géotechnologie 0428
Matières plastiques (Technologie) 0795
Recherche opérationnelle 0796
Textiles et tissus (Technologie) 0794

PSYCHOLOGIE
Généralités 0621
Personnalité 0625
Psychobiologie 0349
Psychologie clinique 0622
Psychologie du comportement 0384
Psychologie du développement 0620
Psychologie expérimentale 0623
Psychologie industrielle 0624
Psychologie physiologique 0989
Psychologie sociale 0451
Psychométrie 0632

AN ENERGY RECOVERY FILTER FOR HVDC SYSTEMS

BY

XIAO JIANG

A Thesis submitted to the Faculty of Graduate Studies of the University of Manitoba in partial fulfillment of the requirements for the degree of

DOCTOR OF PHILOSOPHY

To My Parents

Acknowledgement

The author wishes to express his sincere gratitude to his advisor Prof. A.M. Gole for his guidance and encouragement during the course of this work.

The author appreciates the suggestion and discussion of Prof. D. Woodford of Manitoba HVDC Research Centre. The thanks are due to Prof. R.M. Menzies and Prof. D. Meek for their valuable advice as the members of the advisory committee.

The sponsorship from Manitoba HVDC Research Centre is gratefully acknowledged.

Finally, the author will express the greatest thanks to his parents, wife and brother for their patience, support and sacrifice which the author is in deep debt.

Abstract

The thesis investigates the use of a novel filter arrangement called the Energy Recovery filter (ER–filter) for HVDC systems.

Several operating problems can occur with HVDC schemes operating into weak AC systems. Most of the problems are closely associated to the harmonic resonance and instability between AC and DC systems. The harmonic instability is usually mitigated by either modifying the AC/DC system impedance characteristics or adding extra control circuits to damp the oscillations. The majority of existing approaches deal with eliminating the specific harmonic of the most concern. Sometimes a broadband solution is more desirable because resonance frequencies may change with the system conditions. The filter used for this purpose should have a low quality factor for coving a wide frequency range. However, the use of a conventional low Q filter involves large power losses in the filter resistor. The ER–filter introduced in this thesis will recover the power losses in the filter.

The ER–filter is implemented by replacing the resistors in a conventional filter with a low power back–to–back DC link which takes power from the filter and returns it to the system. The link acts as a resistor to the filter, but does not consume real power.

The studies also show that for certain system conditions a low Q filter is desirable and for other conditions a high Q is better. This inspired the concept of a "Variable Q filter" in which its quality factor is controllable by electronic means. The Variable Q filter provides low Q factor in the steady state to reduce the steady state oscillations, and a high Q factor during fault recovery to help eliminate harmonic currents injected from the saturated

transformer. The ER–filter is able to operate as a Variable Q filter by modifying the firing angle control in the inverter of its DC link.

The investigations in this thesis are conducted through digital computer simulation using an electromagnetic transient simulation program PSCAD/EMTDC. The CIGRE benchmark model, which experiences both steady state and core saturation harmonic instabilities, is selected as the base system. The harmonic instabilities in the CIGRE system are first mitigated by installing a conventional filter on AC bus. Later, the conventional filter is replaced by an ER–filter in order to reduce the high losses in the filter resistor. Finally, the ER–filter is modified to a Variable Q filter to provide an improved system recovery from disturbances.

The results of the studies confirm that installing a conventional low Q filter on the AC bus solves the harmonic instability problems. The ER–filter has a similar performance as the conventional filter but with much reduced losses. And the Variable Q filter gives better performance during system recovery from faults.

Contents

CHAPTER 7

List of the Figures

Chapter 1

Introduction

1 .1 BACKGROUND

HVDC transmission technology is now an important alternative means of long distance transmission or interconnection between large power systems. There are a considerable number of HVDC schemes in operation and several in development.

There are many AC/DC system interactions that should be considered while installing an HVDC link. The interactions become more pronounced as the power rating of HVDC link becomes larger. The Short Circuit Ratio (SCR, which is the ratio of the AC system short circuit MVA to the DC power) indicates the strength of the system. The weaker the system (i.e. the lower the SCR), the greater the interactions. It is suggested that the system with SCR lower than 3 be considered as a weak system. Now there are many HVDC schemes connected to a weak system, which give rise to many challenges to control and operation of the system.

AC/DC system interactions of concern in a weak system are voltage instability, overvoltages, low order harmonic resonances and instability, and poor recovery from disturbances. Some of these are closely associated with the low frequency resonance of the impedances of system/filters combination. Harmonic instability phenomena have gained much attention and a lot of research is being conducted in this area.

The harmonic instability is usually mitigated by either modifying the system impedance characteristics or adding extra control circuits. A filter tuned to the low resonance

frequency on the commutating bus can be added to provide more damping to the oscillations around this frequency. The filter for this purpose should have a low quality factor Q for covering a wide range of resonance conditions.

However, the use of a low Q filter for mitigating instability involves large fundamental power losses in the filter resistors. To reduce the losses of a conventional filter, a new type of filter called the Energy Recovery filter (ER–filter) is introduced. The concept of the ER–filter is to substitute the resistors in the filter by a small back–to–back DC link, which takes the power from the filter, and sends it back to the AC system. The link acts as a resistor to the filter, but does not consume real power. The ER–filter has a very low Q factor but no significant real power losses. Also, an ER–filter has the flexibility of being operated as a variable quality factor filter which is useful for various operating conditions.

1 .2 LITERATURE REVIEW

Low frequency resonance and instability are not new problems due to the inherent non–linear nature of conversion [5][17][20]. With the modern trend where the power transmitted by the HVDC link becomes higher with respect to the power of the AC system, this problem becomes more serious.

It is the inherent nature of the HVDC converter to generate characteristic harmonics. The converter also produces non–characteristic harmonics under unbalanced or transient conditions [6] [7] [8] [18] [19]. Usually the non–characteristic harmonic will be injected into the AC system since there are no filters for such harmonics on the commutating bus.

The harmonics injected into an AC system do not cause much influence on AC/DC operation if the AC system is strong. But if an HVDC link is connected to a weak AC system, there is a possibility of harmonic resonances and instability. To successfully operate an HVDC link with a weak AC system, an additional control circuit or AC filter must be installed or some operating restrictions must be enforced.

The introduction of a phase locked loop oscillator for firing control of the converter was a tremendous success in HVDC control. The phase locked loop oscillator can keep equidistant firing for the converter even if the AC voltages are distorted [9]. There are other approaches of firing angle modulation to minimize the non–characteristic harmonics [10] [11] [16] [21]. All these approaches deal with specific non–characteristic harmonics generated under certain conditions.

Another approach to prevent harmonic instability is to modify the system frequency characteristic. The low order harmonic resonances of a system/filter combination are reduced by installing a filter tuned to the resonance frequency [10] [12] [21]. This method can eliminate the instability mechanism under all circumstances. The filter used here can be a single tuned filter or a high pass filter. The filter is tuned to a low frequency close to the fundamental frequency. Also, the Q factor of the filter cannot be very high as it may shift the resonance problem to another frequency. Due to these factors, the fundamental power losses in the filter can be high. A modified high pass filter called a C–type filter, in which the resistor is short circuited at fundamental frequency by adding a capacitor in series resonance with the inductor at fundamental frequency, is used in several schemes.

Another approach to harmonic filtering that has been recently proposed is that of using active filters[22]. The idea of this method is to cancel the harmonics by re–injecting the current which is exactly the same as the harmonic current of the converter but in phase opposition. To achieve this, exact magnitude and phase angle information must be continuously known.

Not only the system impedance but also its phase angle are important to the harmonic instability, especially during transients. Small system impedance and phase angle at harmonic frequency will help to damp the harmonic oscillations. A low Q single tuned filter will provide low impedance in a large frequency range, which will mitigate the harmonic instabilities over a wide frequency range. But the fundamental power losses in a low Q filter

are too high due to its large resistor. The energy recovery filter proposed here will overcome the drawback of high losses in the low Q filter and, at the same time, solve the problem of harmonic instability. This concept is proposed in this thesis for the first time.

1 .3 WEAK SYSTEM AND INSTABILITY

Because of the nonlinear nature of in the AC/DC or DC/AC conversion process, an HVDC converter station injects harmonics into both the AC and DC sides. The converter is viewed as a harmonic current source from its AC terminal, and a harmonic voltage source from DC line side. At the AC side (either rectifier or inverter end), only the fundamental component (first harmonic) is desired; the remaining harmonics result in system losses and voltage quality degradation. At the DC side, only the DC component is needed; the harmonics interfere with neighboring communication systems. To minimize the harmonics, normal design practice is to add harmonic filters on the commutating buses and use smoothing reactors and filters at both ends of the DC line.

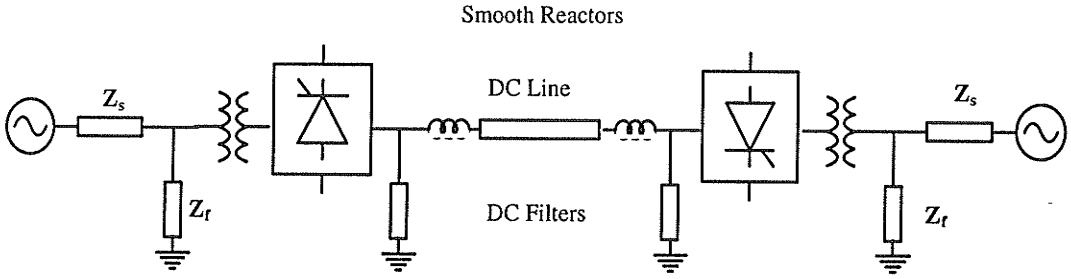

Figure 1 .1 : General HVDC Transmission System

1 .4 WEAK AC SYSTEM

The difficulty of operating an HVDC link is closely related to the "strength" of the AC system. The tendency towards increased size of the HVDC link relative to the AC system power increases this difficulty[4][14].

1 .4 .1 AC SYSTEM STRENGTH

The "strength" of the AC system connected to an HVDC link is indicated by the factor known as Short Circuit Ratio (SCR). The SCR is defined as the ratio of the short circuit MVA of the AC system to the power transmitted by HVDC link :

$$SCR = \frac{Short\ Circuit\ MVA}{HVDC\ Power}$$

The smaller the SCR, the weaker the AC system. Usually, an AC system of SCR less than 3 is considered as a weak system.

Assume $\mathbf{Z}_s$ be the "Thevenin equivalent" source impedance in per unit, we have this relationship:

$$|Z_s| = \frac{1}{SCR}$$

This means a weak AC system has a high system impedance.

The converter (either rectifier and inverter) consumes reactive power which can be supplied by shunt capacitors in the form of capacitor banks or the capacitors in the AC filters connected at the AC bus of a HVDC link. The shunt capacitors can significantly increase the effective AC system impedance. The effective short circuit ratio ESCR is used to allow for the effect of the shunt capacitors on the system strength:

$$ESCR = \frac{Short\ Circuit\ MVA - MVAr\ of\ capacitors}{HVDC\ Power}$$

1 .4 .2 PROBLEMS

An HVDC link connected to a weak AC system may experience several problems. These include:

- voltage instability

- overvoltages
- low order harmonic resonances and instability
- poor recovery from disturbances

Most of these problems are closely associated with the low frequency resonance between the system and filter impedances.

1 .5 RESONANCE AND HARMONIC INSTABILITY

Usually, the filters on the commutating bus contain several tuned filters (sharply tuned to the low order characteristic harmonics) and a high pass filter for the remaining higher order characteristic harmonics. The filters are a series connection of a capacitor and a combination of an inductor and a resistor, either in series or parallel. The power system can be equivalently represented as a pure sinusoidal source with a source impedance $\mathbf{Z_s}$. At a frequency lower than the first characteristic harmonic, the total impedance $\mathbf{Z_f}$ of filters is dominated by the filter capacitors, so the filters can supply the necessary reactive power for converter stations. But the source impedance $\mathbf{Z_s}$ acts much like an inductance at all frequencies.

1 .5 .1 THE RESONANCE

The total system impedance, as viewed from a converter station, is a parallel connection of source impedance $\mathbf{Z_s}$ and filter impedance $\mathbf{Z_f}$. This results in a parallel resonance at a frequency lower than first characteristic harmonic.

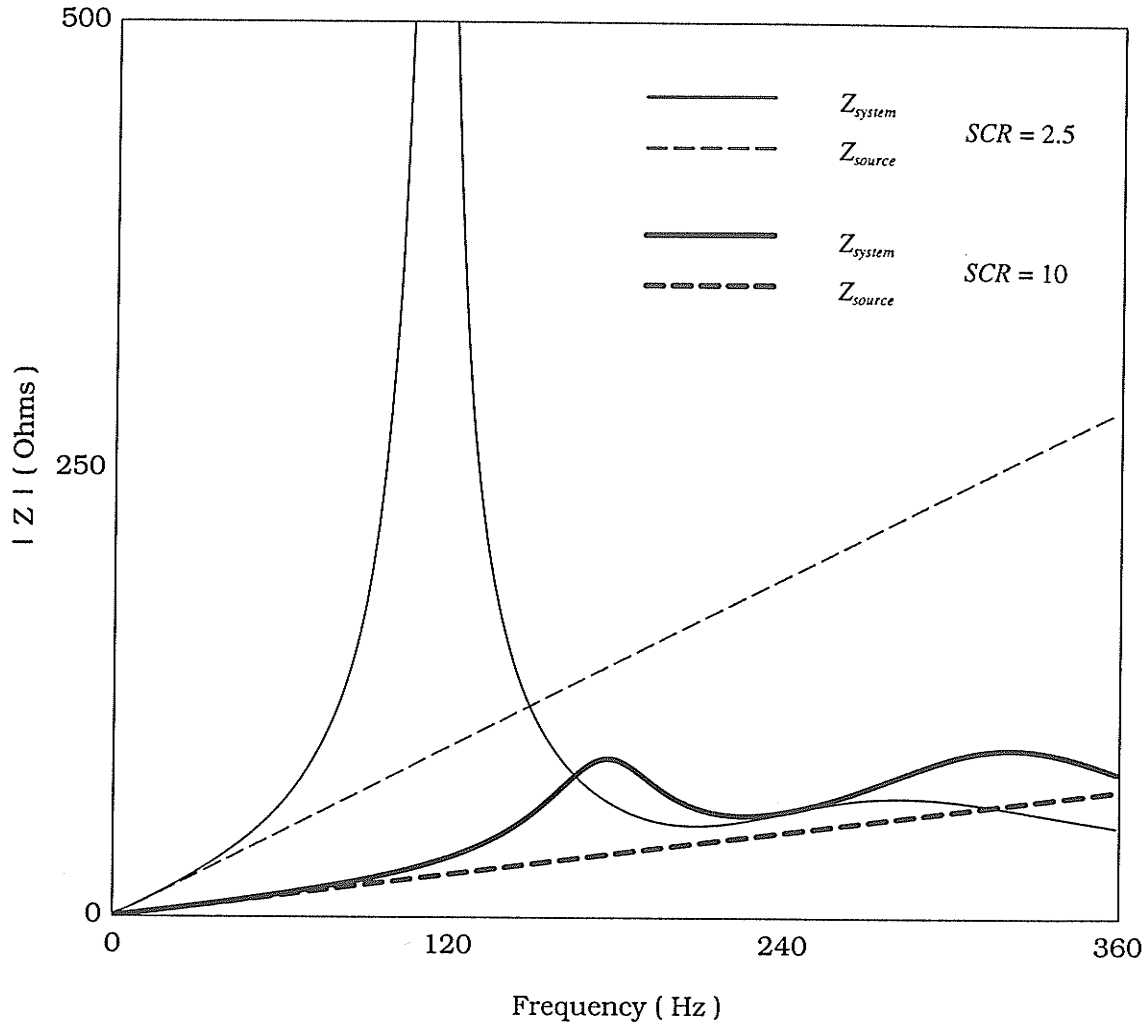

Figure 1 .2 : The System Frequency Characteristics

Fig. 1 .2 shows the source and system impedance characteristics of a typical 12–pulse HVDC scheme. The resonance problem is usually more significant in the case of weak AC systems. The higher the source impedance $\mathbf{Z_{source}}$ (i.e. the lower the SCR or the weaker the AC system), the higher the resonance in system impedance (see Fig 1 .2 for SCR=2.5 and SCR=10). Not only the impedance magnitude but also its phase angle has an effect on the resonance. The phase angle of the system impedance reflects the damping of the system. The higher the phase angle of the AC system, the less damped is the resonance. Schemes which are directly fed by remote generators without any local load have very little

damping from the rest of the AC system on the rectifier side. Sometimes these phenomena may result in harmonic instability for the HVDC scheme.

1 .5 .2 HARMONIC INSTABILITY

According to converter theory, the converter only produces characteristic harmonics under ideal operating condition. Under non–ideal conditions, the converter will also produce non–characteristic harmonics due to unbalances such as:

- unbalanced firing pulses due to control circuit errors
- unbalanced impedances (AC systems, filters and transformers)
- unbalanced AC supply voltages

Also during transients such as system start–up, recover from faults and other disturbances, the converter will also produce non–characteristic harmonics. The converter transformer saturation is a major reason, it can inject all the integer harmonics into the system [13][15]. The transformer can be saturated due to:

- energization of the transformer producing inrush current
- blocking of part of a multipolar scheme producing an overvoltage and hence transformer saturation
- commutation failure producing transformer saturation

Characteristic harmonic filters are usually installed on the commutating bus to prevent the characteristic harmonics injected into AC system. But characteristic filters cannot prevent non–characteristic harmonics from entering into the AC system. Non–characteristic harmonics injected into the poorly damped resonant networks can cause difficulties with the HVDC system operation. Because the system is current–fed, the worst case will be when the impedance is a maximum (i.e. at the parallel resonant frequency).

Harmonic instability is an important problem due to the resonance of the system/filters when the HVDC link is connected to a weak AC system. First the

non–characteristic harmonic current at frequency f_n injected into the system yields a large harmonic voltage at the same frequency superposed on the supply voltage, then the converter modulates the harmonic voltage at frequency f_n into harmonic voltages at frequencies $f_n \pm$ 60 Hz (fundamental frequency of supply) on the DC side. On the DC side, the harmonic voltages at frequencies $f_n \pm 60$ Hz yield harmonic current at same frequencies. The harmonic current at frequencies $f_n \pm 60$ Hz on DC side will reflect on AC side as harmonic current at frequency f_n . This harmonic current injects into the system again so that a harmonic instability may occur, particularly where there are DC side series resonance at the complementary frequencies of resonance in the AC side (i.e. the DC resonance frequency differs from the AC resonance frequency by close to ±60 Hz). In that case, harmonic currents on the DC side are also amplified.

1 .6 SOLUTIONS

The harmonic instability is mitigated by either modifying the AC system impedance characteristics with filters or adding extra control circuits.

1 .6 .1 CONTROL CIRCUITS

Today, most of the new HVDC schemes use a phase locked loop oscillator in the firing control of the converter. The phase locked loop oscillator can track the fundamental component in the AC bus voltage, and then keep equidistant firing for the converter even if the AC voltages are distorted. But the equidistant firing does not solve the particular harmonic instability problems. Additional control circuits must be added to eliminate the problems[21]. There are other approaches of firing angle modulation to minimize the non–characteristic harmonics. But all the approaches deal with eliminating the specific non–characteristic harmonic of the most concern.

1 .6 .2 FILTERS

To modify the AC system characteristics having high impedance at a low order harmonic, a filter tuned to the resonant frequency can be installed on the commutating bus.

The majority of the approaches deal with the harmonic instability at a specific frequency. They are not broadband solutions. Sometimes the broadband solutions are more desirable since resonant frequencies may change with the system conditions. The filter used for this purpose should have a low quality factor Q for covering a wide frequency range of resonance condition. The Energy Recovery Filter is introduced to recover the power loss in the conventional low Q filter.

1 .7 SUMMARY OF THE THESIS

In the thesis, a detailed description of harmonic instability and its solutions is presented. A modified CIGRE benchmark model is selected as a base system for the investigations. A frequency scanning method is introduced in digital simulation for finding the harmonic resonance in a real AC/DC system.

A comparison of the various cases studied indicates that the ER–filter provides broadband damping and elimination of harmonic instabilities without increased losses. Also a novel " Variable Q " filter is investigated in which the Q–factor of the filter can be changed adaptively.

All studies are conducted using digital simulation on an electromagnetic transients simulation program (EMTDC).

1 .7 .1 SCOPE OF THE THESIS

This thesis presents the following aspects:

1. Review of harmonic instability phenomena in a weak HVDC scheme and their solutions.

2. Digital simulation studies of the base system and the solution of harmonic instability with conventional low Q filter.
3. Frequency scanning method for predicting harmonic instability.
4. Component selection of the Energy Recovery filter and its performance.
5. Performance of Energy Recovery filter in solving harmonic instabilities.
6. Implementation of the ER–filter in the " variable quality factor " mode.
7. Performance of the variable quality factor filter during transients.
8. Conclusions

Chapter 2

Study Tool and Base System

2 .1 THE STUDY TOOLS

2 .1 .1 INTRODUCTION

Historically, many power system problems have been studied with powerflow and transient stability computer programs. But those programs are inadequate to deal with the interaction problems associated with HVDC schemes such as harmonic instability and overvoltages. To achieve this, simulation with electromagnetic transients programs must be used. Time domain simulation has the advantage that the differences between small and large signal disturbances can be readily observed. Frequency domain programs using eigenvalue analysis are also sometimes used with the linearization of the nonlinear elements, but this study chooses to use the more complete nonlinear model afforded by electromagnetic transients simulation.

2 .1 .2 EMTDC

The time domain simulation program EMTDC (ElectroMagnetic Transients simulation program for DC) [29] is used as the simulation tool for the studies. EMTDC is a good program for studying complex power systems including HVDC schemes. A graphical user interface for EMTDC (PSCAD/EMTDC) can help users easily use the program.

2 .2 THE BASE SYSTEM

To study harmonic instability problems, we need to select a base system which will represent the main factors that cause the harmonic instability.

2 .2 .1 CIGRE BENCHMARK MODEL

The CIGRE benchmark model [27] is selected as the base system for the studies. The main purpose of the benchmark is to encourage comparisons of performance of different controls and provide a reference for testing of simulators and digital programs. The system is modified slightly as indicated below to heighten the harmonic instability.

2 .2 .2 MODIFICATIONS TO THE MODEL

For the specific studies of the harmonic instability problem, some modifications to the CIGRE benchmark model have been made.

- The base frequency is changed from original 50 Hz to 60 Hz (North American standard).
- The AC system damping angle at the rectifier (sending end) is changed from 84° to 87° to make harmonic instability more serious.
- The damped low frequency filter is changed to the C–type filter, this will reduce real power losses in the filter and also reduce the damping.

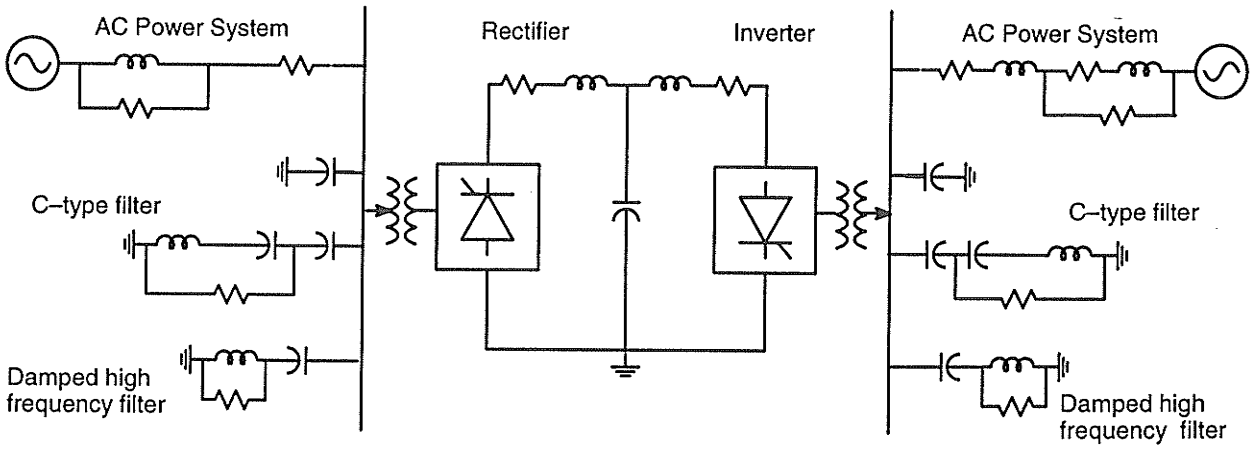

Figure 2 .1 : Modified CIGRE Benchmark Model

2 .2 .3 FEATURES OF THE MODEL

The model represents a 12–pulse 500 kV HVDC link rated at 1000 MW. The DC line is represented by a T–section whose parameters are typical of a medium or long cable. The control at the rectifier is constant current control and at the inverter it is constant extinction angle (gamma) control.

The conventional filter design which uses single tuned filters for characteristic harmonics and a high pass filter for higher harmonics will usually give a more effective reduction of harmonics than required. In modern HVDC schemes, filter design could be simplified by using only damped filters. A damped filter has many advantages in its performance, such as being less sensitive to parameter changes, having a wide range of harmonic filtering, etc. [2].

In weak HVDC schemes (high system impedance), the harmonic filtering is easier than in strong schemes, since the harmonics are injected into the parallel impedance combination of the system/filter. But at low frequency, a high impedance may occur in the weak system. So a damped filter tuned at 3rd to 4th harmonic is installed to reduce the impedance. Because this filter is tuned close to fundamental frequency, a C–type filter is used to reduce its real power losses. A high pass filter (damped) is used to deal with 11th, 13th and higher harmonics. The C–type and high pass filter each supply 250 MVAR reactive power respectively. To totally compensate the reactive power consumption by the capacitor, a 125 MVAR capacitor bank is installed. While a static capacitor provides the cheapest way of reactive power compensation, it will increase the effective system impedance and make HVDC operation more difficult[14]. The Effective Short Circuit Ratio (ESCR) is defined for indicating the system strength with shunt capacitor .

Some of the base values of the CIGRE system are listed in Table 2 .1 .

Table 2 .1 : The System Base Values

	RECTIFIER	INVERTER
SCR	2.5∠–87°	2.5∠–75°
ESCR	1.88∠–86°	1.9∠–70.04°
Bus Voltage (L-L)	345 kV	230 kV
Filter VAR Supply	625 MVAR	625 MVAR
Nominal Angle	15°	15°

2 .2 .4 THE IMPEDANCE/FREQUENCY RESPONSE OF THE MODEL

The total system impedance/frequency plots of the CIGRE benchmark model, as viewed from the terminal buses, are shown in Fig. 2 .2 .

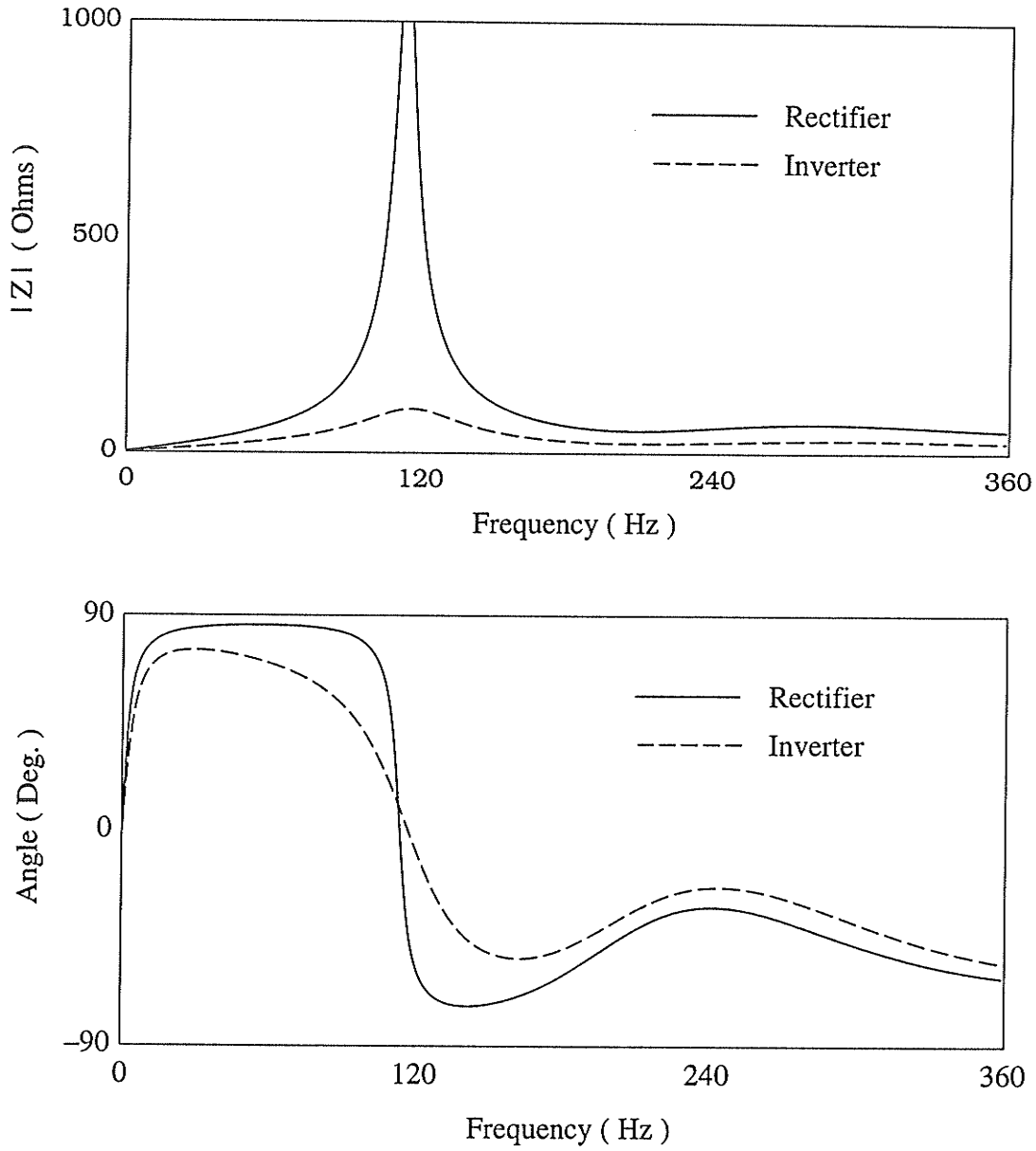

Figure 2 .2 : The Total AC System Impedance / Frequency Plot

Fig. 2 .2 shows that a high parallel impedance (1195 Ω) resonance around 120 Hz (exact at 113 Hz) is 18.88 times of the fundamental frequency impedance (63.31 Ω) at the sending end. At the receiving end, the parallel impedance resonance (100 Ω) at 120Hz which is 3.58 times of the fundamental frequency impedance (27.9 Ω) and is much smaller than that at sending end.

The DC impedance/frequency plot, as viewed from the converter, is shown in the Fig. 2 .3 . There is a series resonance around 60 Hz which is close to the complementary frequency (53 Hz) of the AC system resonance.

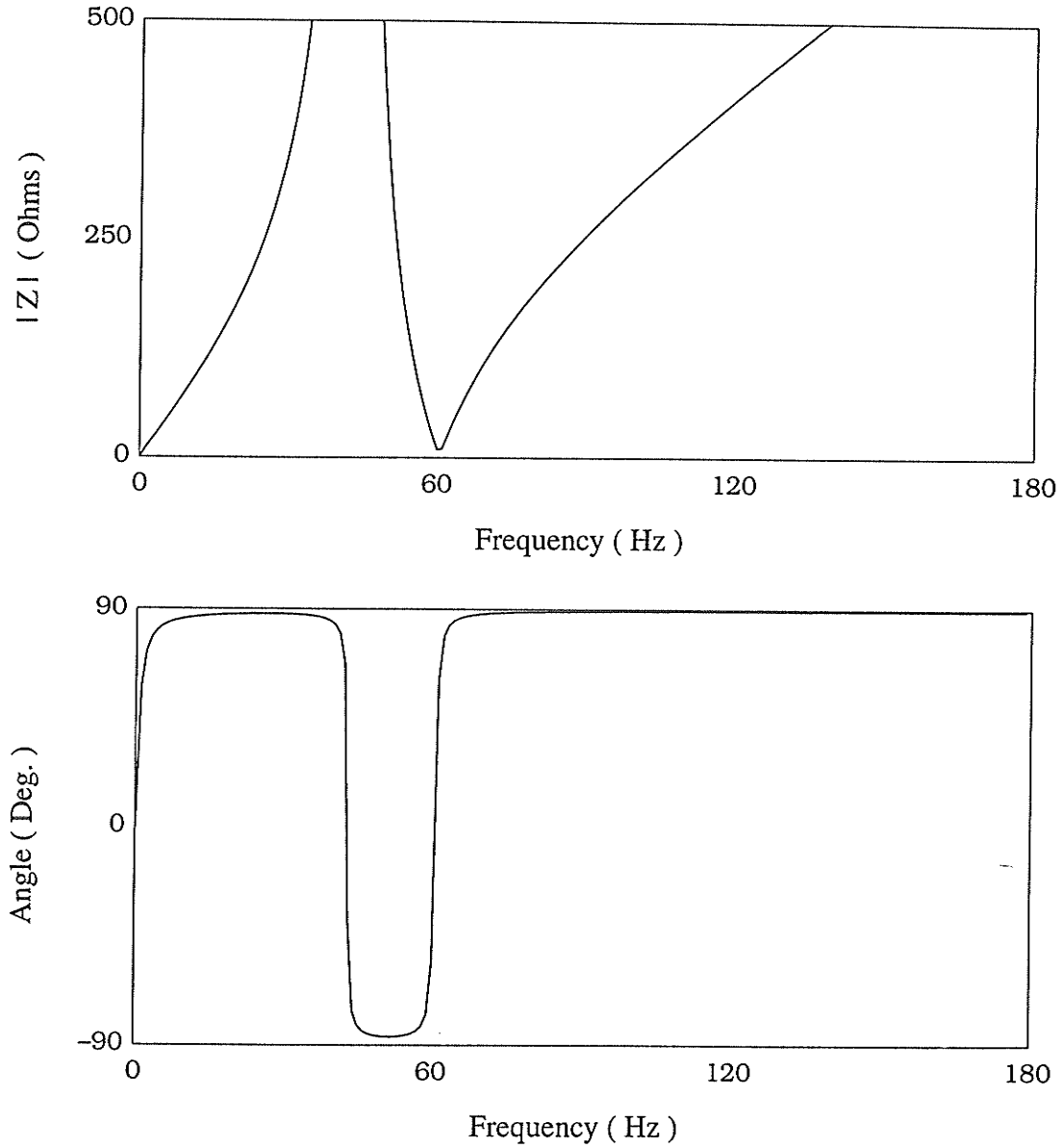

Figure 2 .3 : The DC Side Impedance / Frequency Plot

2 .2 .5 CONCLUSIONS

From the discussions above, it is known that the modified CIGRE benchmark model has the following features:

1. A weak AC system with little damping at the sending and receiving ends.
2. The total local reactive power compensation is via capacitors.
3. Low order harmonic resonance around 2nd harmonic on the AC side, and a complementary resonance on the DC side.

Features 1 and 3 are the major factors contributing to harmonic instability. So the base system gives us a suitable system model for the low order harmonic instability studies.

Chapter 3

System Studies

3 .1 INTRODUCTION

In this thesis, the following four types of HVDC system configuration are simulated to investigate the performances of different filters.

1. Modified CIGRE benchmark model without any additional filter.
2. Modified CIGRE benchmark model with a conventional filter.
3. Modified CIGRE benchmark model with an Energy Recovery filter.
4. Modified CIGRE benchmark model with a variable Q filter.

Each case is simulated on the computer with the EMTDC program. For every simulation, the following waveforms are recorded for the analyses.

- AC bus voltages at both rectifier and inverter sides.
- DC currents and voltages at both rectifier and inverter sides.
- Active and reactive powers at sending and receiving ends.
- Firing angle of both converters.
- Additional data for specific purposes (such as filter currents, extinction angle, some control signals and etc.).

3 .2 THE BASE SYSTEM

The modified CIGRE benchmark model is considered as the base system for the studies. The rectifier AC filter configuration is as in Fig. 3 .1 .

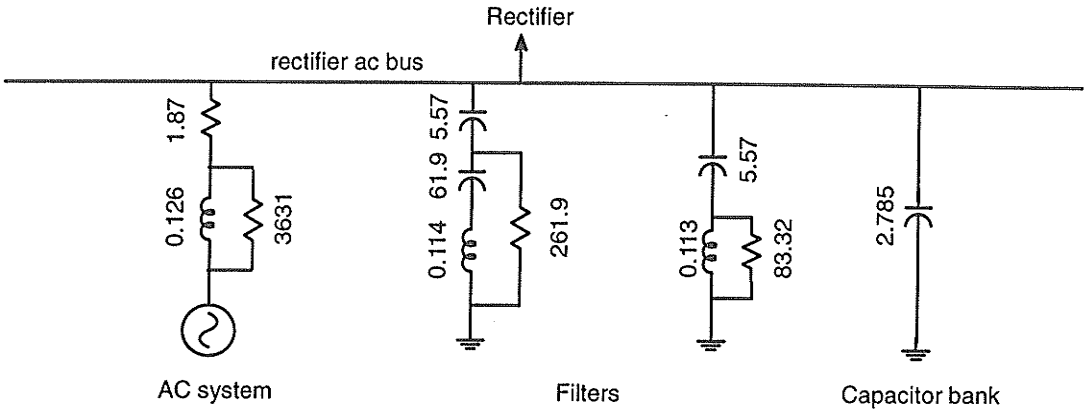

Figure 3 .1 : Rectifier AC Filter Configuration of the Base System

This system is modelled on the computer using the EMTDC program. A suitable timestep of 50 μs is selected for all the simulations. Different operating conditions such as system start–up and fault recoveries are tested. The results for each test are measured and saved in the data files for the later analyses.

3 .2 .1 PERFORMANCE DURING START–UP AND STEADY STATE

Shown in Fig. 3 .2 are the waveforms during system start–up and steady state.

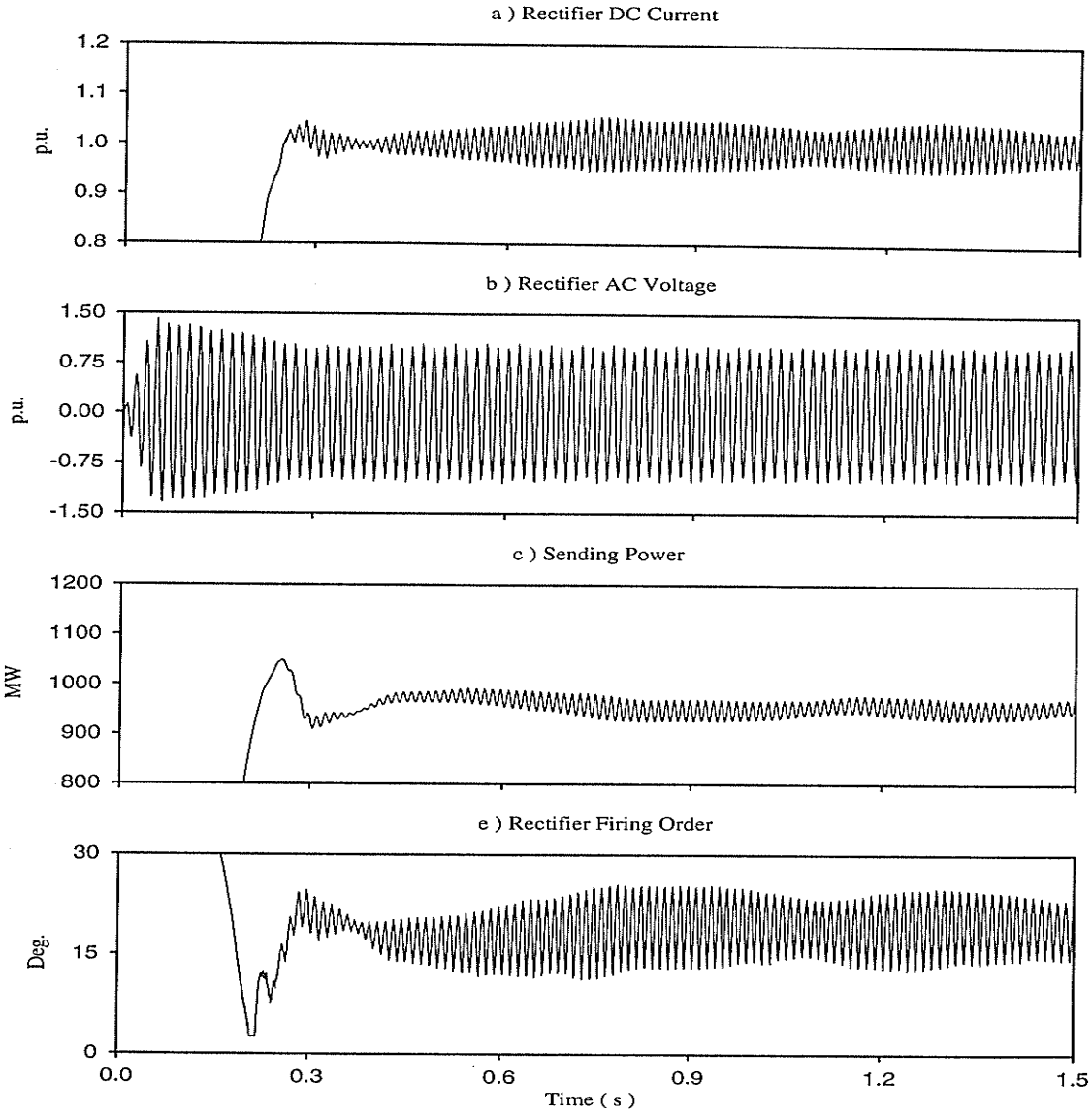

Figure 3 .2 (Continued): Start–up and Steady State in the Base System

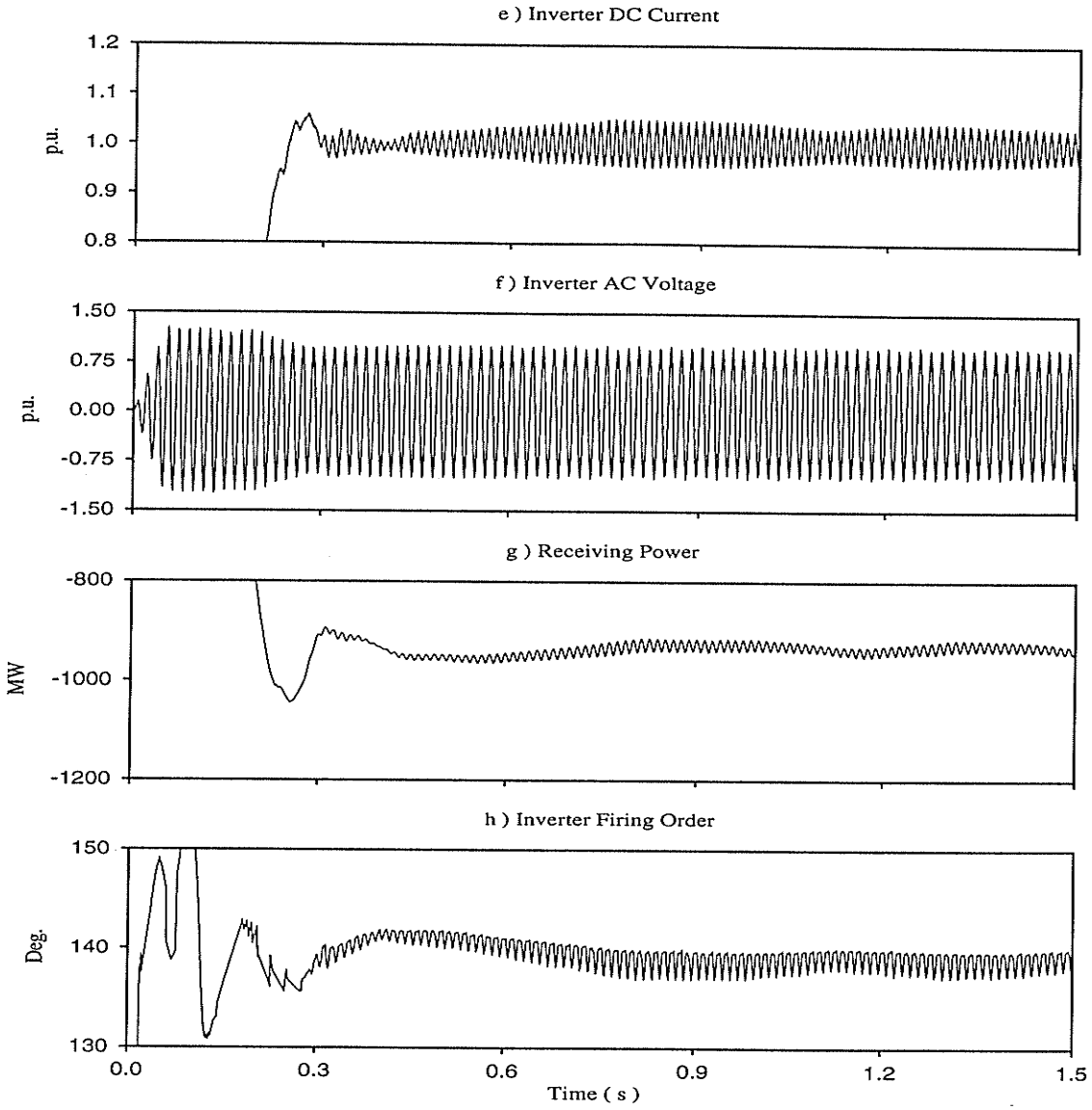

Figure 3 .2 (Concluded): Start–up and Steady State in the Base System

The harmonic instability is evident from the results in Fig. 3 .2 where the oscillations in the DC currents, active powers or firing angles can be easily seen. In the steady state, these quantities should be constant at their nominal values. The oscillations are not present initially but built up in about 0.4 seconds. During steady state, the following facts can be observed:

- The DC currents in both converters have 80 Hz oscillations.

- The active powers at sending and receiving ends have 80 Hz oscillations of about 20 MW and 12 MW respectively.
- The α orders of rectifier and inverter have 80 Hz oscillations of about 5^{o} and 1.5^{o} respectively.
- The sending end AC power is 953 MW and the receiving end AC power is 933 MW. So the total loss of the DC link is 20 MW.

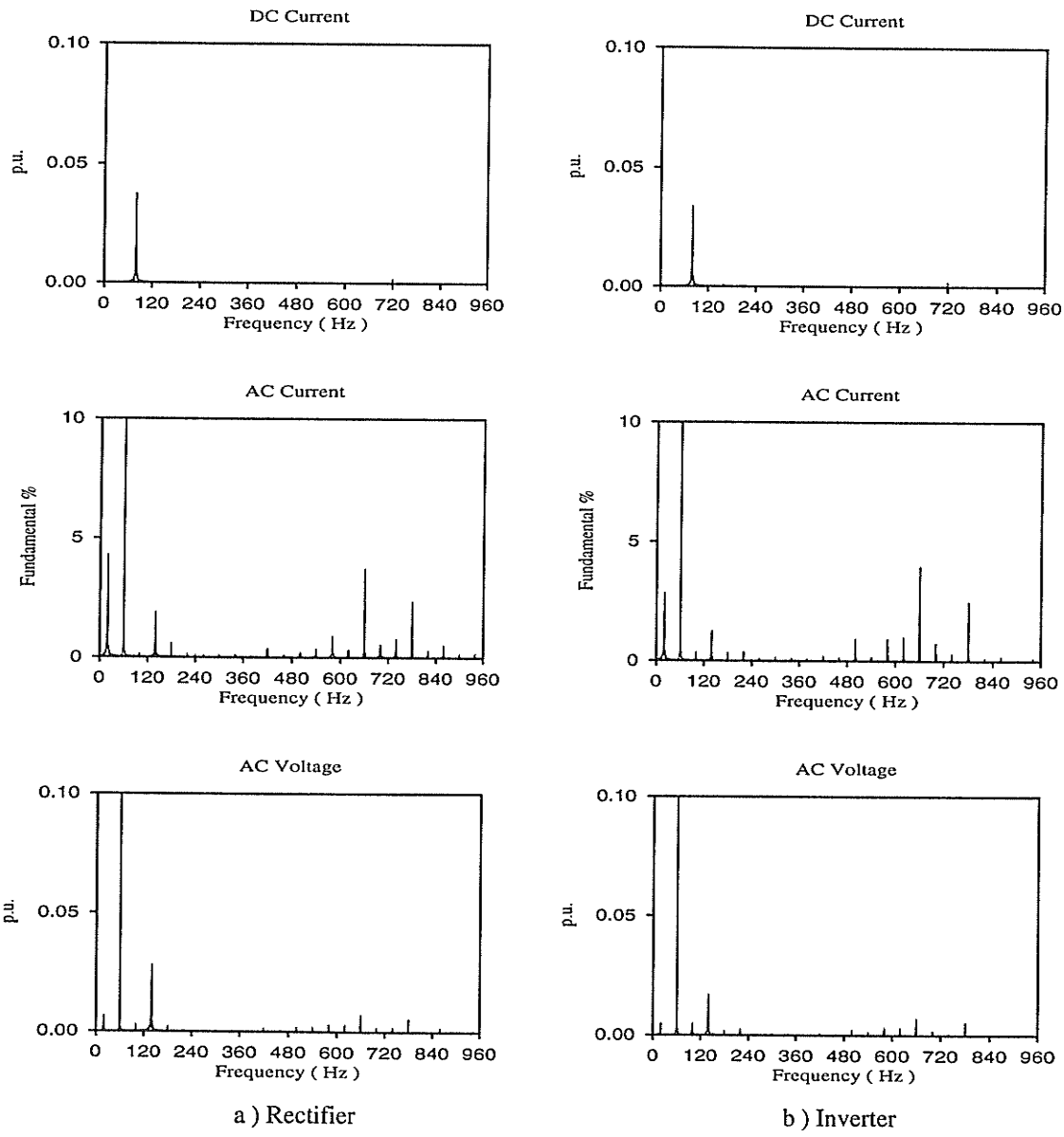

a) Rectifier

b) Inverter

Figure 3 .3 : Fourier Analyses of Base System Waveforms

Fourier analyses of the steady state DC currents, converter currents and AC bus voltages are plotted in Fig. 3 .3 . They show the following effects:

- Besides the DC component, the DC currents on both ends have 80 Hz harmonics of about 3.5 % and 3.2 % respectively.
- Beside characteristic harmonics (660 Hz and 780 Hz), the converters also inject non–characteristic harmonics into the AC system. The major ones are at 20 Hz and 140 Hz due to the modulation effect of the DC bridge of the 80 Hz DC side frequency. The 20 Hz currents are 3.8 % and 2.6 % of the fundamental at the rectifier and inverter respectively, and the 140 Hz currents are 1.7 % and 1.2 % of fundamental at the rectifier and inverter respectively.
- The injected harmonic currents do not produce very high harmonic voltages (all less than 1 % i.e. the individual harmonic limit) on the AC bus voltage. But the 140 Hz harmonic current causes high harmonic voltages (2.6 % for the rectifier and 1.6 % for the inverter) due to the system/filters resonance around 120 Hz.
- The oscillation in the rectifier is larger than that in the inverter due to higher resonant impedance on rectifier side.

The results indicate that the system has a steady state harmonic instability problem. Although the operation does not collapse, the problem is noticeable. The oscillation will remain in the normal operation if no action is taken.

3 .2 .2 PERFORMANCE DURING SYSTEM DISTURBANCE

In steady state, a single line–to–ground 3.5 cycle fault is applied on the phase A in the rectifier AC bus at 0.05 seconds. The system performance during fault recovery is shown in Fig. 3 .4 .

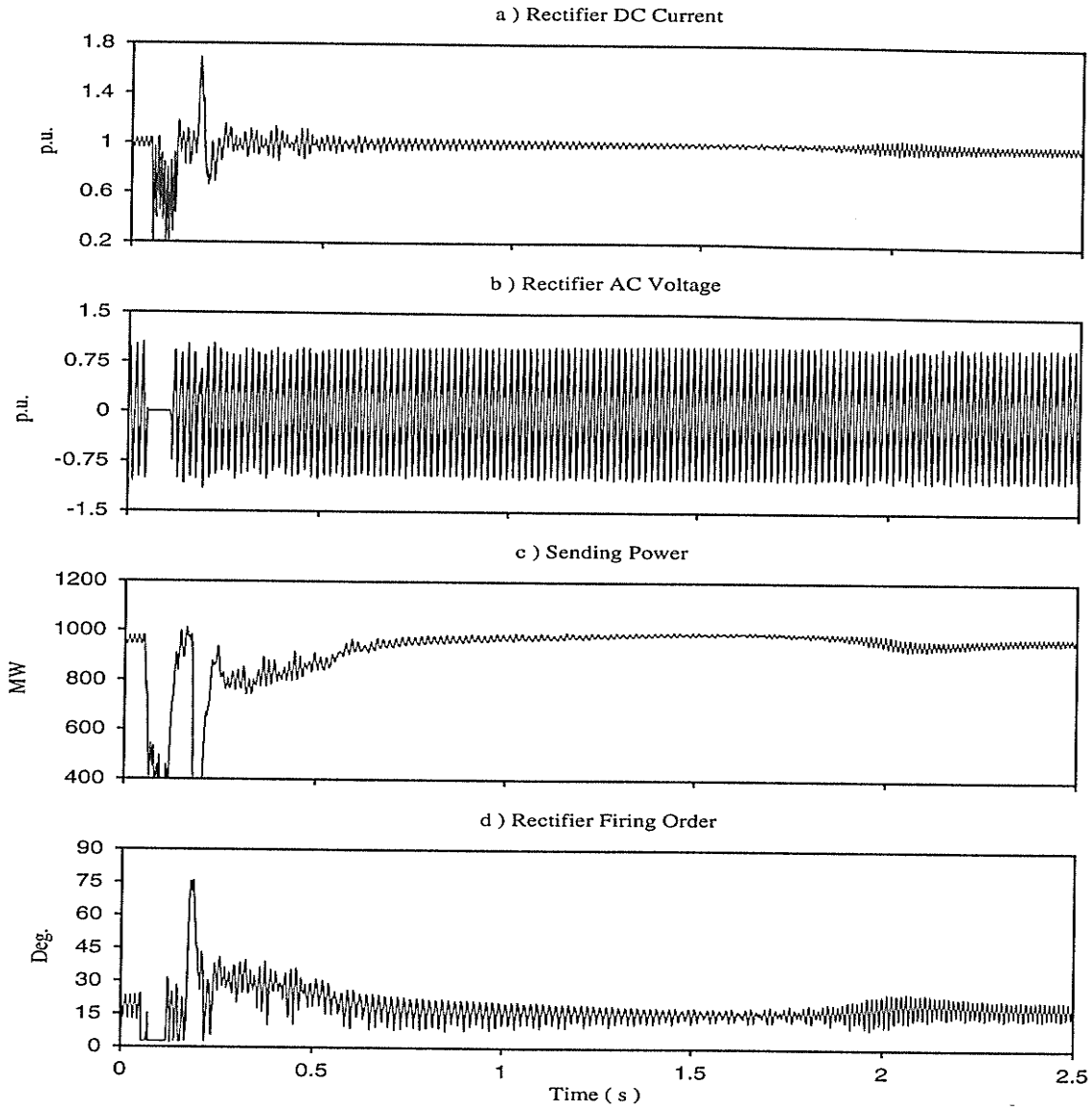

Figure 3 .4 (Continued): Single Line–to–Ground Fault Recovery in the Base System

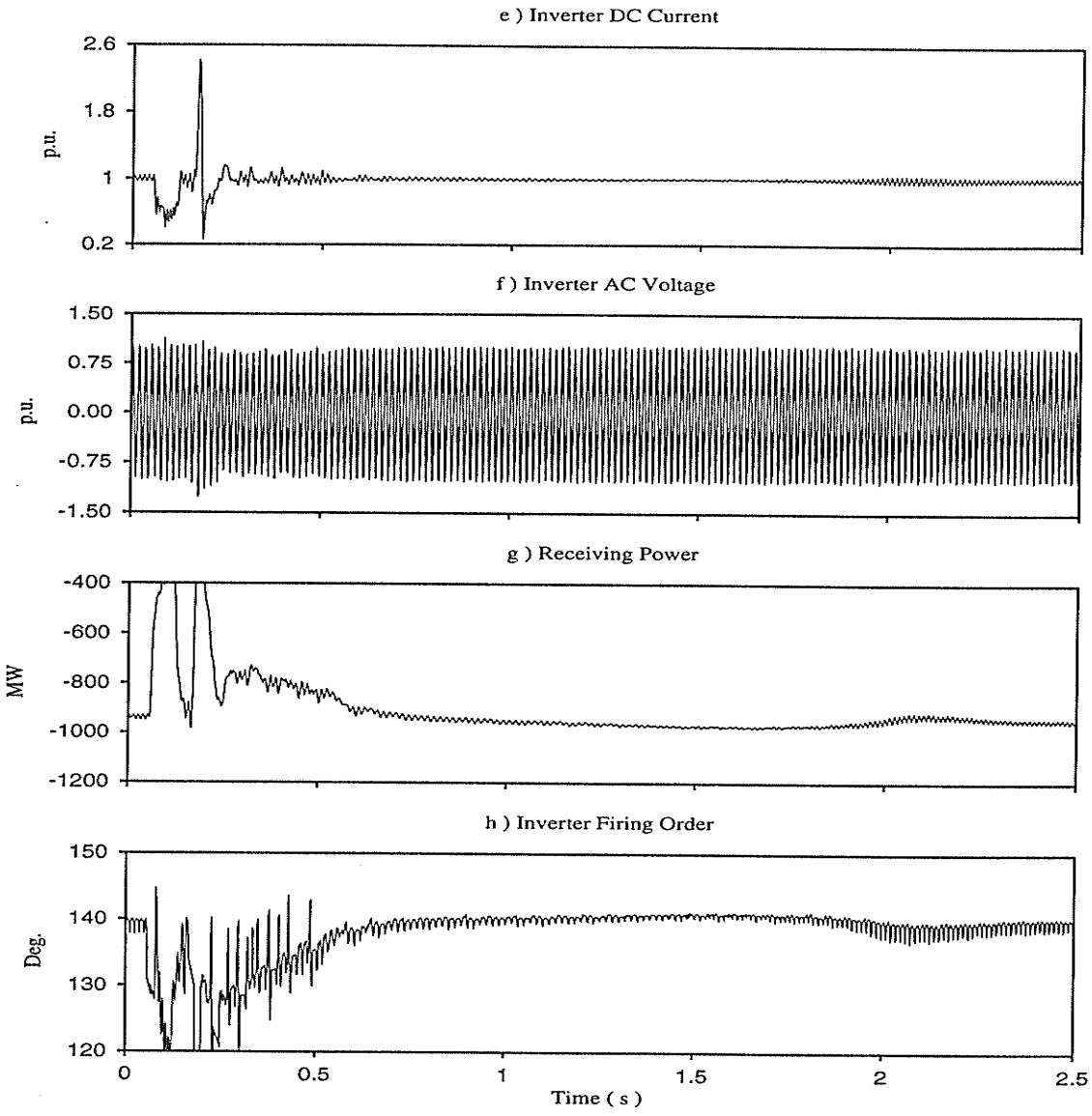

Figure 3 .4 (Concluded): Single Line–to–Ground Fault Recovery in the Base System

From Fig. 3 .4 , following facts can be observed:

- The system returns to the pre–fault condition in about 1.8 seconds.
- After the fault clears (approximately t=0.15 seconds), there is a commutation failure at the inverter. This causes DC overcurrents at both sides (1.7 p.u. and 2.4 p.u. in rectifier and inverter respectively).

- During system recovery, the DC currents have 60 Hz oscillations which decay gradually.
- After 1.8 seconds, the 60 Hz oscillation in DC current dies out and the 80 Hz oscillation (the pre–fault oscillation) returns.

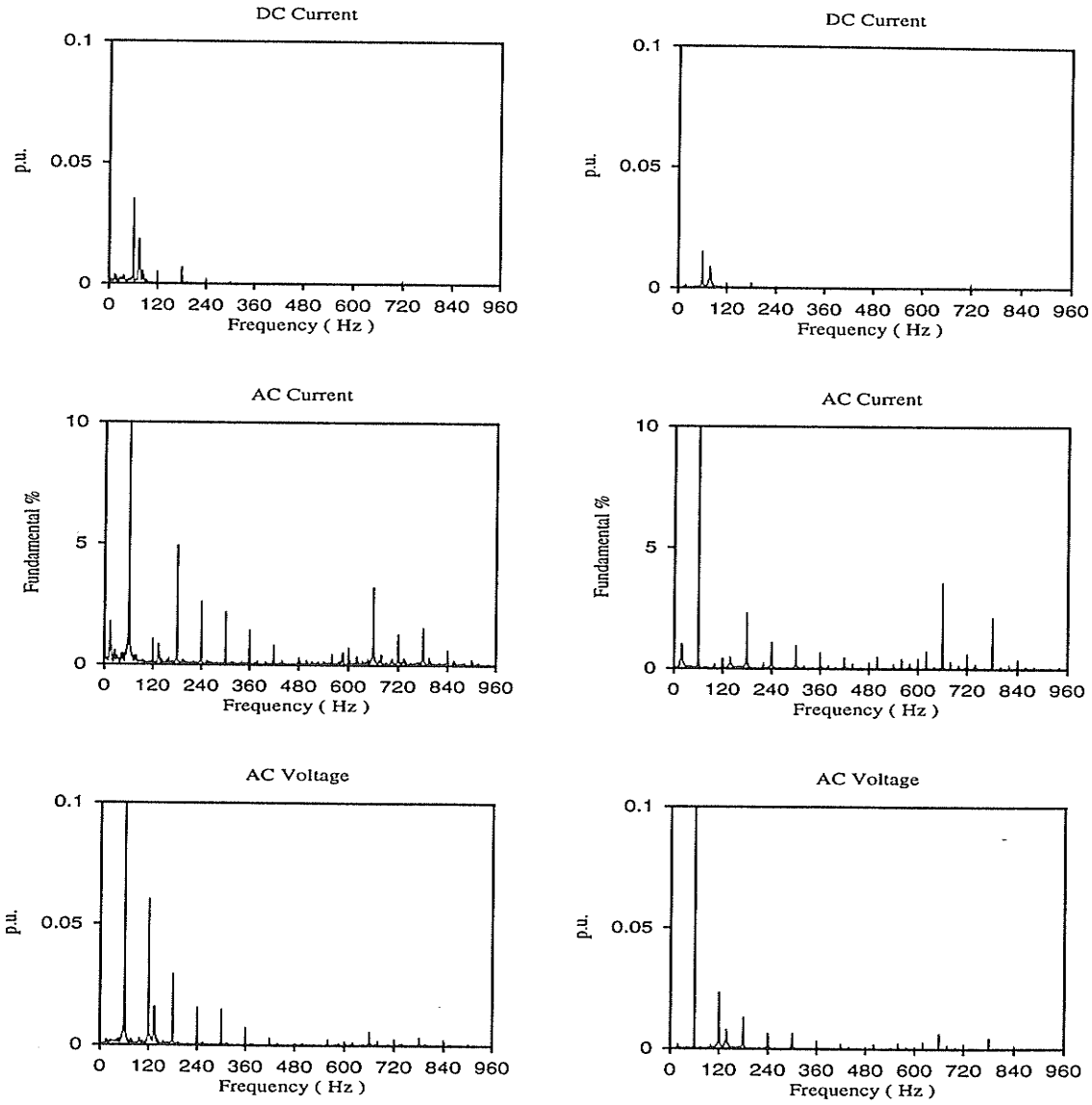

Figure 3 .5 :Fourier Analyses of the Waveforms during Fault Recovery

Fig 3 .5 shows the Fourier analyses of the outputs in rectifier side at 0.25 seconds (just after recovery starts) and 1 second(when the system is partially recovered).

- The rectifier injects all the integer (2nd, 3rd, ...) non–characteristic harmonics due to transformer saturation. The harmonics decay with time as we compare the spectra at 0.25 seconds (Fig. 3 .5 a) and 1 second (Fig. 3 .5 b).
- The harmonic components on the bus voltage also decay gradually as harmonic currents decay.
- The DC current has a major harmonic of 60 Hz which also decays with time.

The analyses indicate that the system experiences core saturation instability as a result of the fault. After fault clearance, the saturated transformer injects all integer harmonics into the AC system. The saturation current dies out very slowly.

3 .2 .3 SUMMARY

The simulation studies of the base system show that the system experiences both steady state and core saturation harmonic instabilities. The steady state instability is at 80 Hz (DC side) frequency, the core saturation instability of 60 Hz (DC side) eventually dies out and is thus not an instability in the strict sense, but we will continue to refer to it as such because of its low damping.

3 .3 BASE SYSTEM PERFORMANCE DURING OTHER SYSTEM DISTURBANCES

Several system disturbances are tested on the base system. Note that the harmonic instabilities in the base system studied earlier can be observed both in DC current and AC voltage. When an 80 Hz oscillation is shown in the DC current, its modulated components 80 ± 60 Hz also can be seen at the same time in the AC current , voltage, power etc. This means in order to observe the instability of an HVDC system, only one of the quantities needs to be monitored. In following studies only rectifier DC current is plotted for demonstrating the instabilities in the HVDC system.

3 .3 .1 THREE LINE–TO–GROUND FAULT ON RECTIFIER AC BUS

In the steady state, a three line–to–ground 3.5 cycle fault is applied on the rectifier AC bus at 0.05 seconds. The system performance during fault recovery is shown in Fig. 3 .6 .

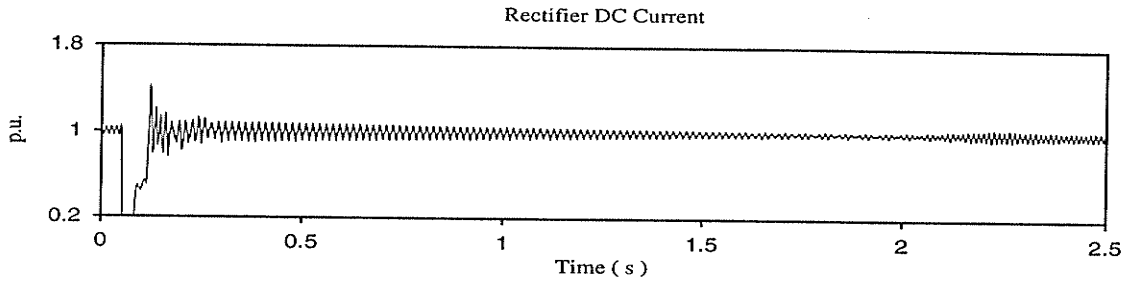

Figure 3 .6 : Three Line–to–Ground Fault on Rectifier AC Bus

Note that during the rectifier AC bus three line–to–ground fault recovery, the performance is similar to the single line–to–ground fault case (Fig. 3 .4 a). The system recovers to pre–fault condition in 2 seconds. During the system recovery, DC current has a 60 Hz oscillation which dies out in 2 seconds.

3 .3 .2 INVERTER AC BUS FAULTS

Faults on inverter AC bus are also tested for the CIGRE system.

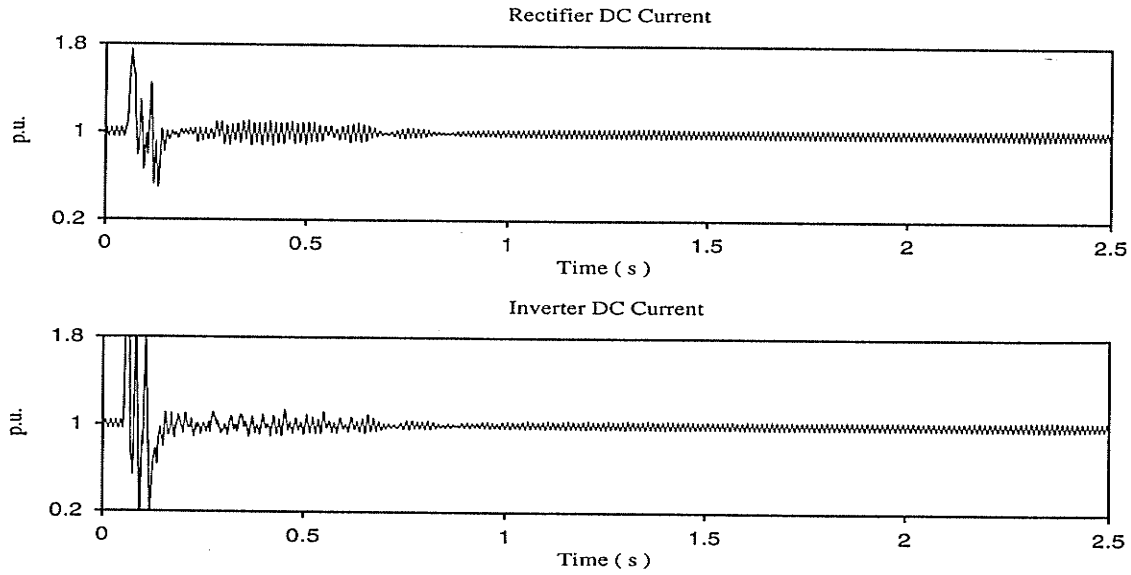

Figure 3 .7 : Single Line–to–Ground Fault on Inverter AC Bus

For the inverter AC bus faults (Fig. 3 .7 for the single line–to–ground fault and Fig. 3 .9 for the three line–to–ground fault), the system recovery performance is much faster (less than 1 second) than the cases for the rectifier AC bus faults (about 2 seconds, see Figs. 3 .17 b & c).

Fourier analyses (At 0.25 seconds) of the outputs (Fig. 3 .8) during the inverter single line–to–ground fault recovery show :

- As in the case of rectifier the single line–to–ground fault discussed earlier (Fig. 3 .5), the inverter injects integer non–characteristic harmonics (2nd, 3rd, ...) due to inverter transformer saturation, which die out in 0.8 second. These harmonics cause few harmonic voltages in AC bus voltage, neither modulated harmonics in DC current, because of much lower resonant impedance on inverter side.
- Unlike the case in the rectifier AC faults, 80 Hz DC oscillation (or 140 Hz AC oscillation) still appear during fault recovery and are even aggravated.

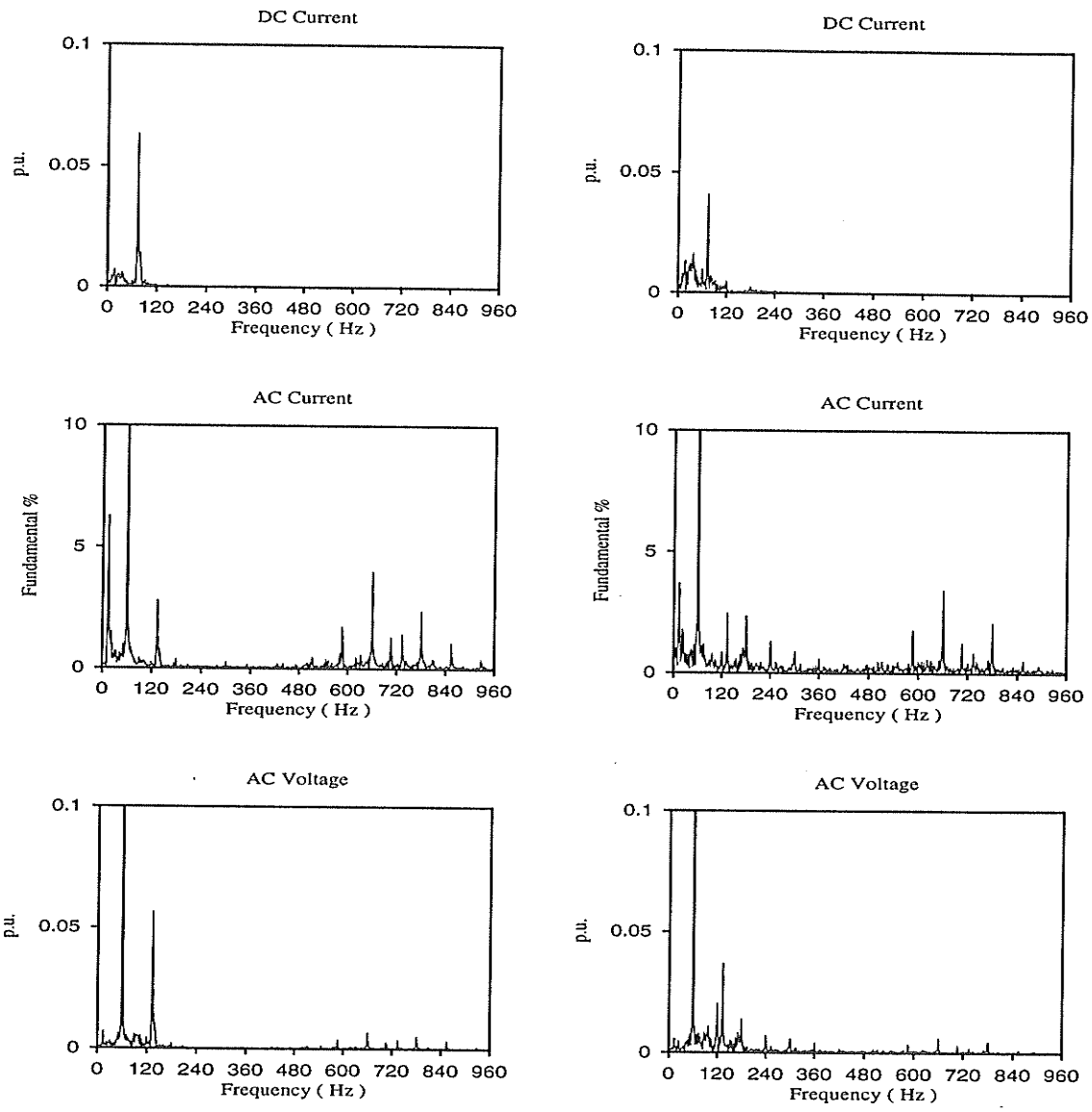

Figure 3 .8 : Fourier Analyses of the Outputs during Inverter Single Line–to–Ground Fault

The system performance during the inverter three line–to–ground fault (Fig. 3 .9) is similar to the case in the inverter single line–to–ground fault. The oscillation during the inverter three line–to–ground fault recovery last the same time but magnitude is smaller than the case with the inverter single line–to–ground fault.

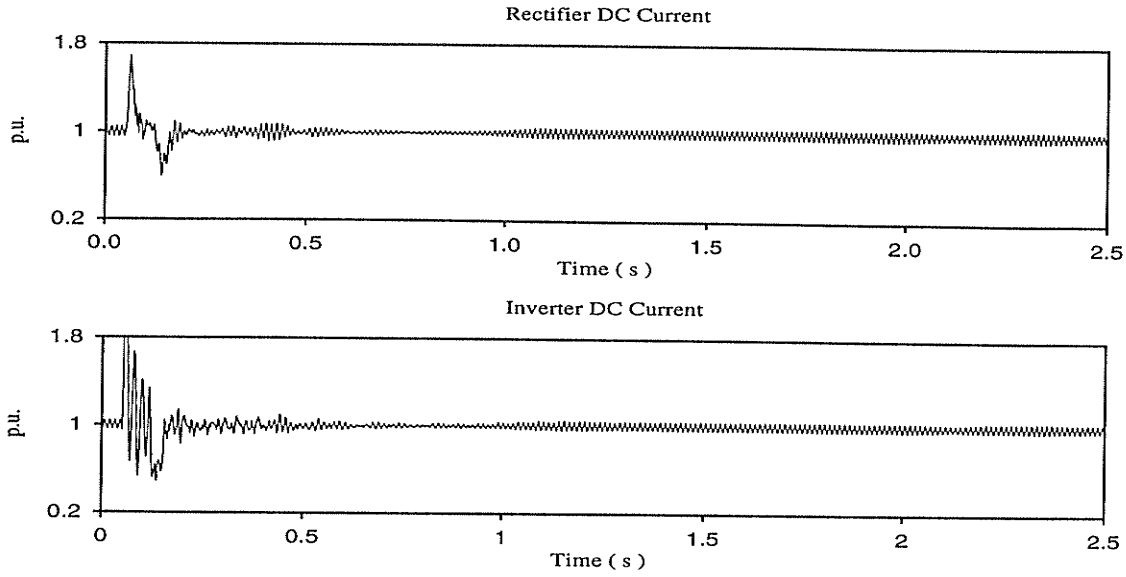

Figure 3 .9 : Three Line–to–Ground Fault on Inverter AC Bus

The base system recovers better in the case of inverter AC bus faults than with rectifier AC bus faults, since the system impedance at resonance on the rectifier side is much higher than the inverter side. The high resonant impedance in the rectifier side is the major reason for harmonic instabilities in the CIGRE benchmark model.

3 .3 .3 DC LINE FAULT

The system can not recover from the DC line faults without control action, because the DC line current does not have zero crossings. The only means of clearing a DC fault is to force the firing angle of the rectifier beyond 90° (called forced retard) thus de–energizing the DC line and then re–starting the system after the fault current is extinguished. Alpha forced retard can be triggered upon detection of the DC fault. After the detection of the DC fault, the rectifier α order is set to 135° for 200 ms to de–energize the DC line and clear the fault, and then the α order is ramped to 0° in 50 ms. A maximum select block is used so that the retard firing angle order is passed on to the firing control during the recovery from the DC fault after which the (normal) current control mode operation is resumed (Fig. 3 .10).

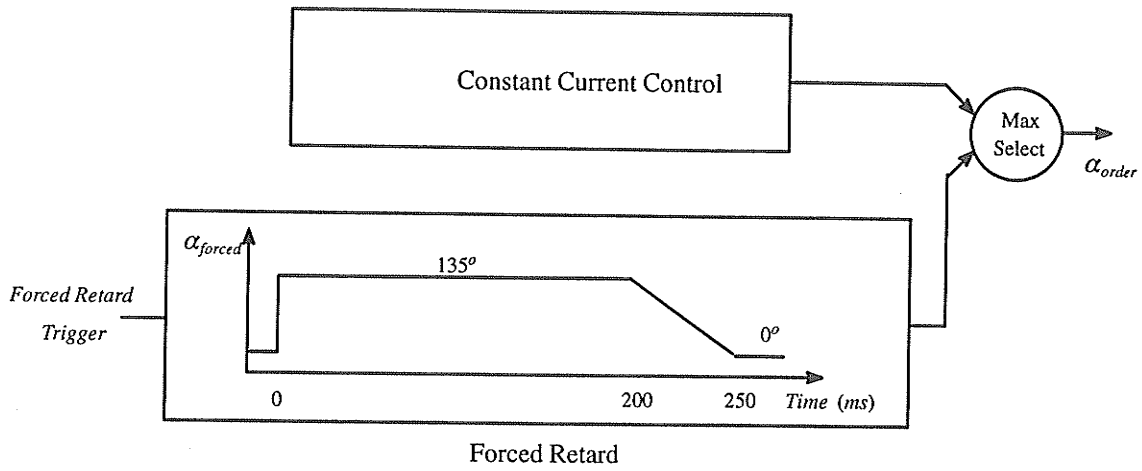

Figure 3 .10 : Forced Retard Block in Rectifier Control

Fig. 3 .11 c shows the rectifier α order during DC line fault recovery. Note that the rectifier α order is set to 135° after the fault detection. The DC current (Fig. 3 .11 a) is quickly extinguished because the rectifier converter now works as an inverter ($\alpha > 90°$). The DC fault is cleared with zero DC current after which the system restarts.

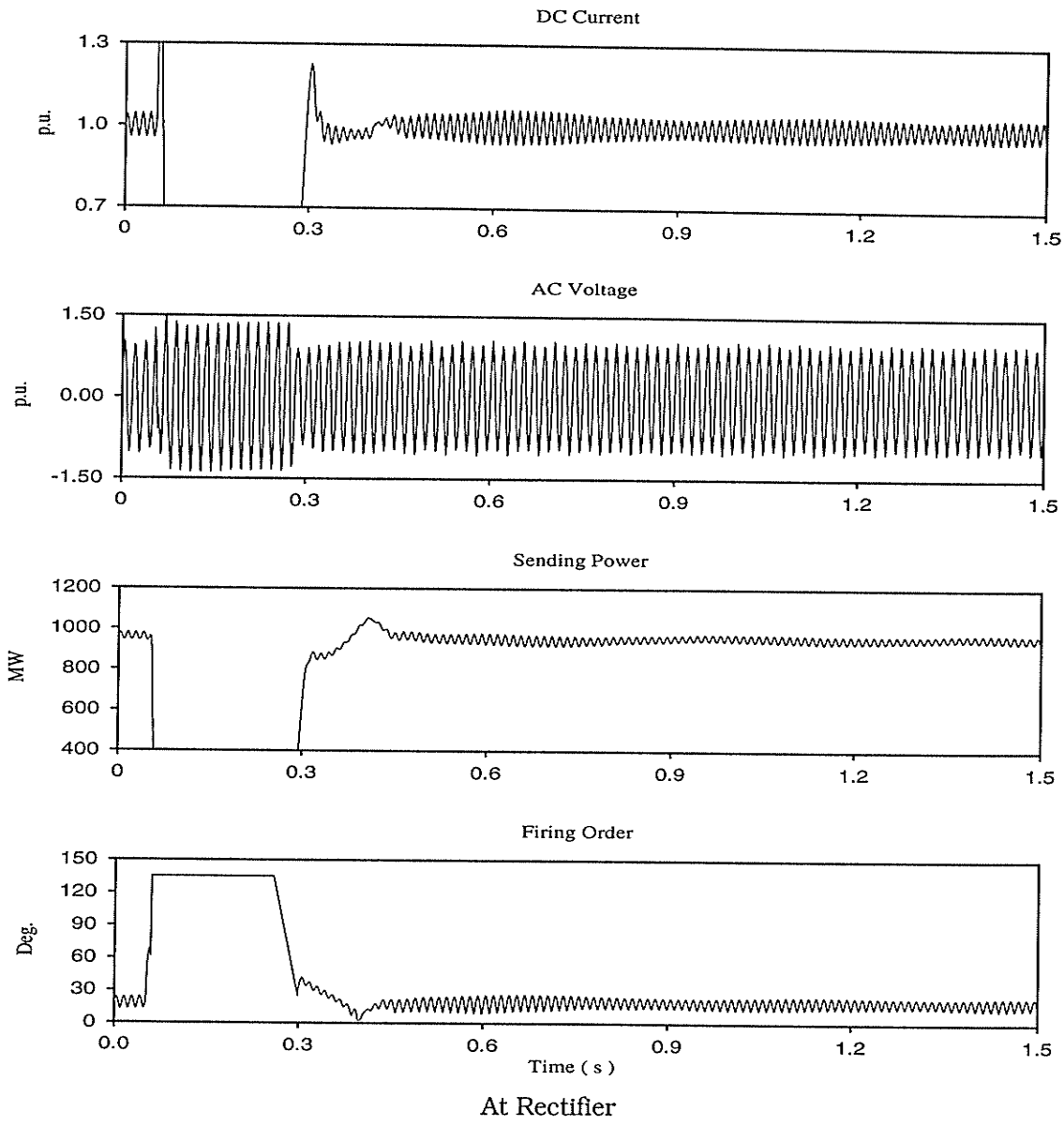

Figure 3 .11 (continued): DC Line Fault Recovery in the Base System

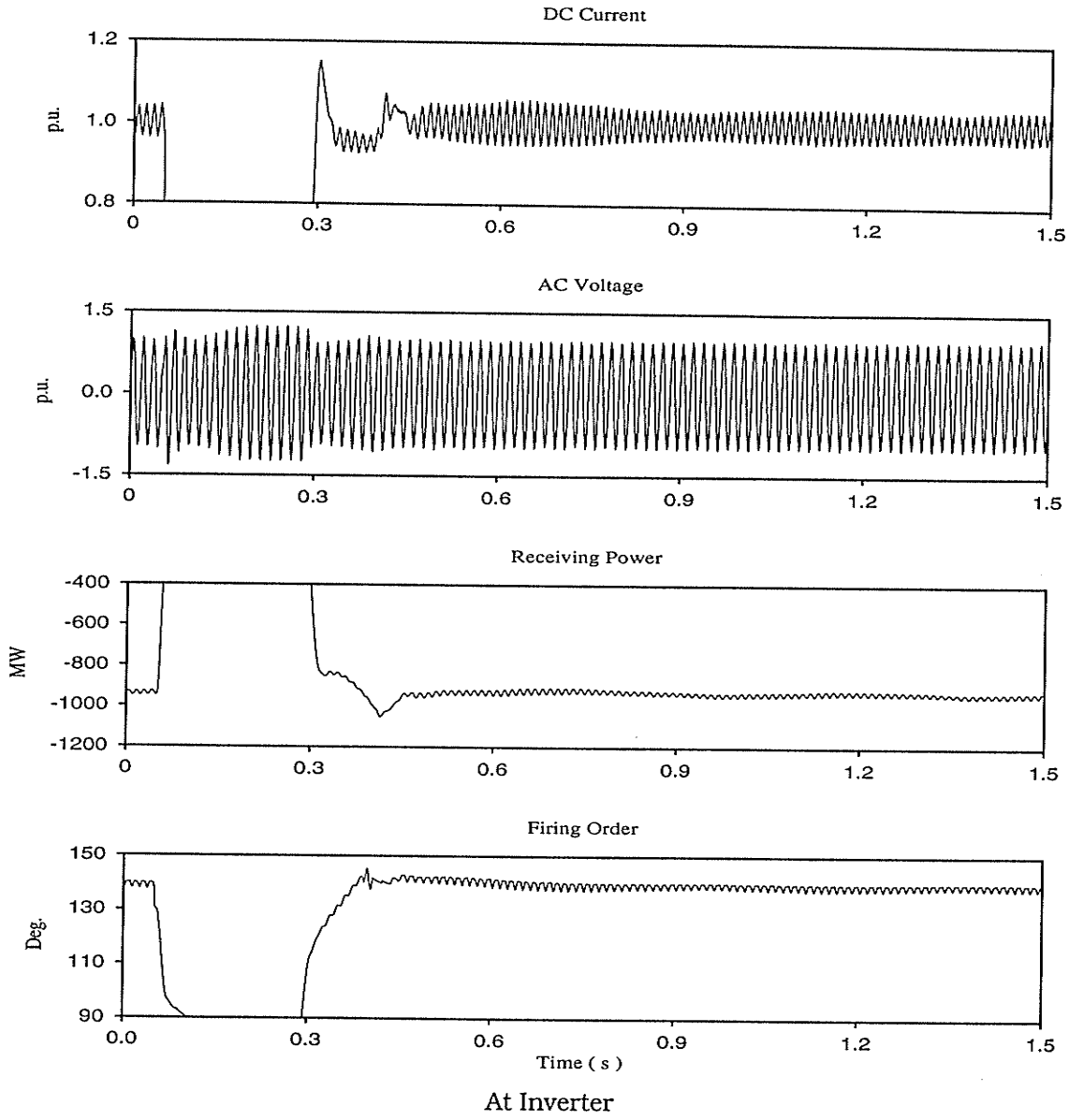

Figure 3 .11 (Concluded): DC Line Fault Recovery in the Base System

Fig. 3 .11 shows the system performance during a rectifier DC line–to–ground fault recovery. The following facts can be observed:

- The system recovers in 0.3 seconds. The system returns to pre–fault condition shortly after the system restart.
- When the DC fault occurs (at 0.05 seconds), the rectifier DC current has a 1.6 p.u. overcurrent which is quickly brought to zero because of forced retard.

- During alpha forced retard, current becomes zero. This causes the voltage drop on system impedance to become zero and results in a 1.4 p.u. overvoltage on the AC bus. The AC overvoltage causes transformer saturation, but no harmonic instability occurs. There is no 60 Hz complementary resonance on the DC side, since no current flows from AC system into the DC side during this period.

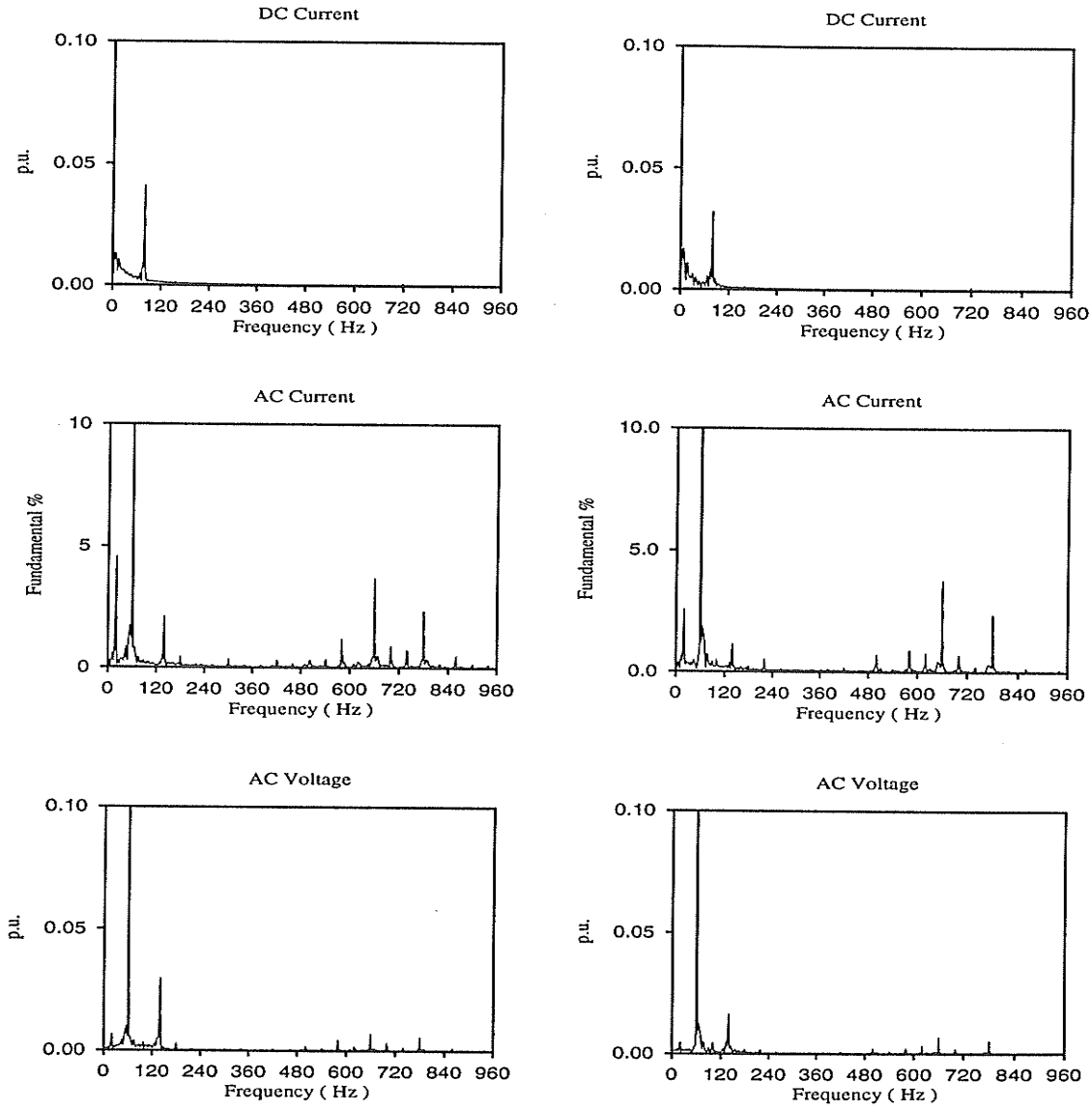

a) At Rectifer

b) At Inverter

Figure 3 .12 : Fourier Analyses of the Waveforms during DC Fault Recovery

Fourier analyses of the DC Currents, converter current and AC bus voltages during fault recovery (0.3 to 0.8 seconds) are plotted in Fig. 3 .12 . They show that:

- Unlike AC faults, there are no integer non–characteristic harmonics injected from the transformer.
- The DC current contains no 60 Hz oscillation.

With force retard, the DC system recovers following DC fault quickly and there are no harmonic instability problems during fault recovery.

3 .3 .4 SUMMARY

The simulation studies of the base system in different fault conditions show that the faults on the rectifier AC bus (where the system impedance is much higher than that of the inverter AC bus) present the most difficult situations for the system to recover. So in the later studies, only the system response to the rectifier AC bus faults are presented.

3 .4 FREQUENCY SCANNING METHOD FOR IMPEDANCE RESPONSE

The system impedance responses have been calculated by assuming that AC and DC systems are operated separately. Under this condition, the DC system is considered as an ideal current source feeding into the AC system. Therefore, the DC system has no effect on the AC system. However, in the actual system the impedance might be affected by the DC system especially for the weak system condition.

In order to identify the presence of a possible instability in a real AC/DC system more accurately compared to precious methods, the frequency scanning method[23] is introduced in this thesis. This method as applied to digital transients simulations of HVDC system is an important contribution of this thesis. In the steady state simulation, a small individual harmonic current is injected into the AC bus. The system impedance can be calculated by measuring the AC bus harmonic voltage $\mathbf{V_h}$ in response to the injected harmonic current $\mathbf{I_h}$.

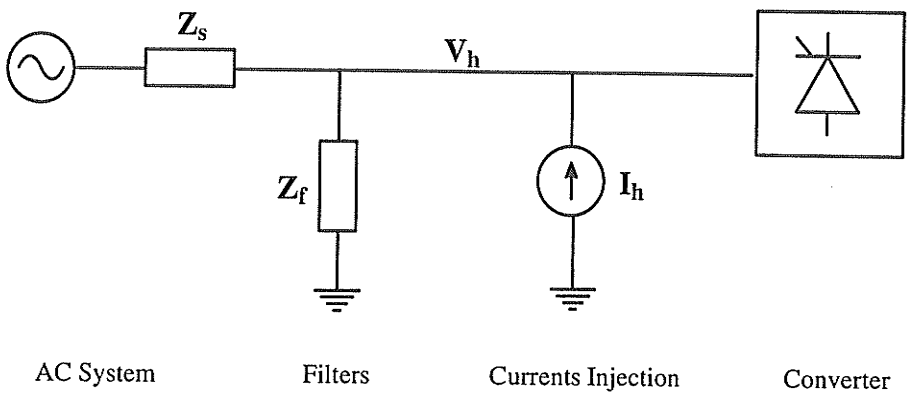

Figure 3 .13 : Frequency Scanning method for System Impedance

Since the DC system behavior is nonlinear. The superposition principle which is true only for a linear system does not apply. But if the disturbance caused by the injected harmonic is small enough, the DC operation can be considered as nearly linear around the operating point.

The injected harmonic currents should be small enough to not affect the normal operation of the HVDC system nor cause any disturbance. This can be checked by monitoring the firing angle of the HVDC converter. Normally, if the oscillation in firing angle cause by injected harmonics is less than half degree (0.5^o), the Frequency Scanning Method is considered valid.

From the experience of the studies in the CIGRE system with this method, following points are helpful in the application of this method:

1. Use a harmonic current injection that is as small as possible (the harmonic current must be large enough however, to show a significant voltage response without being unduly buried in noise).

2. Use nonlinear phase shift between each injected harmonic (with linear shift, the harmonics result in a constrictive interference peak that causes an unduly large disturbance in the HVDC system, Fig. 3 .14).

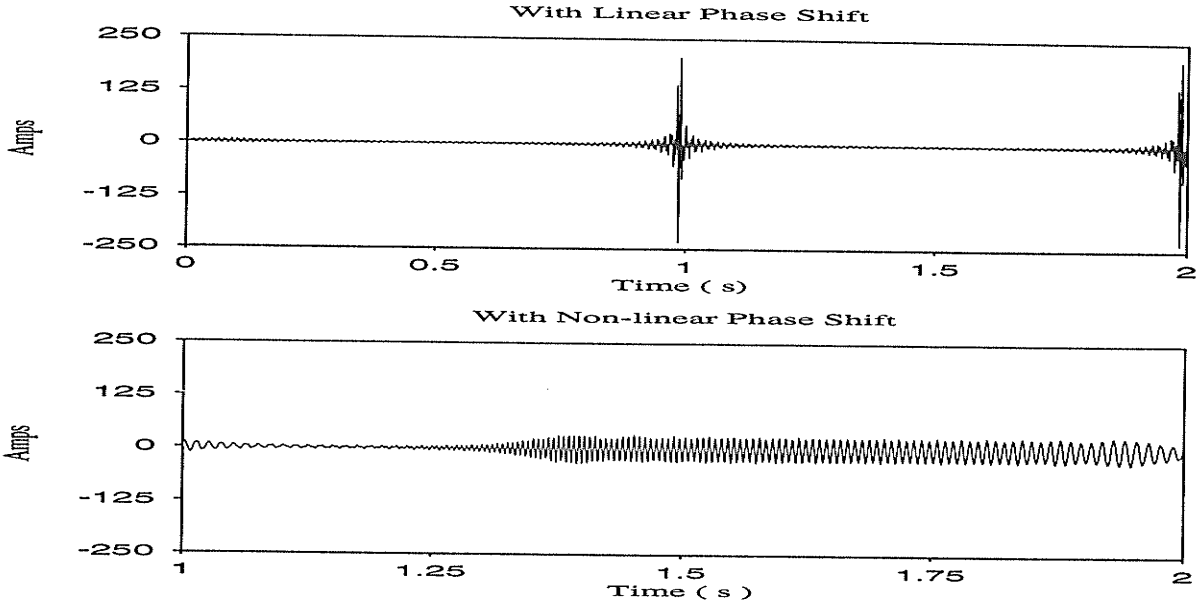

Figure 3 .14 : Effect of Phase Shift between Harmonics in the Total Injected Current

3 .4 .1 FREQUENCY SCANNING FOR THE BASE SYSTEM

The actual system impedance response of base system was obtained by the frequency scanning method described above. In steady state, a series of small harmonic currents (i.e. 80 Hz, 81 Hz, ... 200 Hz at the magnitude of 2 Amps, or less than 0.1% of the fundamental current in AC source) are injected into the rectifier AC bus. Then the harmonic components at those frequencies will build up in the AC bus voltages due to the impedances at the harmonic frequencies.

Fourier analysis of the AC bus voltage is shown in Fig. 3 .15 .

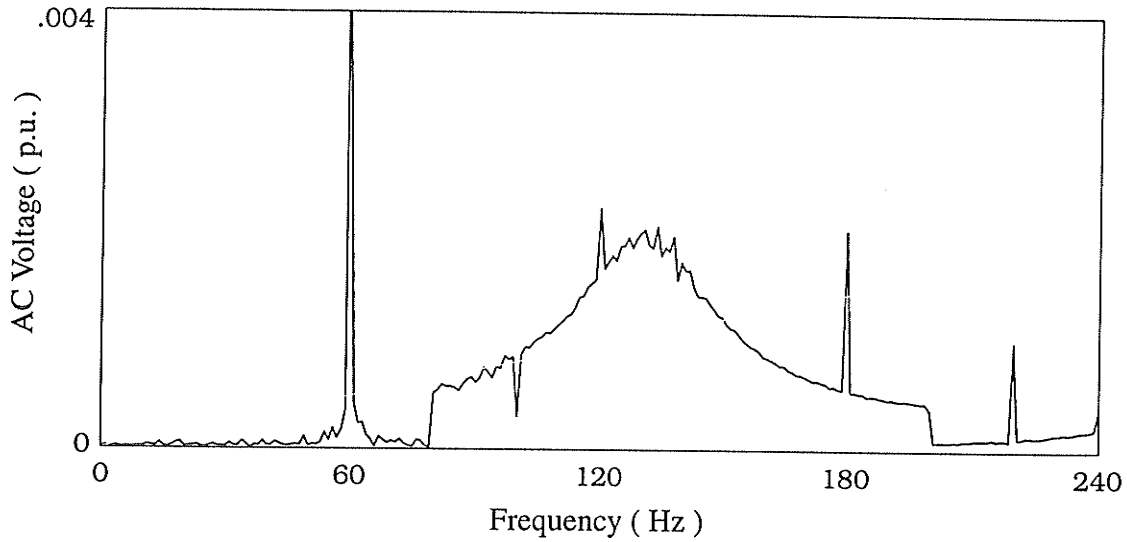

Figure 3 .15 : Fourier Analysis of Rectifier AC Bus Voltage

The frequency spectra of the AC bus voltage contains harmonic components from 80 Hz to 200 Hz in response to the injected harmonic currents. Note that the harmonic components in AC bus voltage are very small ($< 0.2\%$) and thus guarantee the assumption of a small disturbance that does not significantly change the operation of the DC system.

From Fig. 3 .15 , the rectifier AC impedance can be easily obtained by calculating the ratio of AC bus voltage to the injected harmonic current (known, 2 Amps) at each frequency. The measured rectifier AC impedance/frequency characteristics by frequency scanning method is shown in Fig. 3 .16 . The results are plotted with the calculated frequency response for comparison.

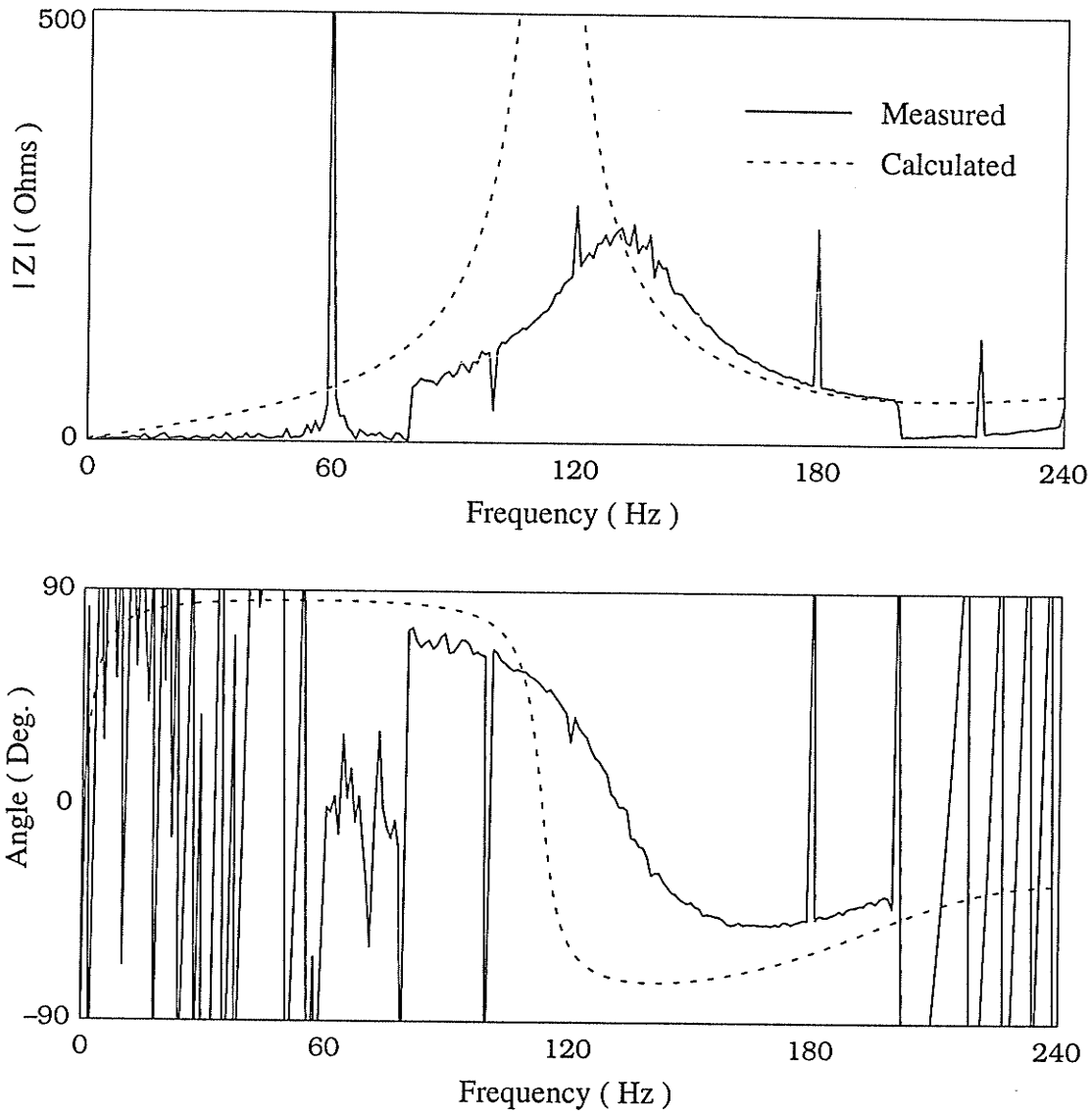

Figure 3 .16 : AC System Impedance / Frequency Characteristic

The results indicate that the frequency scanning method is able to find the resonance and damping of the AC/DC system.

Comparing the spectra of calculation and measurement from 80 Hz to 200 Hz in Fig 3 .16 , there are some differences between the linear analysis method and frequency scanning method. Note that the resonant frequency measured by the frequency scanning method is shifted to a higher frequency (about 140 Hz instead of 120 Hz in calculation).

This is affected by the impedance from DC system. In linear analysis, the DC system is assumed as a current source with infinite impedance. As in the frequency scanning method, the high (not infinite) equivalent impedance of DC system is reflected in the simulation result. This causes the shift of the resonance peak. Also, the DC system provides some damping to the harmonics which results in lower resonant impedance measured in frequency scanning method.

The simplistic picture presented in the linear analysis is often not observed in practice. This is because the AC and DC systems are inherently coupled and it is not always correct to consider individual resonances on each side. Thus a 2nd harmonic resonance may be calculated at the AC side by considering only the system and filters, but in reality the resonance may be different from this frequency.

However, the impedance at 2nd harmonic is still significantly high enough to cause the post–fault harmonic instability at 120 Hz. Also, the resonant frequency of 140 Hz is confirmed by the presence of 80 Hz oscillation (140 – 60 Hz) as seen in Fig. 3 .2 etc.

3 .5 SUMMARY OF THIS CHAPTER

In this chapter, the modified CIGRE benchmark system (which is selected as a base system for the studies) has been simulated on the EMTDC program. Several simulation studies are conducted on the different system situations such as system start–up and disturbances. The general performance of the system can be monitored through the rectifier DC current waveforms as in Fig. 3 .17 .

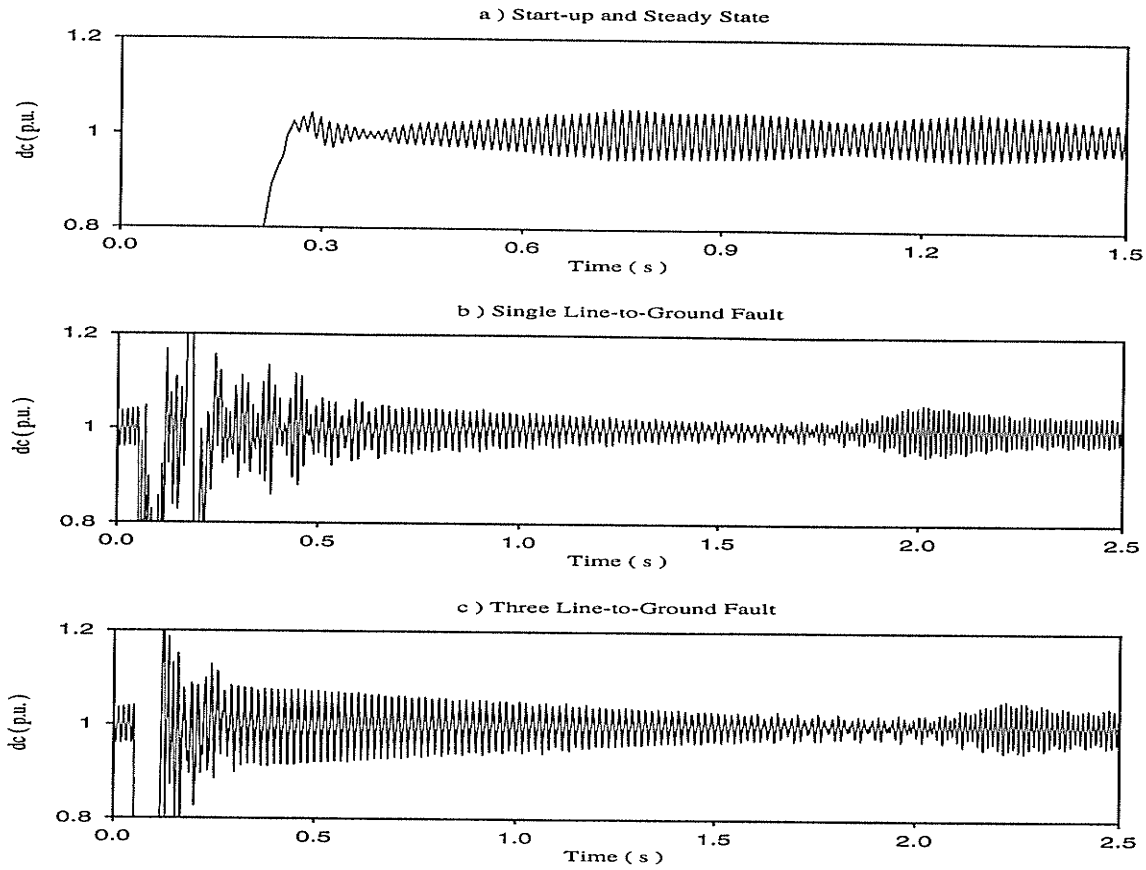

Figure 3 .17 : Rectifier DC Current in the Base System

Following conclusions are obtained in this chapter:

1. The modified CIGRE benchmark system experiences both steady state and core saturation harmonic instabilities. It is a good candidate as a base system for the studies.
2. Different system disturbances have been tested on the base system. The rectifier AC bus faults are the most series conditions for the base system recovery.
3. The Frequency Scanning Method provides a more accurate frequency impedance characteristic measurement for the real AC/DC system.

Chapter 4

System with Tuned Filter

4 .1 THE SYSTEM WITH TUNED FILTER

To cure the harmonic instabilities in the original system, the system impedance/frequency characteristic is modified by installing an additional filter on the commutating bus. Since the resonant impedance on the inverter side is much lower than the resonant impedance on the rectifier side (see Fig. 2 .2), only the rectifier side needs modification. In a later Chapter, this lossy filter will be replaced with an energy recovery type filter.

4 .2 SELECTION OF THE FILTER

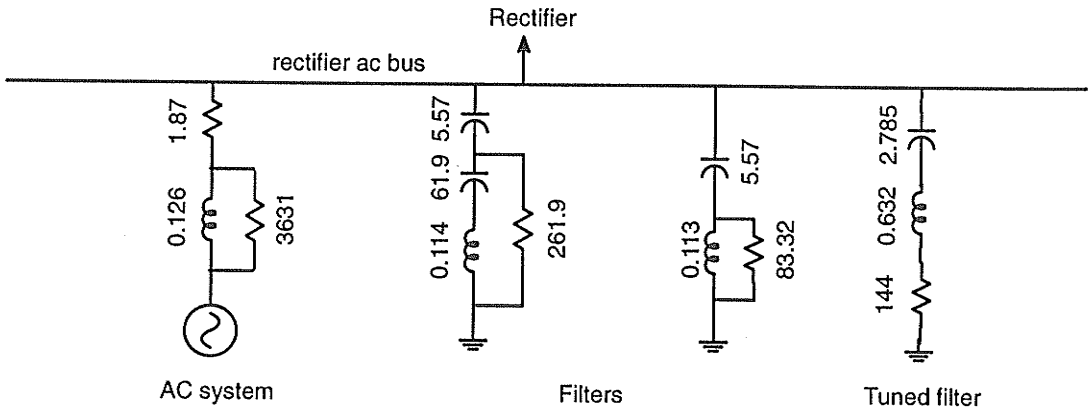

Figure 4 .1 : Rectifier AC Filter Configuration of the System with Tuned Filter

The purpose of this filter is to reduce the peak impedance at the resonance of the system/filter and so an R–L–C filter tuned at 120 Hz is used. In order to keep the same reactive power supplied by the capacitor in the base case, this filter replaces the capacitor bank in the original case (Fig. 4 .1).

4 .3 SELECTION OF THE QUALITY FACTOR OF THE FILTER

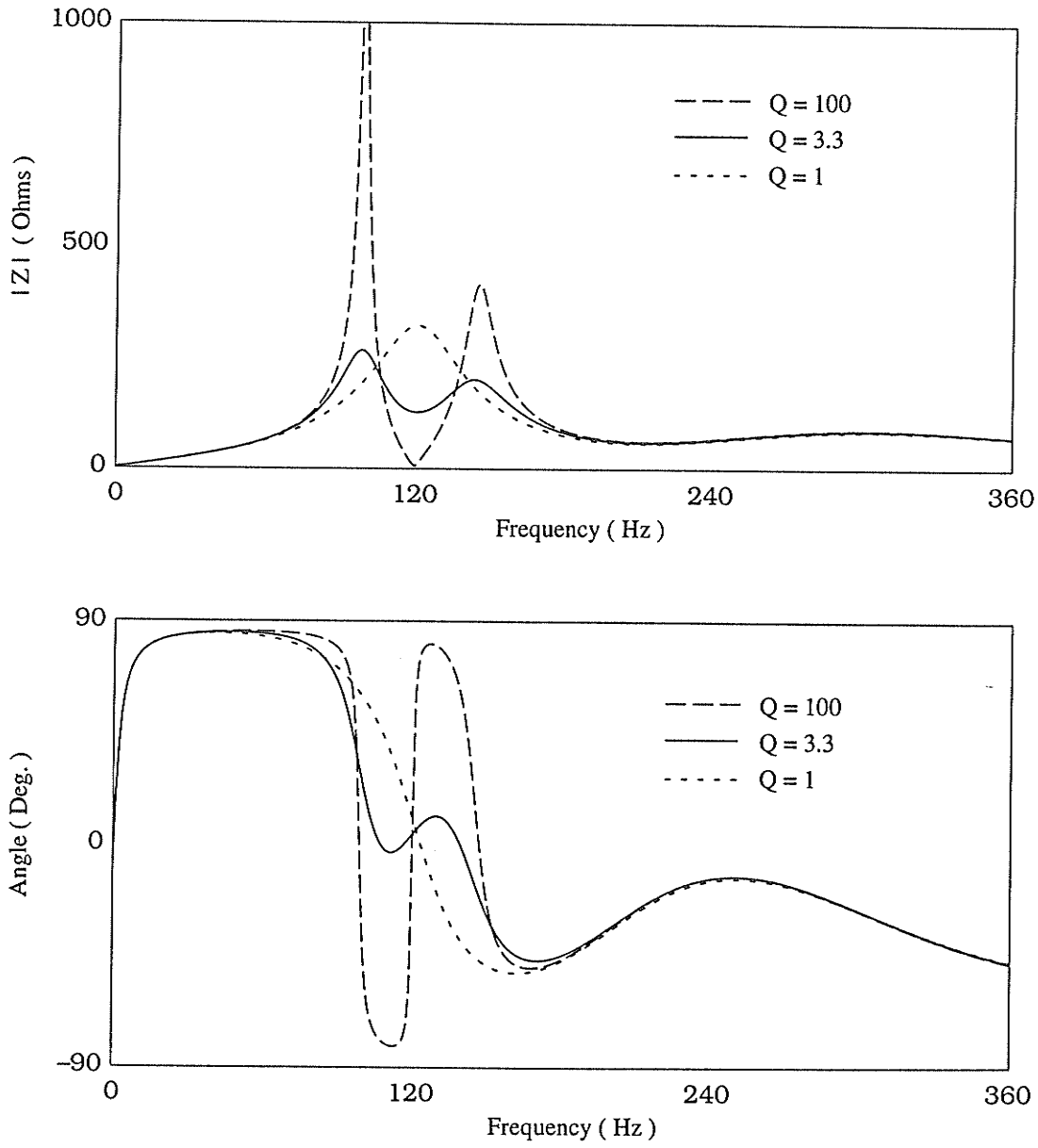

Figure 4 .2 : Modifying the Impedance / Frequency by Tuned Filter

As stated earlier, a low Q factor R–L–C filter is used here to provide a broadband solution for harmonic instabilities.

It can be seen that a high Q filter gives a very low impedance at the tuned (resonant) frequency, but also results in two high sideband resonances which may cause other instability problems (Fig. 4 .5). Reducing the Q factor reduces the high impedance peaks at nearby frequencies but increases the value of the filter impedance at the tuned frequency. Thus there is a compromise between tuned impedance and sideband impedances in selecting the Q factor of the filter. So in this application, a Q factor of 3.3 was selected which gives a maximally flat response as seen in Fig. 4 .2 . The parameters of the filter are:

$$C_f=2.785\mu F \quad L_f=0.632H \quad R_f=144\Omega$$

4 .4 IMPEDANCE/FREQUENCY RESPONSE BY FREQUENCY SCANNING METHOD

The frequency scanning method described in Chapter 3 is used here to measure the rectifier impedance/frequency characteristic in the systems with the filters of different Q factor.

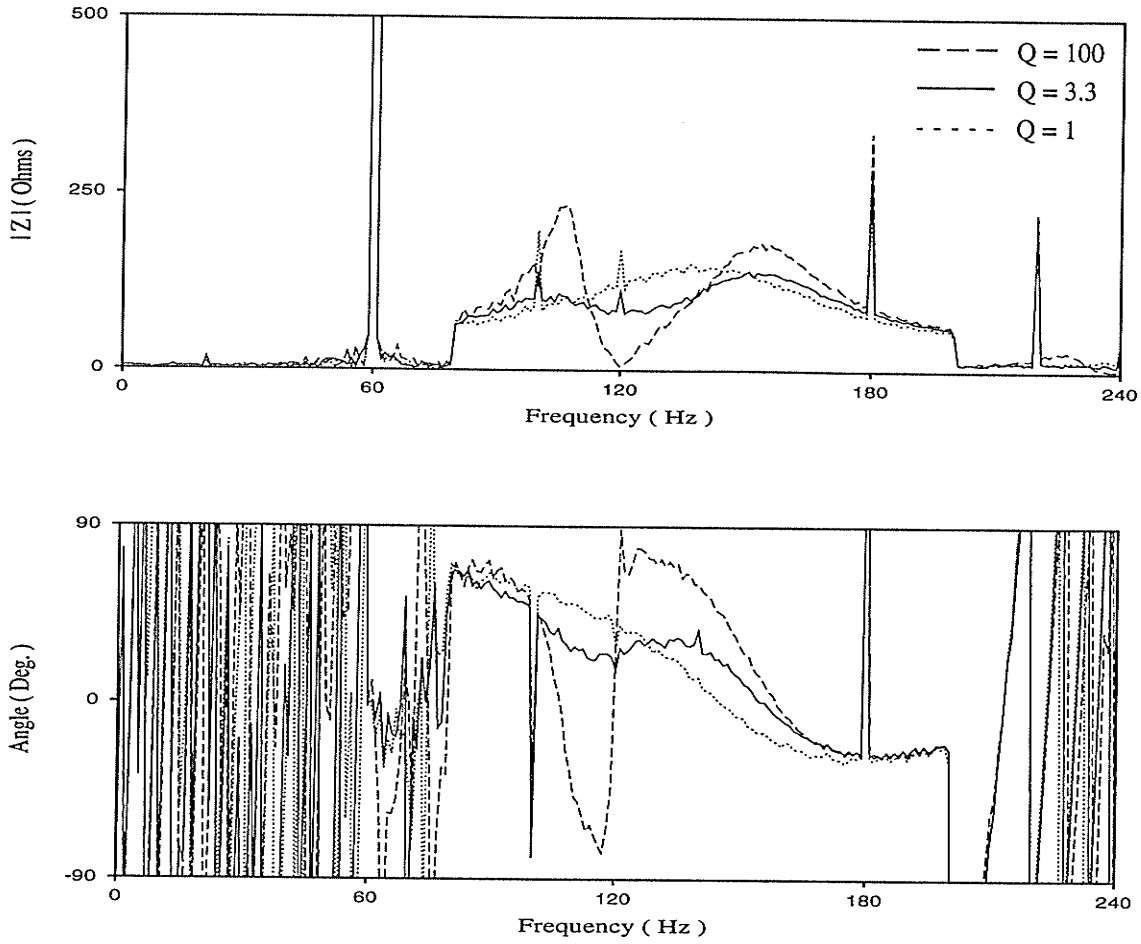

Figure 4 .3 : Measured Frequency Responses by Frequency Scanning Method

The measured frequency response of the system is shown in Fig. 4 .3 . The systems with different Q factor (Q=1, Q=3.3 and Q=100) tuned filters are simulated and plotted in the same graph. Again, the resulting characteristics are slightly different from the calculated results (Fig. 4 .2) due to the effect from the DC link as discussed in Chapter 3.

4 .5 PERFORMANCE OF THE SYSTEM WITH TUNED LOW Q FILTER

A simulation of the start–up shows no buildup of oscillations in the system with the tuned filter (Fig. 4 .4 a) unlike the base case result (Fig. 3 .17 a).

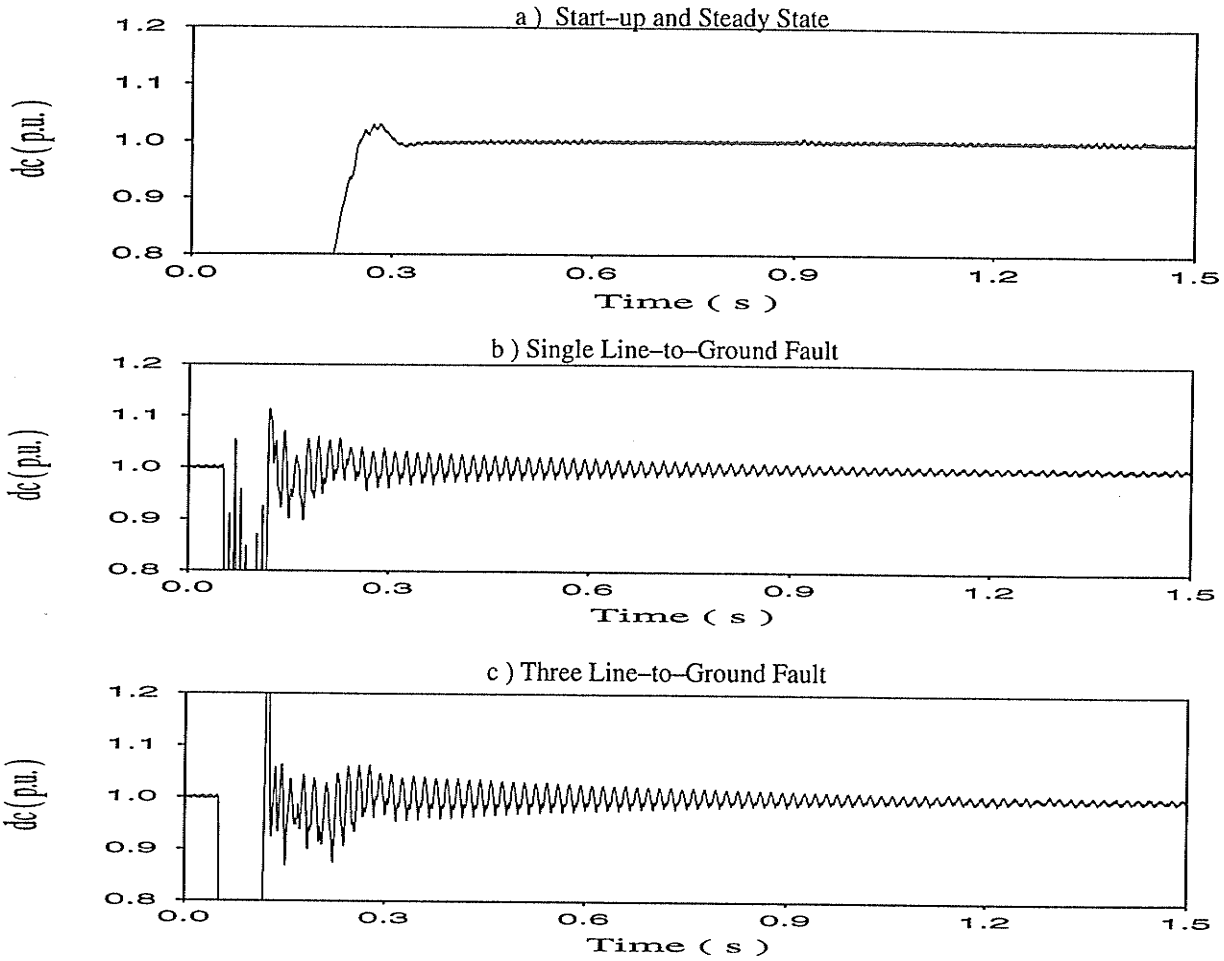

Figure 4 .4 :Rectifier DC Current in the System with Tuned Low Q (Q = 3.3) Filter

From a Fourier analysis of waveforms (not shown) we observe the following:

- Reduced harmonic content in dc current at the resonance frequency (< 1 %).
- The rectifier injects mainly characteristic harmonics : 660 Hz (3.72 %) and 780 Hz (2.35 %), and few non–characteristic harmonics.
- The injected harmonic currents do not produce high harmonic voltages (all less than 1%; i.e. the individual harmonic limit) on the bus. The steady state oscillations are eliminated.
- The sending end AC power is 1040 MW and the receiving end AC power is 987.5 MW. However, as a drawback, the power loss is increased from 20 MW to 52.5 MW. This indicates a filter loss of 32.5 MW.

From the steady state, a single line–to–ground 3.5 cycles fault is applied on phase A of the rectifier AC bus at 0.05 seconds. Results (Fig. 4 .4 b) and their Fourier analyses (not shown) show that:

- The system recovers to pre–fault condition in about 1 second.
- There is no commutation failure in the inverter.
- During system recovery, the DC current has a 60 Hz oscillation which decays quickly and its magnitude is less than that in the base case (Fig. 3 .17 b).
- The rectifier injects all the integer non–characteristic harmonics due to transformer saturation. The non–characteristic harmonics however decay quickly as compared with the base case.

A similar improvement from the base case is also observed for the three line–to–ground fault at the rectifier AC bus (Fig. 4 .4 c).

Results show that the system with a tuned low Q (Q = 3.3) filter has a much better performance than that of the base system (comparing Fig. 4 .4 with Fig. 3 .17). However, there is a drawback of high losses in this solution due to the power consumption in the filter resistor.

4 .6 STEADY STATE CONDITION OF THE TUNED FILTER

The steady state conditions of the low Q tuned filter can be calculated according to the system parameters. The rectifier bus voltage is V_{bus} = 345 kV (l–l rms), so:

The fundamental voltage (l–g rms) drop on the filter resistor is

$$|V_f| = \left| \frac{R_f V_{bus}/\sqrt{3}}{R_f + j\omega L_f + \frac{1}{j\omega C_f}} \right| = 39.46kV$$

The current flow in the filter is

$$|I_f| = \left| \frac{V_{bus}/\sqrt{3}}{R_f + j\omega L_f + \frac{1}{j\omega C_f}} \right| = 0.27kA$$

The power consumption in the filter resistor is

$$MW = 3|I_f||V_r| = 32.2MW$$

The simulation results confirm this calculation. Note that the resistor in the low Q filter produces power loss. In the final implementation, the resistor is replaced with the Energy Recovery link.

4 .7 EFFECT OF THE Q FACTOR OF THE FILTER

As shown in Fig. 4 .2 , increasing the Q factor of the filter will reduce the impedance at tuned frequency but increase the sideband peaks. The effects on the system performance can be observed in the simulation results in Fig. 4 .5 , where a high Q filter (Q=100) is installed on the rectifier AC bus.

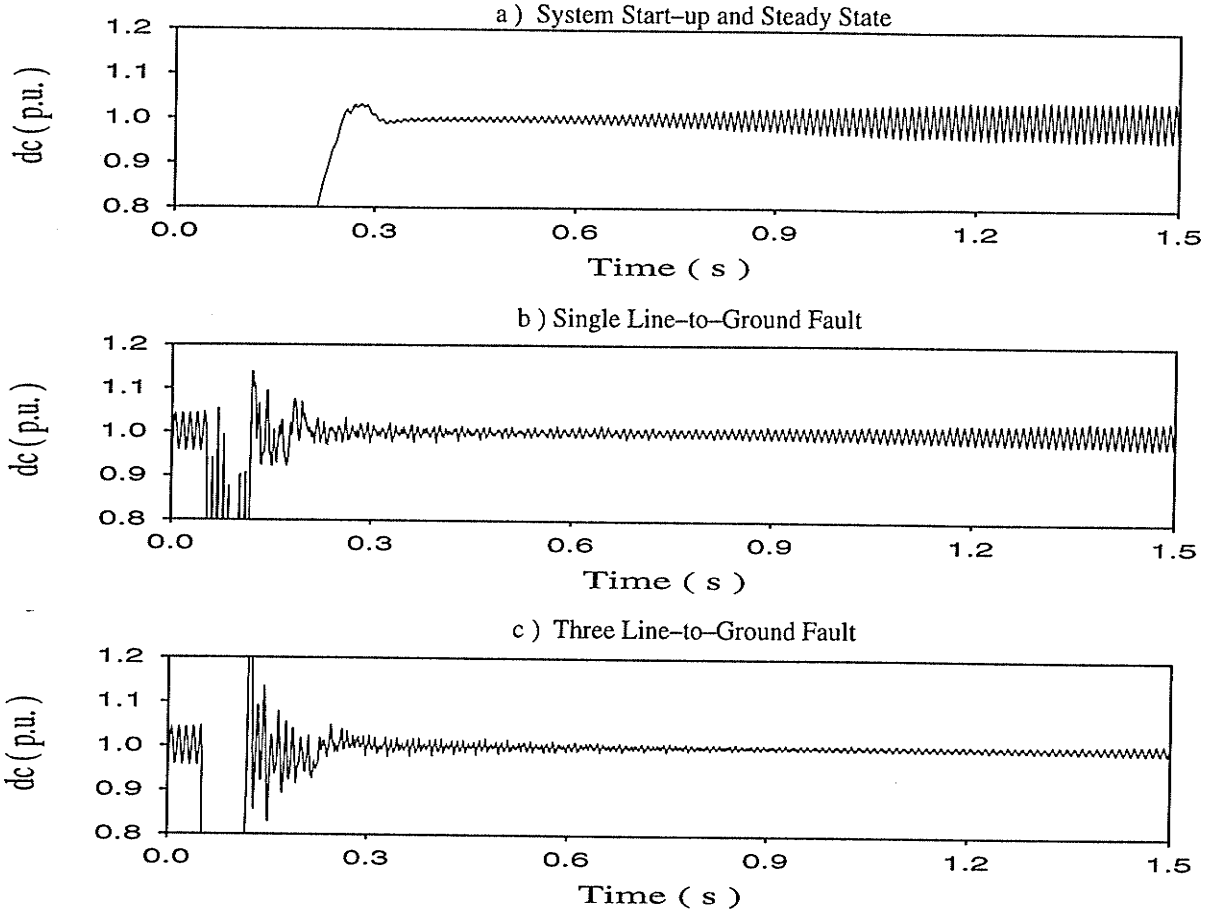

Figure 4 .5 : Rectifier DC Current in the System with a High Q (=100) Filter

In the system start–up and steady state (Fig. 4 .5 a), the oscillations in DC current are clearly visible. The steady state harmonic instability remains as in the CIGRE system (Fig. 3 .17 a) due to the sideband resonances. However as seen in Figs. 4 .5 b&c the system recovery from AC faults is much better in the high Q filter case than in the low Q filter case (Figs. 4 .4 b&c) before the steady state oscillations return. This phenomenon can be explained as follows: After fault clearance, the saturated transformer injects a large amount of 2nd harmonic into the AC system which cause the core saturation oscillation[1]. Since the filter is sharply tuned at 120 Hz, the 2nd harmonic current injected from the saturated converter transformer is completely absorbed by the filter. The 2nd harmonic will not build up in the AC voltage to cause the oscillation.

Thus the high Q filter shows poor steady state performance because of the low damping. On the other hand a low Q filter gives better performance during the steady state. However, the small impedance of the high Q filter at tuned frequency (120 Hz) helps the system recover from faults.

The above discussion suggests that a " variable Q filter " on the AC bus could be used. The " variable Q filter " provides low Q factor in the steady state to reduce the steady state oscillations, and a high Q factor during fault recovery to help absorb harmonic currents generated due to the fault. The Energy Recovery filter to be introduced in the next section can be controlled electronically to have variable Q and can thus implement the feature discussed above.

4 .8 CONCLUSIONS

1. Installing the low Q filter tuned at 120 Hz on the rectifier commutating bus solves the harmonic instability problems in the CIGRE system.
2. The total losses of the system with the low Q tuned filter are 32.3 MW higher than in the original system due to the losses in the low Q tuned filter.
3. The quality factor of the tuned filter has a different effect on the system performance during steady state and transient operation. A variable Q factor filter could be designed to achieve improved performance for different operating modes.

Chapter 5

Energy Recovery Filter

5 .1 INTRODUCTION

Adding the low Q tuned filter on the rectifier commutating bus solves the harmonic instability problems in the original system. The total losses of the system increase due to the high losses in the tuned filter. The proposed Energy Recovery filter (ER–filter)[24][25] will recover the losses and still solve the problems.

5 .2 THE ENERGY RECOVERY FILTER

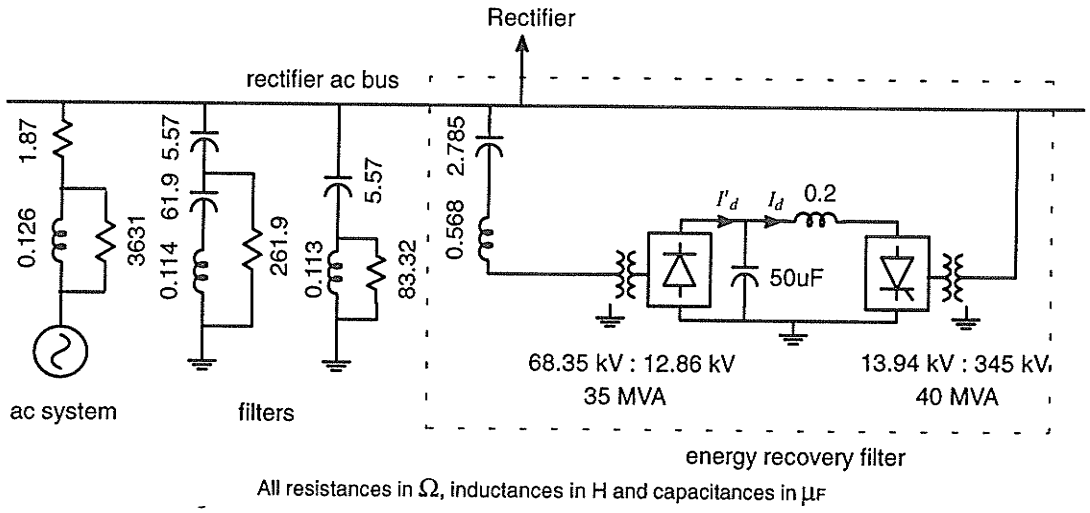

Figure 5 .1 : Rectifier AC Filter Configuration of the System with an Energy Recovery Filter

The ER–filter is constructed by replacing the resistors in a tuned filter with a back–to–back DC link. The rectifier of the DC link is connected to the tuned filter and the inverter to the commutaing bus as shown in Fig. 5 .1 .

Looking from the filter side, there is a certain amount of real power flow in the filter. This means the Q factor of the filter is low. This power flows through the back–to–back DC link and returns to the AC system. So, to the sending AC system there is almost no loss due to the ER–filter.

The diode bridge rectifier of the filter DC link is uncontrolled and accepts power from all frequency components of current in the filter. However the filter DC link capacitor and smoothing reactor combination feed a relatively constant DC current to the filter link inverter. Thus on the inverter side the link behaves more like a source of (predominantly) 60 Hz power, whereas on the rectifier side it behaves more like a resistor. Thus the tuning characteristics of the filter remain more like that of a low Q filter, but the loss power is recovered at 60 Hz frequency on the inverter side.

5 .2 .1 SOME COMMENTS ABOUT THE ER–FILTER

1. Because of the relatively well defined currents in the filter, the input to the bridge is like a current source. In conventional HVDC converters, the firing angle of the bridge is measured from the commutating bus voltage, and so the conventional definition of firing angle is not applicable here. We could define the firing angle as measured from the zero crossing of the fundamental frequency current. Rather than build a firing control scheme for the thyristor using this concept, we just investigate the use of a diode bridge for rectification.
2. The power rating of ER link is small, for simplicity and economics, a 6–pulse diode bridge is selected for the rectifier of the ER link. And a 6–pulse thyristor bridge is selected for the inverter.
3. In the DC link, a capacitor and an inductor are used to maintain a constant voltage on the DC side, and isolate the interactions between rectifier and inverter.
4. The harmonics generated from the converters of the ER link are negligible because the rating of ER–filter is small compared to the main DC link.

5 .2 .2 SPECIAL FEATURES OF ENERGY RECOVERY FILTER

The operation of the rectifier in the ER–filter is different from the converter in a conventional HVDC link which has a constant sinusoidal voltage supply from the AC system[28]. The rectifier in the ER–filter has a near sinusoidal current supply instead of a sinusoidal voltage. So the rectifier operates as a current source rectifier. The simulated steady state current and voltage waveforms are shown in Fig. 5 .2 .

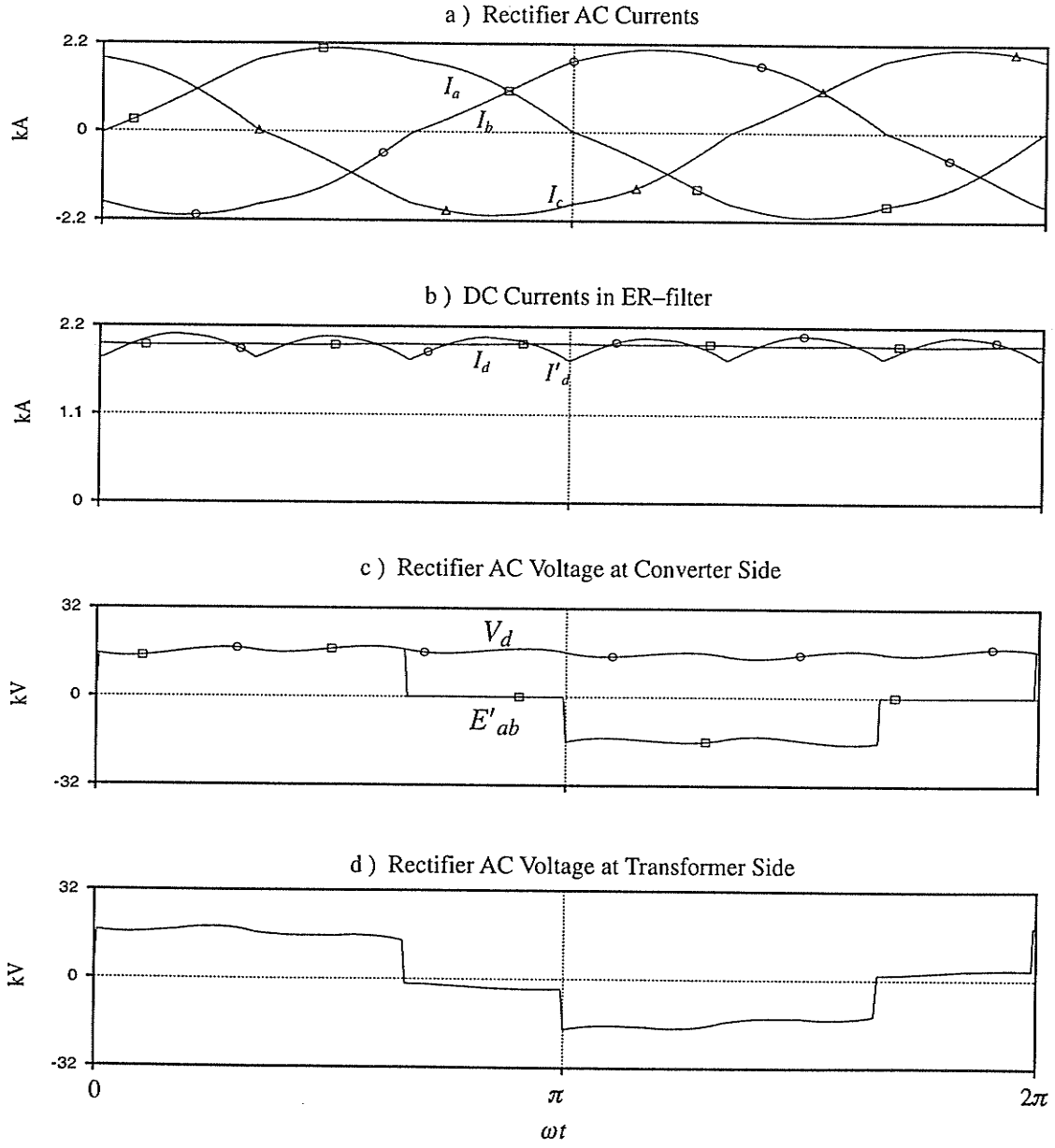

Figure 5 .2 : Steady State Waveforms in the ER–filter

The equivalent circuit of the rectifier in the ER–filter is as below:

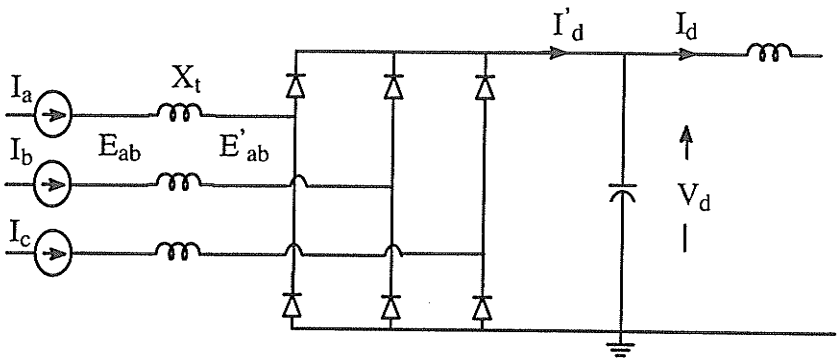

Figure 5 .3 : Equivalent Circuit of the Rectifier in the ER–link

5 .2 .3 RELATIONSHIPS IN THE CURRENT SOURCE CONVERTER

Developed below are some analytical relationships between various filter components that will be useful in the selection of filter components.

Assume that three phase AC currents are:

$$
\begin{aligned}
I_a\ (\ t\ ) &= I_m\ Sin\ (\ \omega t\ ) \\
I_b\ (\ t\ ) &= I_m\ Sin\ (\ \omega t - \frac{2}{3}\pi\ ) \\
I_c\ (\ t\ ) &= I_m\ Sin\ (\ \omega t + \frac{2}{3}\pi\ )
\end{aligned}
\qquad (5.1)
$$

where I_m is the rms value of the AC current

and the DC voltage V_d is constant provided by the capacitor.

Then the current on DC side I'_d is:

$$I'_d(t) = \begin{cases} -I_b & 0 \le \omega t < \frac{\pi}{3} \\ I_a & \frac{\pi}{3} \le \omega t < \frac{2\pi}{3} \\ -I_c & \frac{2\pi}{3} \le \omega t < \pi \\ I_b & \pi \le \omega t < \frac{4\pi}{3} \\ -I_a & \frac{4\pi}{3} \le \omega t < \frac{5\pi}{3} \\ I_c & \frac{5\pi}{3} \le \omega t < 2\pi \end{cases} \qquad (5.2)$$

and the average (DC component) of I'_d is:

$$I_d = \frac{3\sqrt{2}}{\pi} I_m \qquad (5.3)$$

The AC voltage of the rectifier is:

$$E'_{ab}(t) = \begin{cases} V_d & 0 \le \omega t < \frac{2\pi}{3} \\ 0 & \frac{2\pi}{3} \le \omega t < \pi \\ -V_d & \pi \le \omega t < \frac{5\pi}{3} \\ 0 & \frac{5\pi}{3} \le \omega t < 2\pi \end{cases} \qquad (5.4)$$

then the rms value of E'_{ab} is:

$$E_{rms} = \sqrt{\frac{2}{3}}\, V_d \qquad (5.5)$$

and the fundamental component of E'_{ab} is:

$$E_{fund} = \frac{\sqrt{6}}{\pi}\, V_d \qquad (5.6)$$

The rectifier AC voltage E_{ab} (including the drop on transformer leakage impedance) is:

$$E_{ab}(t) = E'_{ab}(t) + X_t(I_a(t) - I_b(t)) \qquad (5.7)$$

5.2.4 SELECTION OF COMPONENT VALUES FOR ER-FILTER

To make the ER–filter work the same as the 120 Hz tuned filter discussed in Chapter 4, the filter DC link should be operated to perform as the resistors in the tuned filter. That is:

- Filter DC link sending end L–L voltage as viewed from the filter must be the same as the voltage drop on the resistor in the tuned low Q filter (i.e. 68.35 kV l–l rms).
- The power rating of filter DC link must be the same as the power consumed in the filter resistor, i.e. 32.3 MW.

According to these data and the formula derived earlier, the rating of the ER–filter can be calculated. The rectifier is assumed to be a diode bridge and an extinction angle of 18^o is assumed at the inverter, the leakage impedance of converter transformers is chosen to be 18%. The DC link is operated at a suitable rating of 2 kA DC current.

The DC voltage of the ER–link:

$$V_d = \frac{MW}{I_d} = \frac{32.3MW}{2kA} = 16.15kV$$

According to (5.3), the AC current at rectifier

$$I_{mr} = \frac{\pi}{3\sqrt{2}} I_d = 1.481kA$$

Assume rectifier transformer rating of 35 MVA (leakage impedance X_{tr} is 0.957 Ω, 18% of the base impedance). According to (5.7), the L–L voltage at the sending end is:

$$E_r = \sqrt{\left(\frac{\sqrt{6}}{\pi} V_d\right)^2 + \left(X_{tr}\sqrt{3}\ I_{mr}\right)^2} = 12.86kV$$

The inverter is operated as a conventional converter, the AC current at inverter is:

$$I_{mi} = \sqrt{\frac{2}{3}} I_d = 1.633kA$$

Assume the inverter is operated in Constant Extinction Angle control ($\gamma = 18^{o}$) and the inverter transformer rating is 40 MVA (leakage impedance X_{ti} of 0.9 Ω, 18% of the base impedance), the L–L voltage can be calculated as:

$$V_i = \frac{V_d + \frac{3}{\pi} X_{ti} I_d}{\frac{3\sqrt{2}}{\pi} \cos\gamma} = 13.94kV \qquad (5.8)$$

The leakage impedance of rectifier converter transformer will affect the filter characteristic, because it acts as an inductor in series with the filter inductor. The inductance of the transformer can be calculated as below:

The base impedance of rectifier transformer is

$$Z_{base} = \frac{68.35kV^2}{35MVA} = 133.48\Omega$$

so , the actual impedance is

$$\omega L_T = X_{tr}(p.u.) * Z_{base} = 0.18 * 133.48 = 24.03\Omega$$

and the transformer leakage inductance is

$$L_T = \frac{24.03}{376.9} = 0.064H$$

and because of L_T, the actual series inductance needed in the filter is

$$L_f = 0.63 - 0.064 = 0.568H$$

Thus the designed values are summarized below and also shown on the diagram in Fig. 5 .1 .

DC Link:

Rated Power : 32.3 MW

DC voltage : 16.15 kV DC current : 2 kA

Capacitance = 50 μF Inductance = 0.2 H

Rectifier:

α order : Nil (Diode bridge operation)

Transformer rating: 35 MVA, 68.35 kV : 12.86 kV

Inverter:

$\gamma = 18^{o}$ (Constant Extinction Angle control)

Transformer rating: 40 MVA, 13.94 kV : 345 kV

5 .3 FREQUENCY RESPONSE OF THE SYSTEM WITH ER-FILTER

The rectifier impedance/frequency characteristic in the system with ER–filter is measured by frequency scanning method. Fig. 5 .4 shows the result:

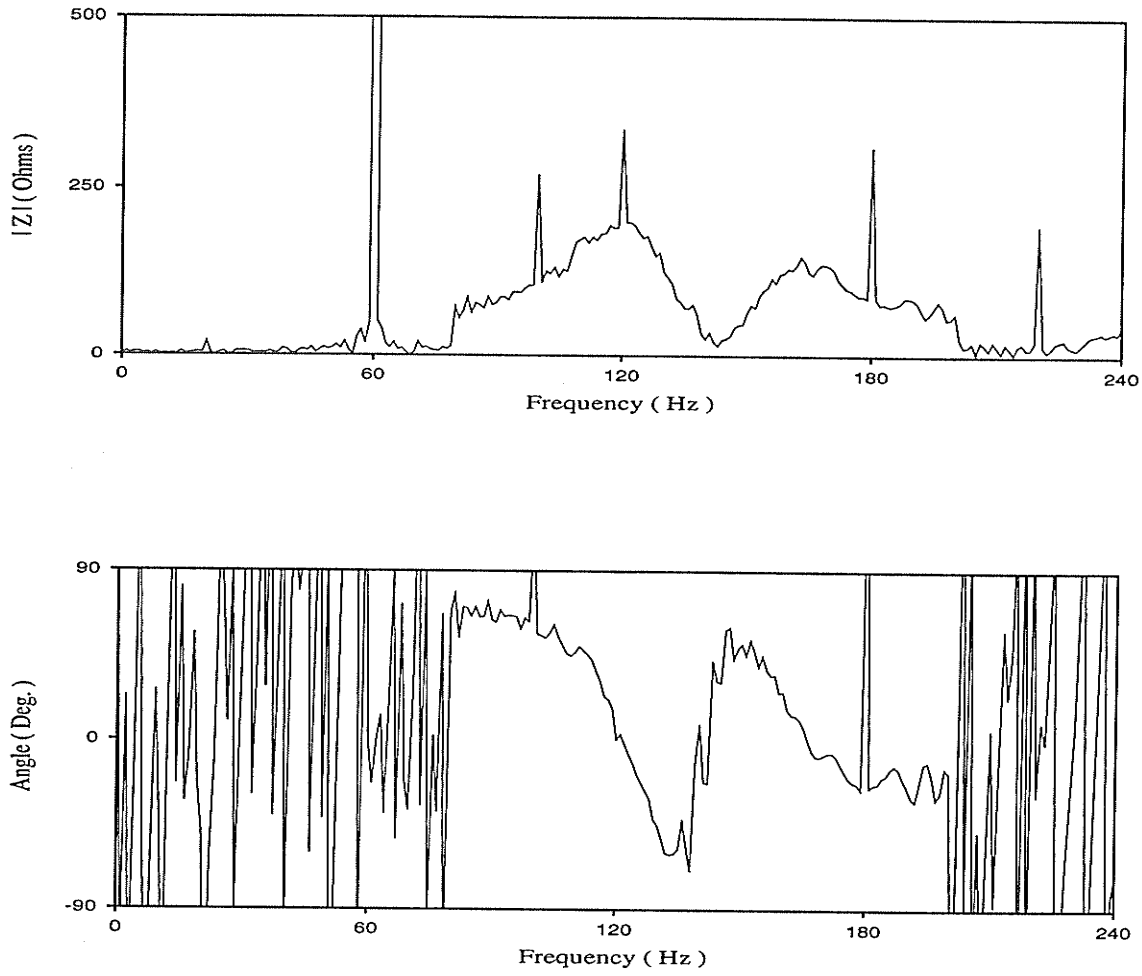

Figure 5 .4 : Measured Frequency Response of ER–filter by Frequency Scanning Method

The ER–filter is designed to have an equivalent quality factor Q of 3.3. The frequency response demonstrates good match with the conventional tuned filter of a quality factor of 3.3 (solid line in Fig. 4 .3). This proves the applicability of the ER–filter concept in tuning the filter.

5 .4 THE SYSTEM WITH ENERGY RECOVERY FILTER

To reduce the power losses in the tuned filter, the ER–filter is used to substitute for the tuned filter. The rectifier AC filter configuration thus is as in Fig. 5 .1 .

5 .4 .1 PERFORMANCE DURING START–UP AND STEADY STATE

A simulation of the start–up and steady state shows no buildup of oscillations in the system with the ER–filter. System performance is virtually identical to the system with the tuned filter of Q=3.3 (comparing the Fig. 5 .5 a with the Fig. 4 .4 a).

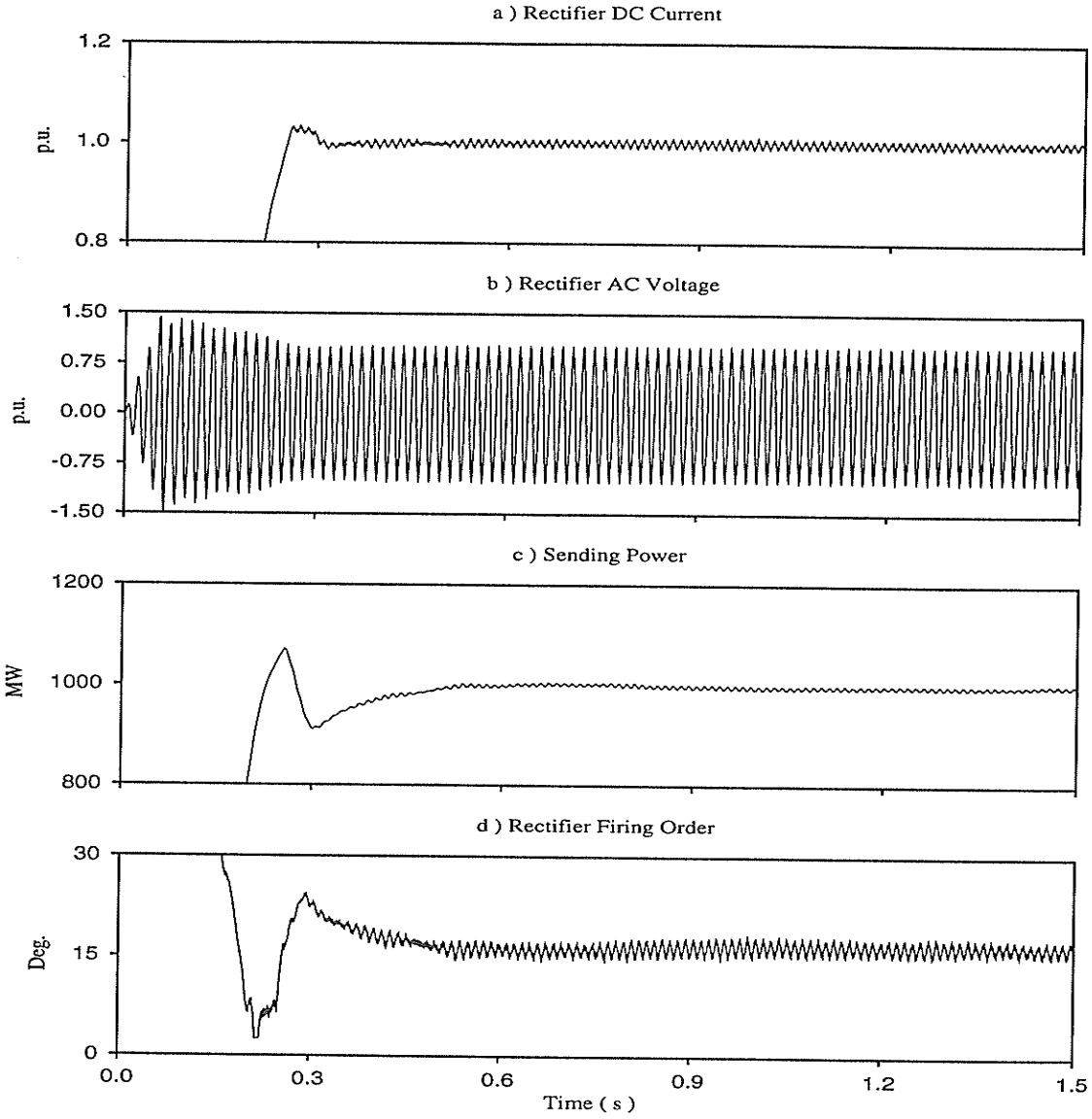

Figure 5 .5 (Continued): Start–up and Steady State in the System with ER–filter

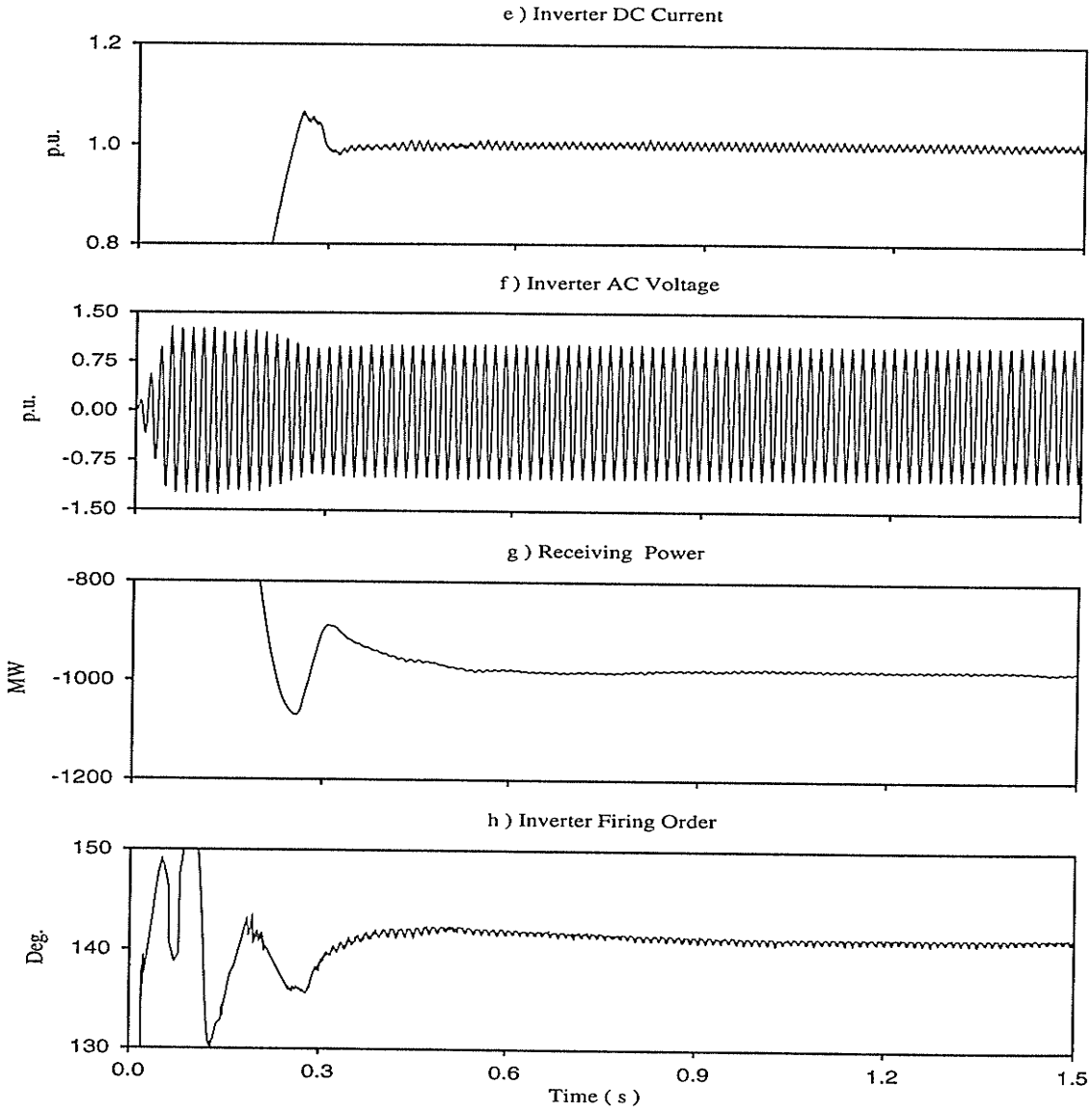

Figure 5 .5 (Concluded): Start–up and Steady State in the System with ER–filter

During the steady state, following facts can be observed:

- The DC current is significantly ripple free compared to that in the base system.
- The oscillation in active power at both ends is significantly reduced (< 2 MW).
- The oscillations in the α order of the rectifier and inverter are small (< 1°).

- The sending end AC power is 998 MW and the receiving end AC power is 977 MW. So the HVDC link power loss is 21 MW, which is close to the total power loss in the base case (20 MW). That means ER–filter does not consume any significant amount of power.

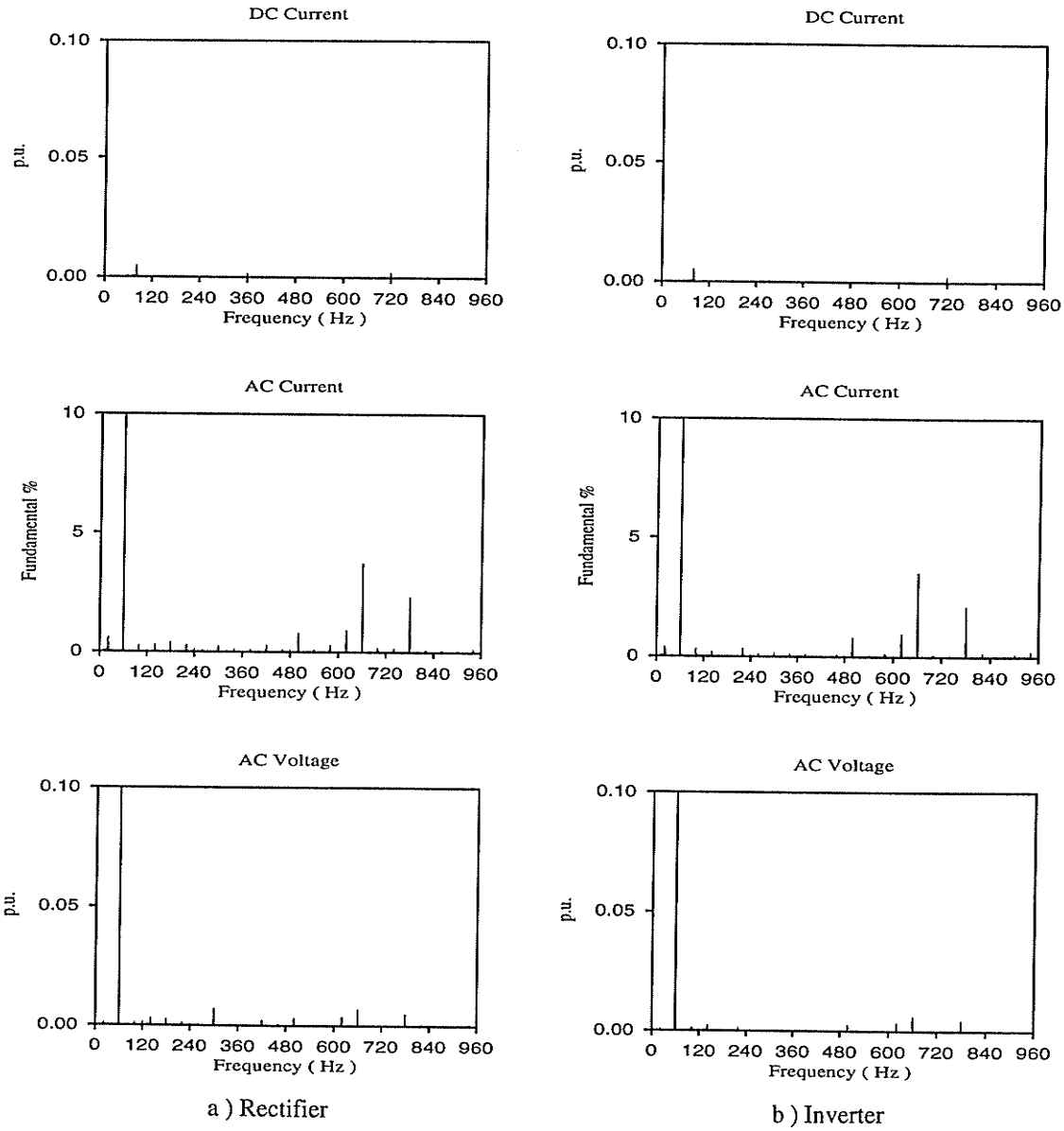

Figure 5 .6 : Fourier Analyses of the Waveforms in System with ER–filter

Fourier analyses of the steady state DC currents, converter currents and AC bus voltages are plotted in Fig. 5 .6 (This should be compared with Fig. 3 .3 of the base system). It can be seen that:

- The harmonic content in the DC current is much reduced.
- The converters inject mainly characteristic harmonics : 660 Hz (4 %) and 780 Hz (2.47 %), and a few of the non–characteristic harmonics.
- The injected harmonic currents do not produce high harmonic voltages (all less than 1% i.e. the individual harmonic limit) on the bus voltage.

5 .4 .2 PERFORMANCE DURING SYSTEM DISTURBANCE

In steady state, a single line–to–ground 3.5 cycle fault is applied on the phase A in rectifier AC bus at 0.05 seconds. Fig. 5 .7 shows the system recovery. The graphs should be compared with the Fig. 3 .4 which are for the base system.

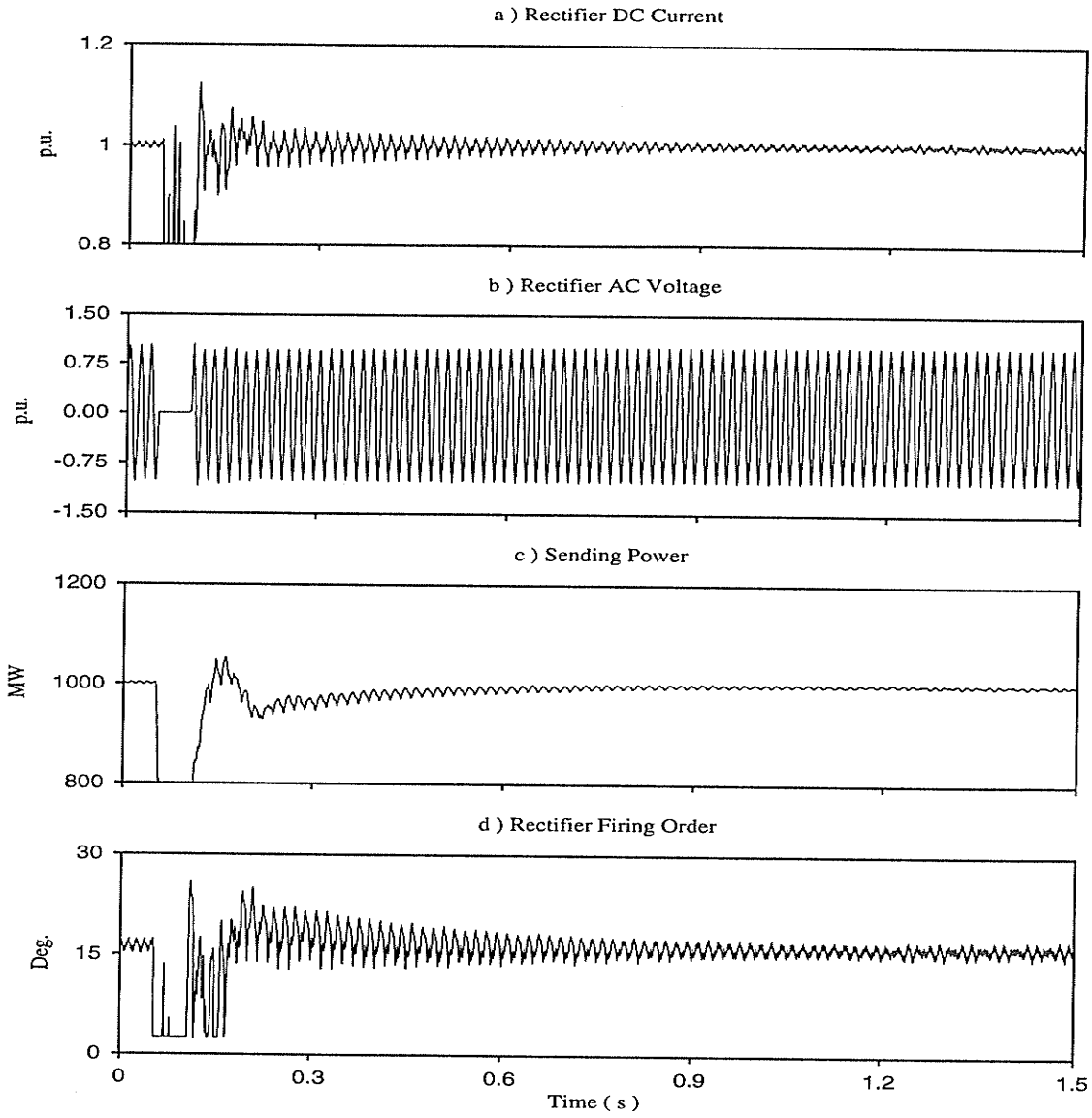

Figure 5 .7 (Continued): Single Line–to–Ground Fault Recovery in the System with ER–filter

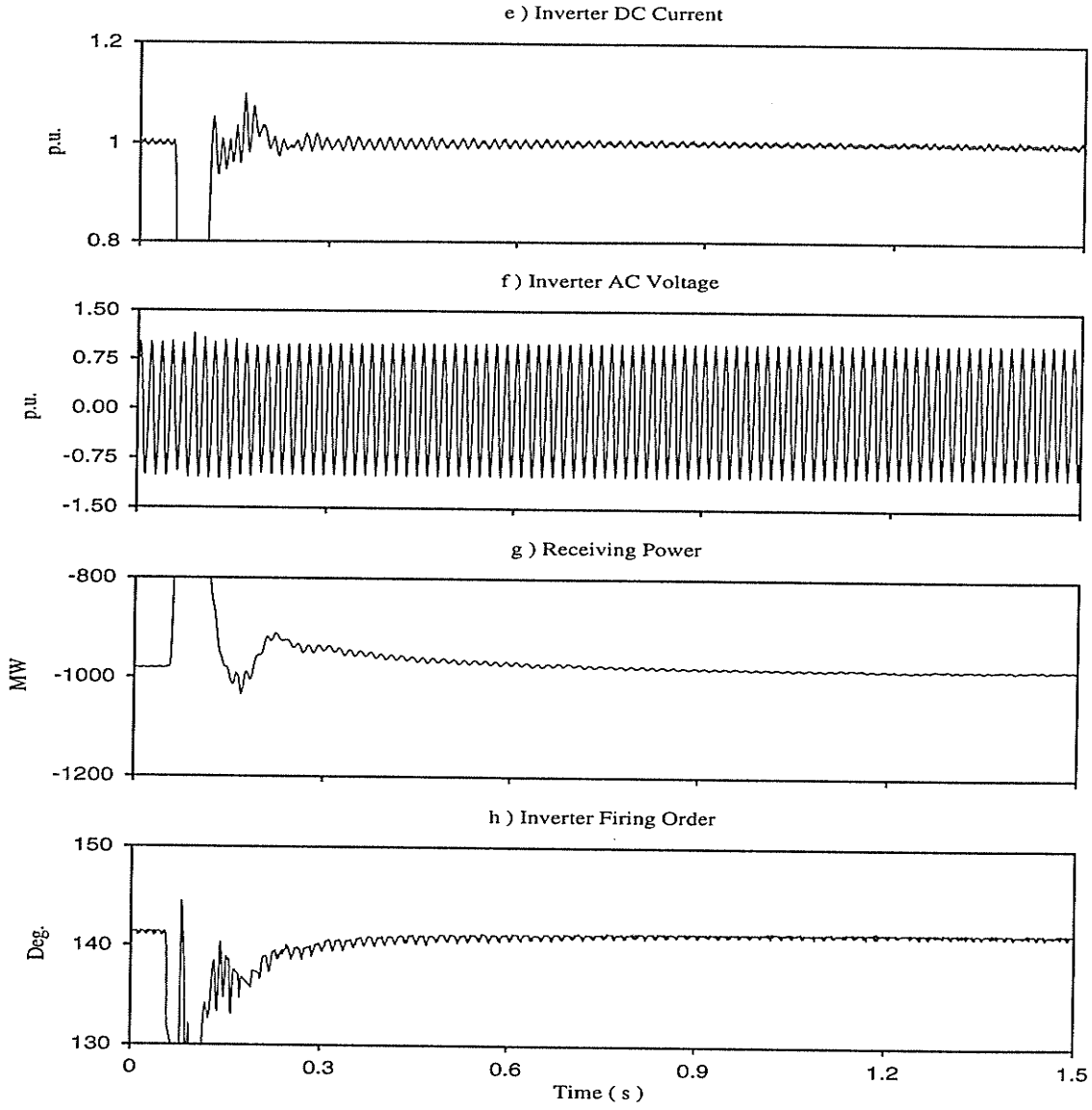

Figure 5 .7 (Concluded): Single Line–to–Ground Fault Recovery in the System with ER–filter

- The system recovery is much faster than the original system and similar to the system with tuned filter (see Fig. 3 .4 and Fig. 4 .4 b).
- There is no commutation failure in the inverter, nor any DC overcurrent.
- During system recovery, the DC currents have 60 Hz oscillations which decay quickly.

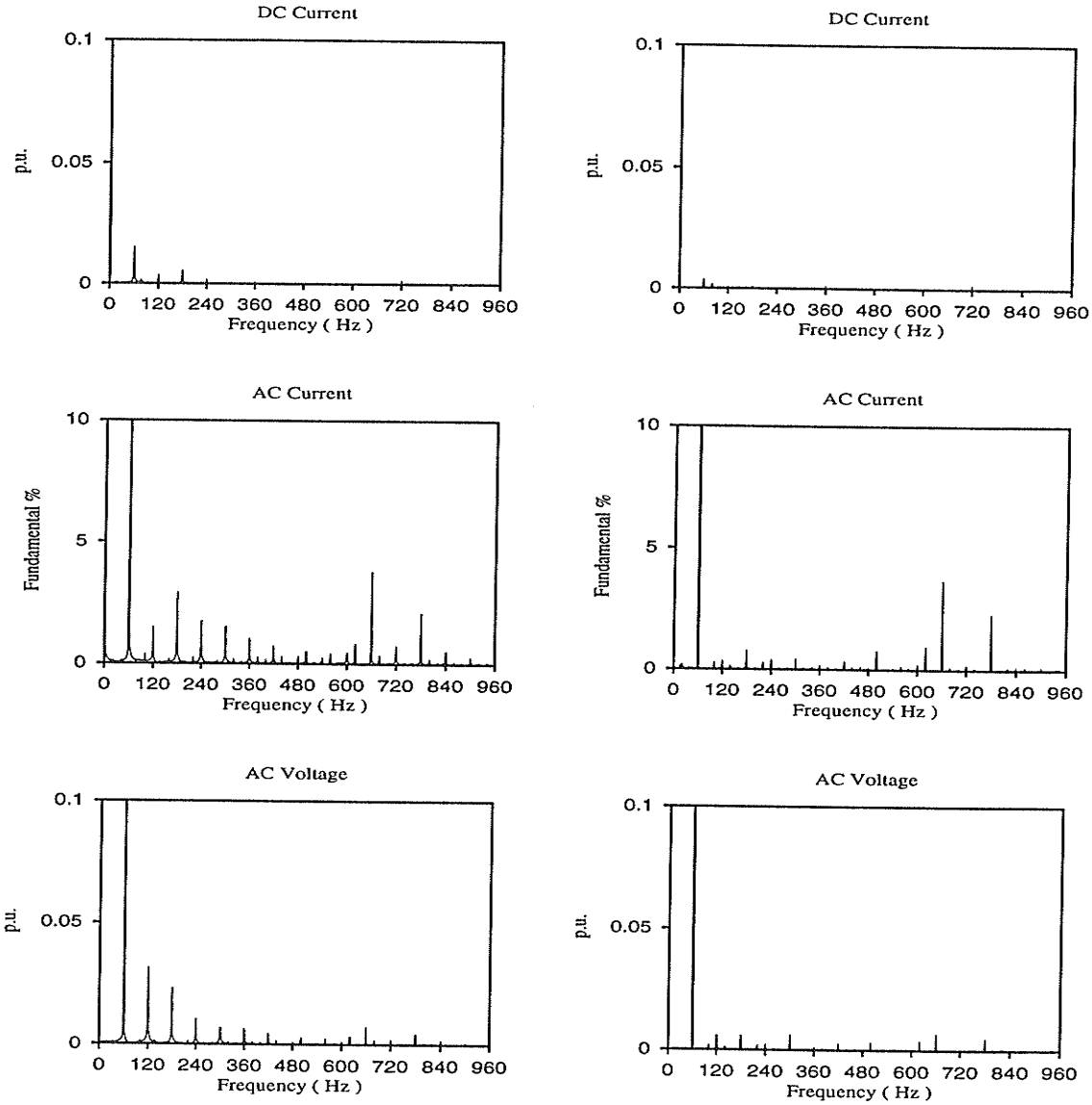

Figure 5 .8 : Fourier Analysis of the Wavforms during Fault Recovery

Fig. 5 .8 shows the Fourier analysis of the outputs at 0.25 and 1 seconds.

- The rectifier injects all the non–characteristic harmonics due to transformer saturation, the non–characteristic harmonics decay quickly with time as we compare the spectrum at 0.25 and 1 seconds.
- Harmonic voltages on bus voltage also decay quickly as harmonic currents decay.
- The DC current has a major 60 Hz component which also decays quickly with time.

A similar response is observed for the three line–to–ground fault. The rectifier DC current is plotted in Fig. 5 .11 b with the rectifier DC current during start–up and single line–to–ground fault recovery.

5 .5 ER–FILTER PERFORMANCE DURING FAULT RECOVERY

The ER–filter contains a small back–to–back HVDC system, its operation is also affected by the fault in the main HVDC system.

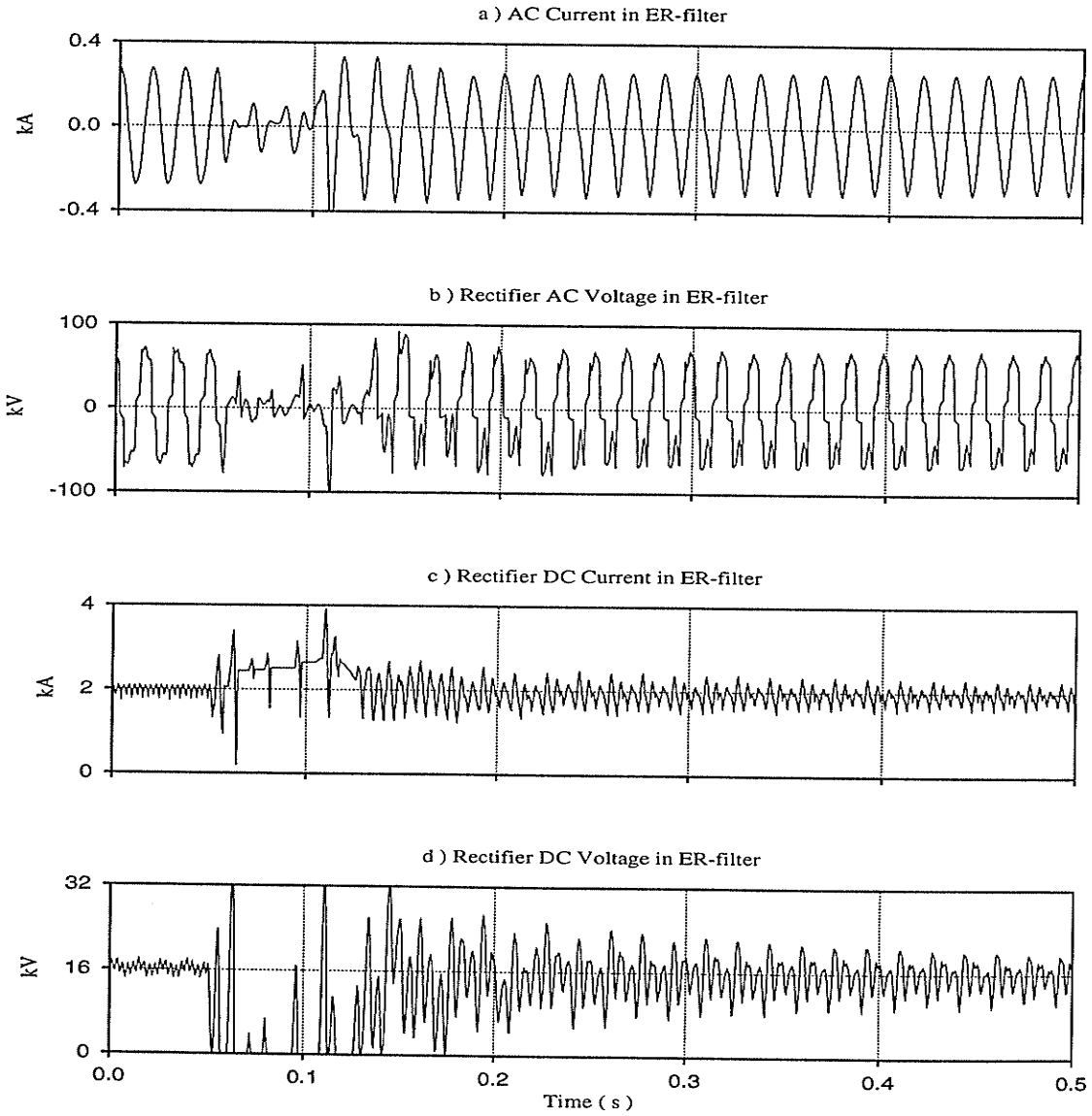

Figure 5 .9 (Continued): Waveforms in ER–filter during Main System Fault Recovery

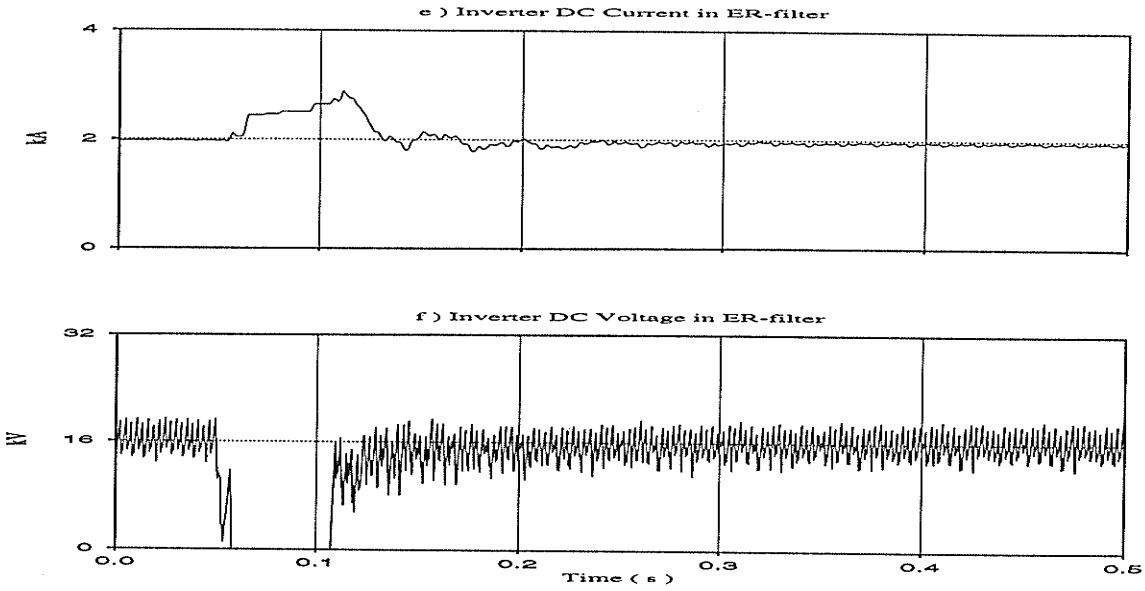

Figure 5 .9 (Concluded): Waveforms in ER–filter during Main System Fault Recovery

Fig. 5 .9 shows the waveforms in the ER–filter during the main system fault recovery. The ER–filter returns to normal operation shortly after the fault clears. During fault recovery, AC and DC quantities on the rectifier side are highly distorted (Figs. 5 .9 a, b, c & d) but the DC current and voltage on inverter side are almost unchanged due to the filtering of the link (Figs. 5 .9 e. & f).

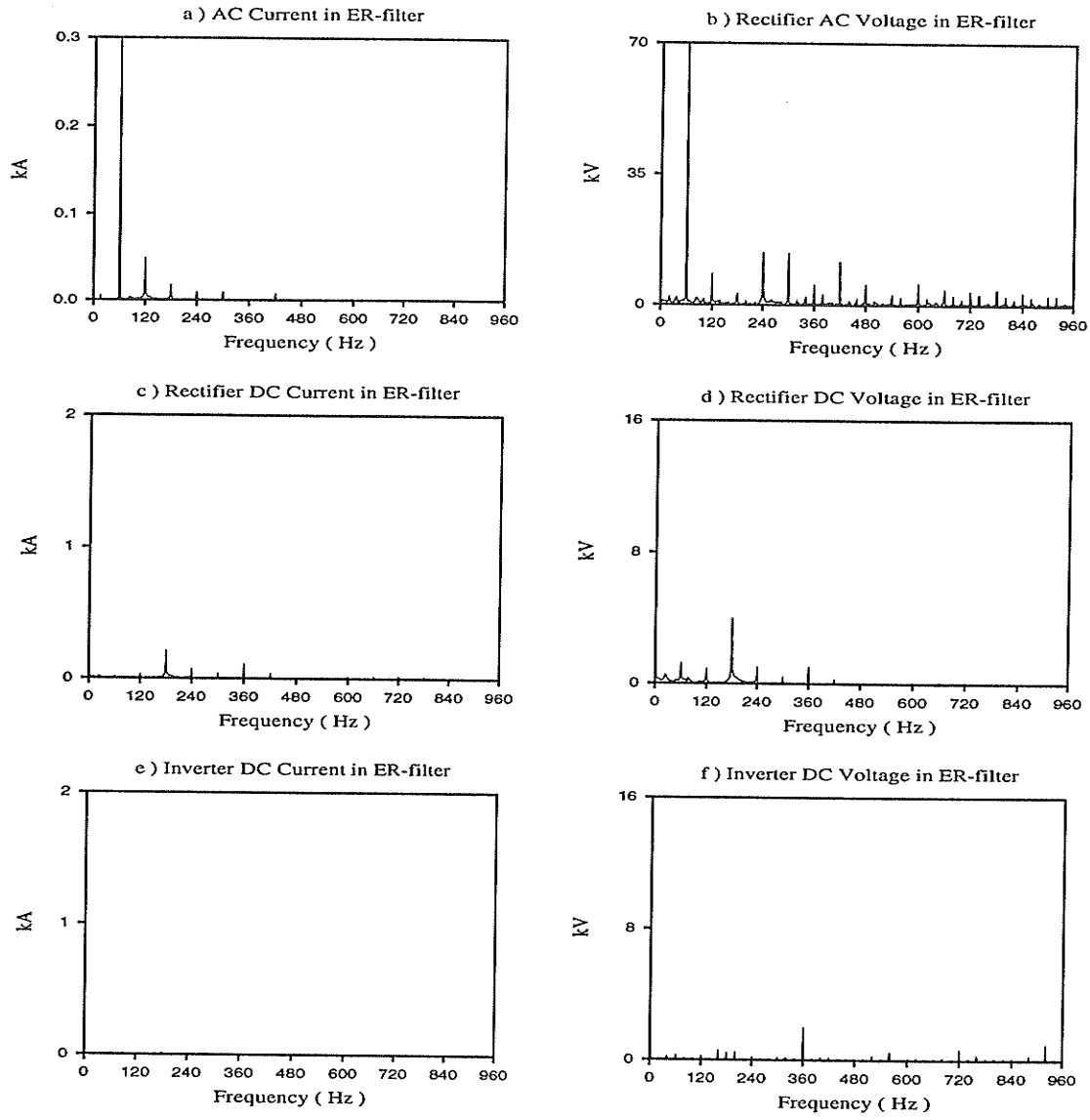

Figure 5 .10 : Fourier Analyses of the Waveforms in ER–filter during Fault Recovery

The Fourier analyses of the waveforms in the ER–filter during the main system fault recovery are plotted in Fig. 5 .10 . Notice the excessive distortion on the rectifier AC voltage. Also the filter AC current has a significant 2nd harmonic component shortly after the fault indicating that the filter is removing the 2nd harmonic current from the system. The 2nd harmonic on AC side is modulated into the 3rd and 1st harmonics on the DC side (see Figs. 5 .10 c & d), which are filtered out by the L and C components on the DC link in ER–filter (see Figs. 5 .10 e & f).

5 .6 SUMMARY

The Energy Recovery filter has been investigated in this chapter. The filter components were chosen from a steady state design, and the performance was investigated by using digital simulation. General performance of the system with an Energy Recovery filter is observed.

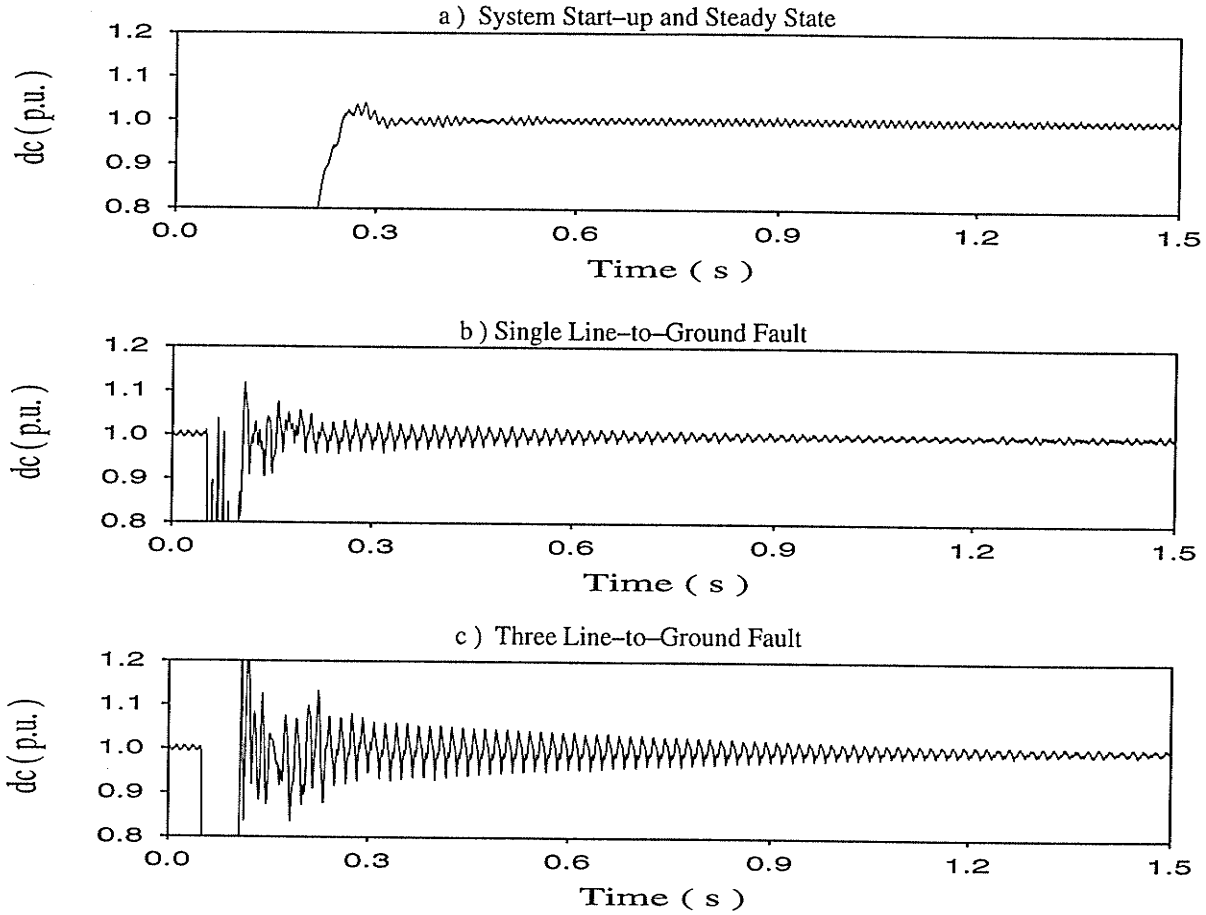

Figure 5 .11 : Rectifier DC Current in the System with an Energy Recovery Filter

The following conclusions are obtained:

1. The ER–filter solves the harmonic instability problems of the original system with much reduced losses.
2. The DC link in an ER–filter simulates the resistor in a conventional filter. The ER–filter recovers both fundamental and harmonic power losses and returns them to the AC system at fundamental frequency.

3. The fault tests indicate that the transient performance of the filter is satisfactory. The summarized results for the current response for three transient conditions: start–up, single phase and three phase faults are shown in Fig 5 .11 , which should be compared to Fig. 4 .4 and Fig. 3 .17 .

Chapter 6

Filter with Variable Quality Factor

6 .1 INTRODUCTION

In the Chapter 4.7, it is shown that a " Variable Q filter " on the AC bus could be used to provide good performance in different system situations. The " Variable Q filter " can be implemented by modifying the firing angle control of the inverter in the ER–filter[26].

6 .2 QUALITY FACTOR CONTROL OF THE ER–FILTER

We now investigate the feasibility of varying the quality factor of the energy recovery filter. It is known that the amount of the power flow through the ER–filter reflects the Q factor of the filter. The more the power flow in the filter, the lower the Q factor of the filter due to higher damping. So if the power flow in the ER–filter can be controlled, the Q factor of ER–filter is controllable.

6 .2 .1 THE RELATIONSHIP BETWEEN Q–FACTOR AND FIRING ANGLE

As the DC link in the ER–filter is operated at a constant DC current of 2 kA, changing the DC voltage of the ER–link will affect the power flow in the ER–filter and thus its Q factor. The DC voltage of the ER–link is determined by the firing angle (α) of the inverter. Thus the equivalent Q factor can be derived as shown below:

The inverter is operated as a conventional voltage source converter. Assume that the inverter has AC voltage of E_{lli}, transformer leakage impedance of X_{ci} and firing order of α, then the DC voltage of the ER–link is:

$$V_d(\alpha) = \frac{3\sqrt{2}}{\pi} E_{lli} \cos(180^o - \alpha) + \frac{3}{\pi} X_{ci} I_d \qquad (6.1)$$

The current I_d remains virtually constant due to the current source nature of the rectifier AC currents.

According to equations 5.6 and 5.3 in Chapter 5, the fundamental component of the l–l AC voltage at the rectifier is:

$$E_{llr}(\alpha) = \frac{\sqrt{6}}{\pi} V_d(\alpha) \qquad (6.2)$$

and the AC current at the rectifier:

$$I_m = \frac{\pi}{3\sqrt{2}} I_d \qquad (6.3)$$

Accordingly, the equivalent resistance of the ER–link is:

$$R_{eq}(\alpha) = \frac{E_{llr}(\alpha)}{\sqrt{3} I_m} = \frac{6}{\pi^2 I_d} V_d(\alpha) \qquad (6.4)$$

Then the Q factor of the ER–link is :

$$Q_{eq}(\alpha) = \frac{\sqrt{\frac{L}{C}}}{R_{eq}(\alpha)} \qquad (6.5)$$

For example in Fig 5 .1 , E_{lli}=13.94 kV, X_{ci}=18% and I_d=2 kA. The relationship between the quality factor of the ER–filter and α order of the inverter is plotted in Fig. 6 .1 .

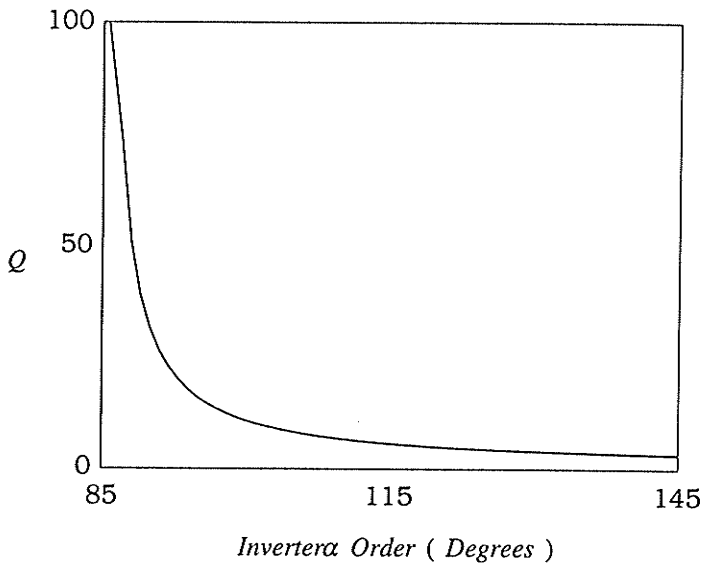

Figure 6 .1 : Equivalent Q Factor of the ER–filter vs. α Order

The ER–filter can operate at any Q factor by firing the inverter at corresponding angle α are seen in Fig. 6 .1 . For example, if a low Q factor (say Q=3.3) is required, an α order of 140° should be selected. And for α=85° at the inverter, a very high Q factor (Q>100) is obtained. It appears at first glance as though for α=85°, the inverter is operating in rectification region. This is however not true, because when the overlap angle is included, the power flow is still (slightly) into the AC system.

However, due to the CEA control and losses in the circuit elements, the equivalent Q factor can only be from 3.3 up to a certain value.

6 .2 .2 FREQUENCY RESPONSES OF ER–FILTER AT DIFFERENT α ORDER

The frequency responses of the ER–filter at different α order are measured by frequency scanning method. The results are shown in Fig. 6 .2 .

Since the α order of ER–filter corresponds to the equivalent Q factor of the filter (Fig. 6 .1), the frequency responses in Fig. 6 .2 should match the frequency responses of

the conventional tuned filter at different Q factor (Fig. 4 .3). The comparison shows a good match between the ER–filter of α=140° (solid line in Fig. 6 .2) and the tuned filter of Q=3.3 (solid line in Fig. 4 .3) and a reasonable match between the ER–filter of α=85° (dotted line in Fig. 6 .2) and the tuned filter of Q=100 (dotted line in Fig. 4 .3)

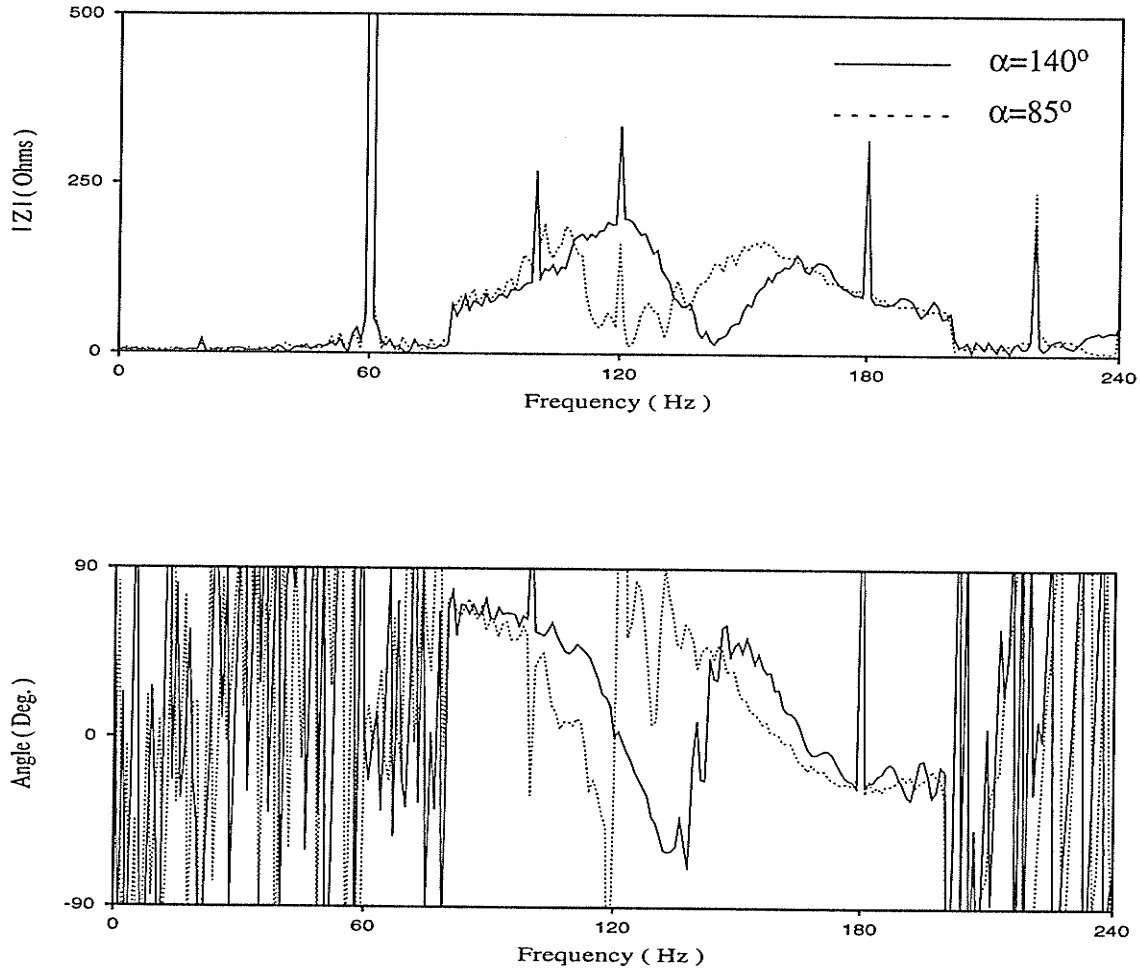

Figure 6 .2 : Frequency Responses of ER–filter at Different α Order

6 .2 .3 CONTROL MODIFICATIONS TO IMPLEMENT VARIABLE Q FILTER

Constant extinction angle control of the inverter in the ER–filter maintains an extinction angle of 18° to prevent commutation failure of the inverter. At normal operation, the inverter has an α order of about 140° which provides a DC voltage of 16.15 kV to give a power rating of 32.3 MW (equivalent Q=3.3). Reducing the α order of the inverter will

reduce the DC voltage provided by the inverter and will thus cause lower power flow through the filter and hence a high Q factor (Fig. 6 .1).

As discussed earlier, a low Q filter is desired to mitigate oscillations in the steady state and a high Q filter is required during fault conditions for better fault recovery. So the firing angle control of the inverter in the ER–link is modified as in Fig. 6 .3 . Note that the minimum select circuit ensures that the extinction angle controller's order is never exceeded and thus the extinction angle always remains at 18° or larger, so as to reduce the risk of commutation failure.

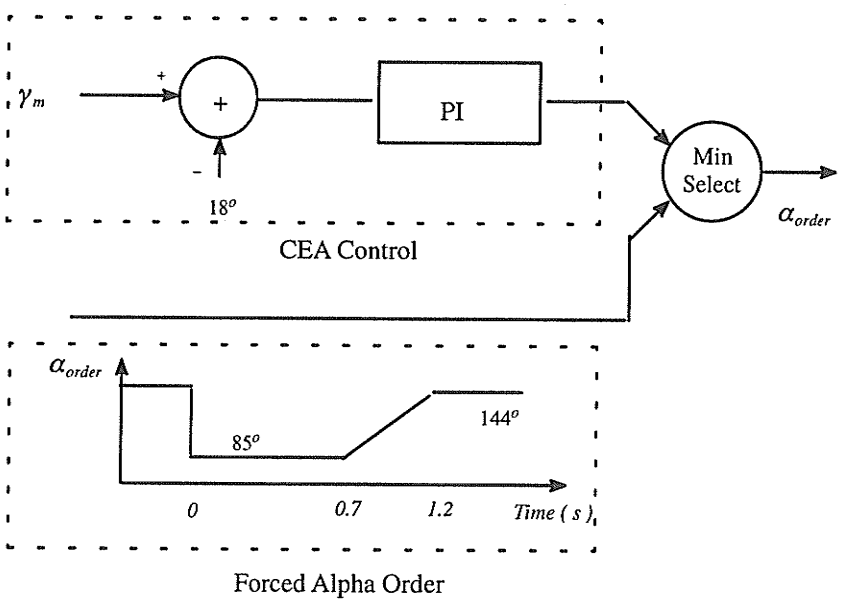

Figure 6 .3 : α Order Control of the Inverter in the ER–link

At the steady state, Constant Extinction Angle (CEA) control is selected to provide an equivalent Q of 3.3 for the ER–filter. During fault recovery, the α order is forced to 85° for 0.7 seconds and then ramped to 144° in 0.5 seconds (Fig. 6 .4 b). This gives a very small DC voltage during fault recovery (Fig. 6 .4 a) which means an equivalent high Q factor for the ER–filter. The forced α order is triggered by detecting undervoltage in any phase.

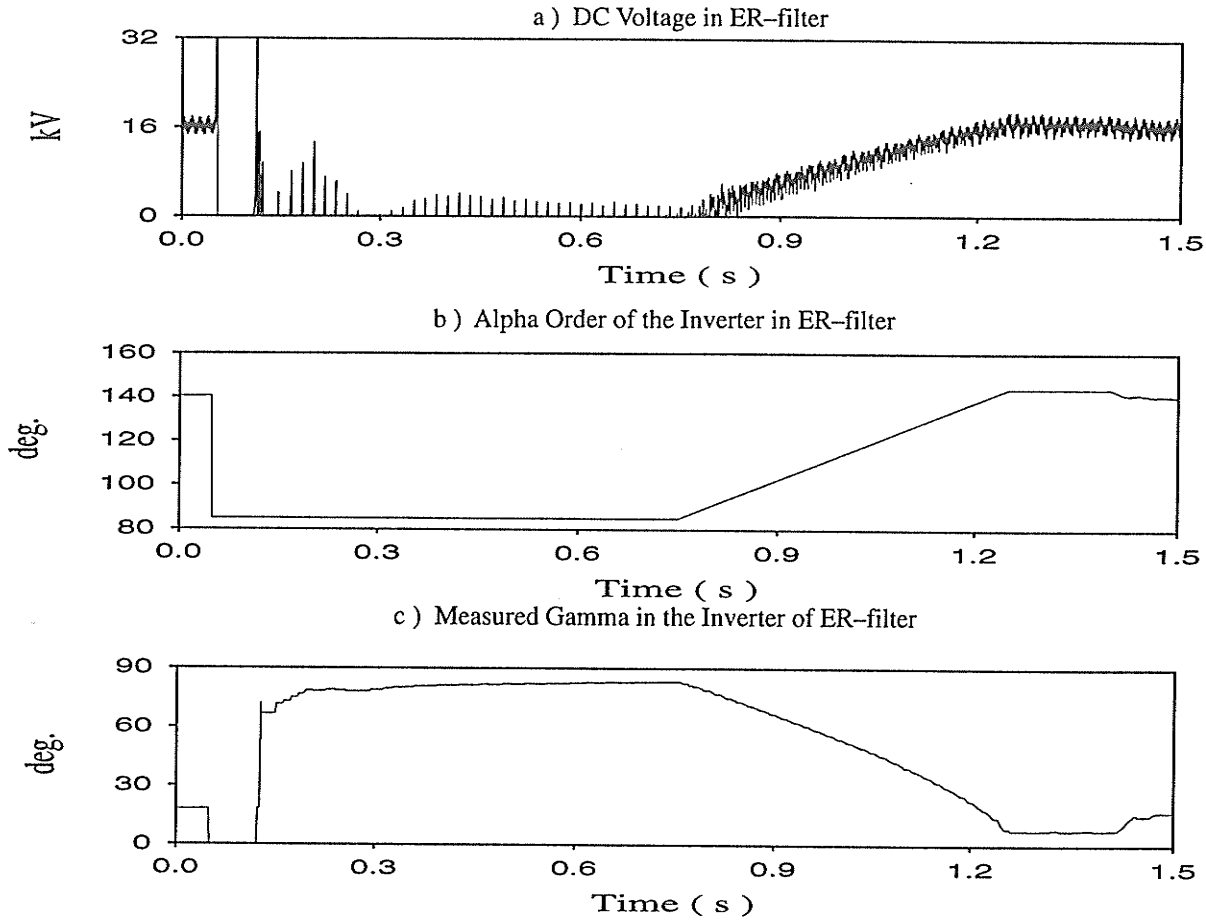

Figure 6 .4 : Controllable Q Filter Performance during Fault Recovery

6 .3 PERFORMANCE DURING SYSTEM DISTURBANCES

Shown in Fig. 6 .5 is the rectifier DC current during fault recovery in the system with the variable Q factor filter. It shows better recovery than the ER–filter with only CEA control in the inverter (Figs. 5 .11 b&c), where the harmonics in the rectifier DC current decay much slowly.

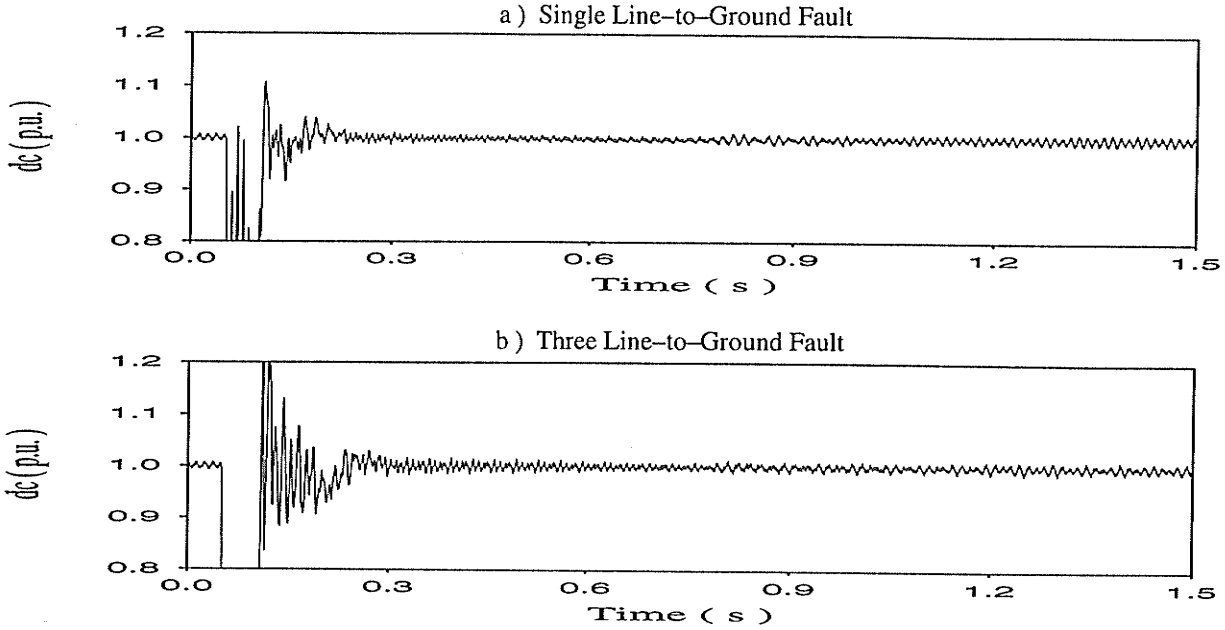

Figure 6 .5 : Fault Recovery of the System with Variable Q Filter

Note that the response is very similar to that of the system with the high Q tuned filter (Fig. 4 .5 b&c). This is corresponding to the fact that the variable Q filter has high a equivalent Q factor during fault recovery (from 0.05 second to 0.75 second). After that the α order of the inverter is ramped back to 144° in 0.5 second, which results in the variable Q filter returning from a high Q factor to a low Q factor. The integer harmonics (mainly 2nd) generated from the saturated transformer after the fault will decay in this time period. Changing the variable Q filter to a low Q factor will not affect the filtering performance to the 2nd harmonic in the main system because there is no 2nd harmonic in the system after the disturbance vanishes.

Since the CEA control (low Q factor) at the inverter is selected in the steady state, there are no steady state oscillations during normal operation. The results will be the same as the ER–filter case in Fig. 5 .5 .

In conclusion, the advantage of the variable Q filter is to combine the good features of high Q factor during fault recovery and low Q factor during steady state, which results in a solution for mitigating harmonic instabilities in all circumstances.

6 .4 VARIABLE Q FILTER PERFORMANCE DURING FAULT RECOVERY

Fig. 6 .6 shows the waveforms in the variable Q filter during main system fault recovery. Note that during the fault recovery, the voltages (AC and DC sides) are reduced by the forced alpha order but the currents (AC and DC sides) remain relatively constant due to the current source nature of the AC side infeed to the rectifier (The current is mainly determined by th L–C components of the ER–filter.

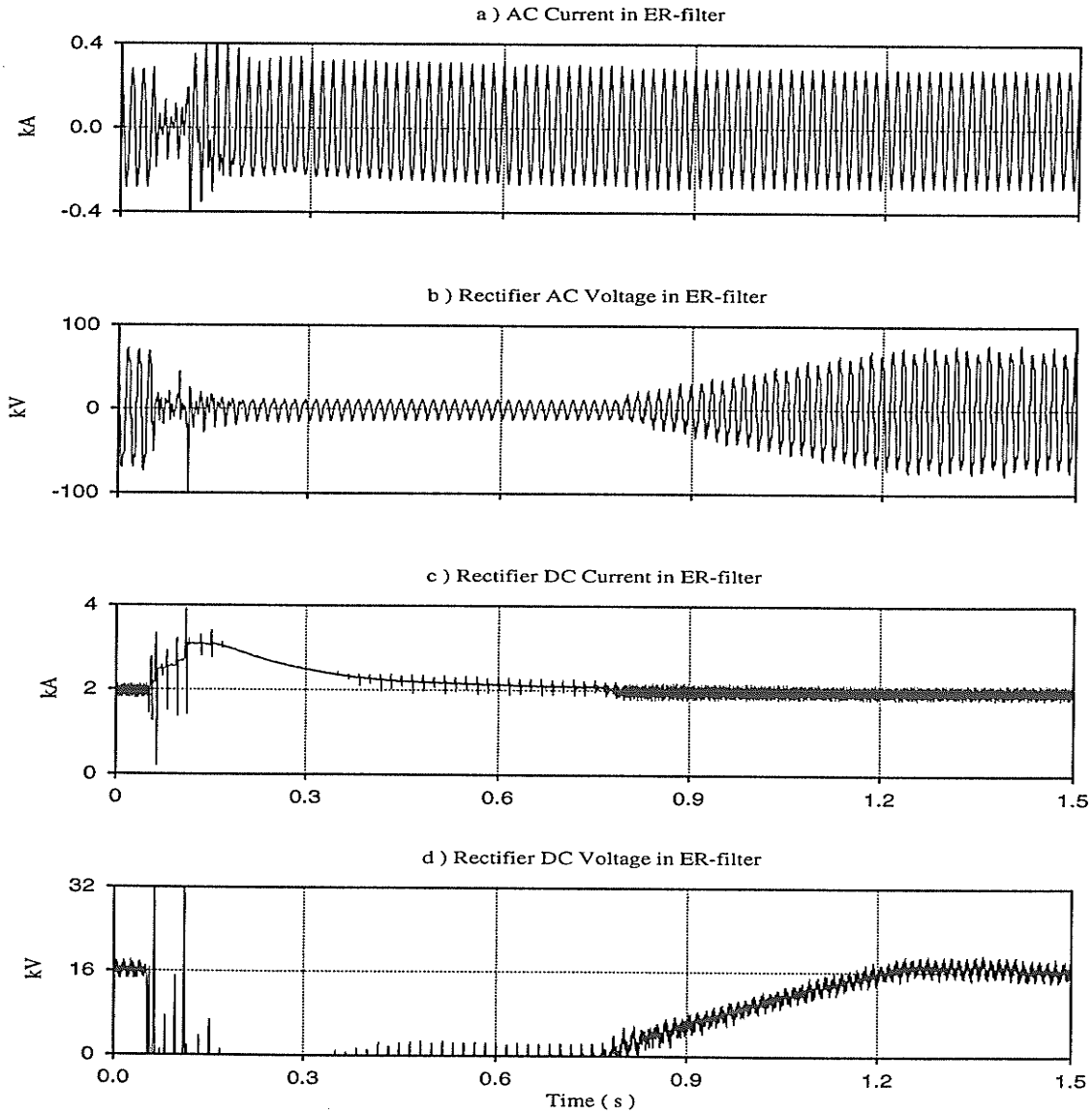

Figure 6 .6 : Waveforms in Variable Q Filter during Fault Recovery

Shown in Fig. 6 .7 is the Fourier analysis of the AC current and voltage in the variable Q filter. Note that the AC current in the ER–filter have fundamental and 2nd harmonic components. That is different from the case of the ER–filter (Fig. 5 .10 a) where more harmonic components (3rd, 4th, etc) are observed. This is because the variable Q filter (equivalent Q of 100 during fault recovery) is more sharply tuned to the 2nd harmonic than that of ER–filter (equivalent Q of 3.3).

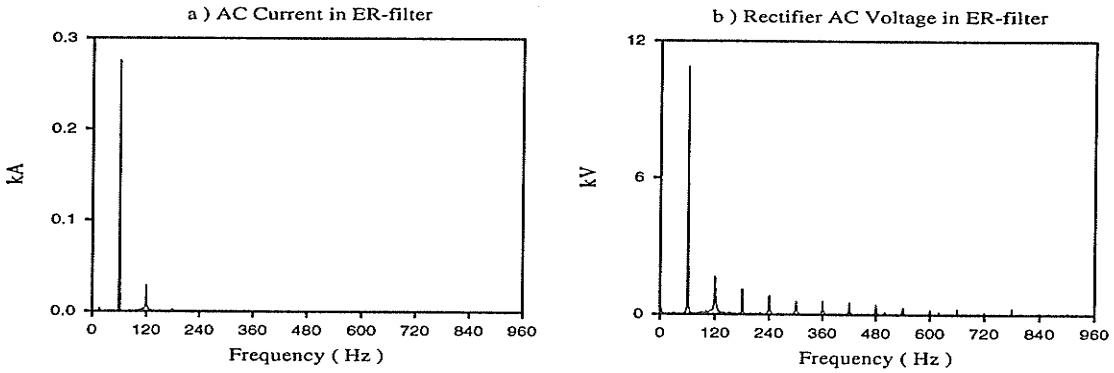

Figure 6 .7 : Fourier Analyses of the Waveform in Variable Q Filter during Fault Recovery

6 .5 SUMMARY

The variable Q filter can be implemented by adding an α order control in the inverter of ER–link. The relationship between the Q factor and firing angle α has been derived. During normal operation the Q factor is kept low thereby providing broadband damping. During faults when it is known that mainly 120 Hz current are excited, the filter switches to the high Q mode to quickly eliminate the oscillations. The simulations show successful operation of this concept. The following conclusions are obtained:

1. The variable Q filter allows operating at any desired Q factor by controlling the firing angle α.
2. This control action helps the system to damp out the oscillations quickly and return to normal operation faster.

3. The variable Q filter combines both advantages of the low Q factor during steady state operation and the high Q factor during fault recovery.

Chapter 7

Conclusions

7 .1 INTRODUCTION

In this thesis, the following contributions have been made:

1. Prediction of harmonic instabilities using the frequency scanning method.
2. Criteria in selecting filter for damping harmonic instabilities.
3. Component selection of an Energy Recovery filter.
4. Relationship between Q factor and α order in a ER–filter and the implementation of a variable Q filter.
5. Transient tests prove the efficiency of the ER–filter in various configurations and for various contingencies.

7 .2 THE COMPARISON OF DIFFERENT CASES IN STEADY STATE

Table 7 .1 is the data of the three cases in steady state (the steady state results in the system with a variable filter are the same as the ER–filter case, since the variable Q filter is set to the same Q factor (Q=3.3) as ER–filter in the normal operation). It shows that both the tuned filter and the ER–filter can eliminate harmonic instability. The performance is similar in steady state but the system with the tuned filter has much higher losses.

Table 7 .1 : The Steady State Feature of the Systems

	BASE SYSTEM	SYSTEM WITH TUNED FILTER	SYSTEM WITH ER–FILTER
DC CURRENT (REC.)	1. ± 0.038 P.U.	1. ± 0.002 P.U.	1. ± 0.008 P.U.
DC CURRENT (INV.)	1. ± 0.034 P.U.	1. ± 0.002 P.U.	1. ± 0.007 P.U.
α OSCILLATION (REC.)	5^o	$<0.5^o$	$< 1^o$
α OSCILLATION (INV.)	1.5^o	$<0.1^o$	$<0.2^o$
SENDING POWER	953 ± 20 MW	1040 ± 2 MW	998 ± 3 MW
RECEIVED POWER	933 ± 12 MW	987.5 ± 2 MW	977 ± 2 MW
POWER LOSSES	20 MW	52.5 MW	21 MW

To elaborate further, the frequency scanning method proved to be useful in defining the resonances in the highly nonlinear AC/DC system.

7 .3 THE COMPARISONS OF THE DIFFERENT CASES DURING TRANSIENTS

7 .3 .1 COMPARISON OF SYSTEM START–UP

Fig. 7 .1 shows the DC currents of three cases at system start–up (again the variable Q filter case is not shown here because it is the same as ER–filter). The results suggest that

- The systems start–up in about 0.4 second.
- The base system has much higher oscillations than other cases.
- The systems with the tuned filter and the ER–filter have similar performances, although both cases have a little oscillation, there are no harmonic instabilities in either case.

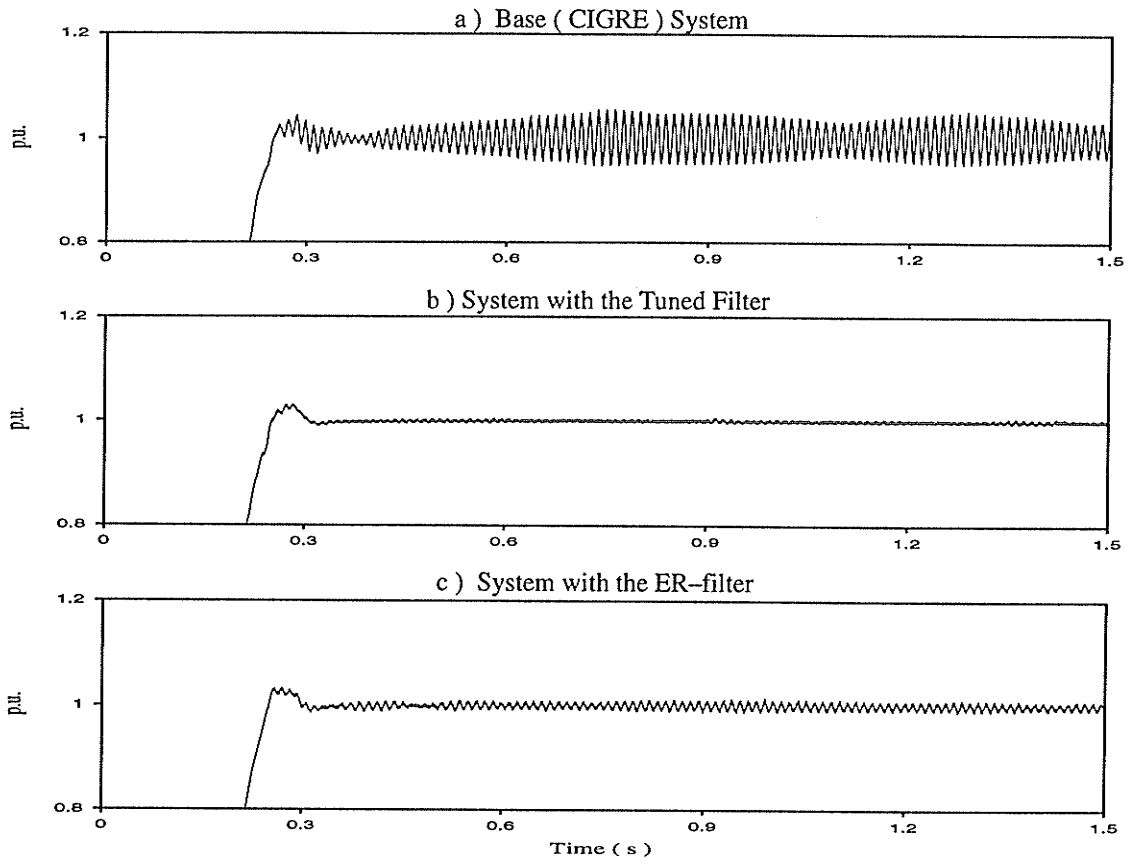

Figure 7 .1 : The DC Currents during System Start–up

7 .3 .2 COMPARISON OF SINGLE LINE–TO–GROUND FAULT RECOVERY

Fig. 7 .2 shows the DC currents of the four cases in a rectifier AC bus single line–to–ground 3.5 cycle fault recovery. The results suggest that:

- The system with filters (conventional tuned, Energy Recovery or variable Q filter) return to the pre–fault condition much faster than that in the base case.
- In the systems with the filters, the oscillations are much less than that in the base case, also the oscillations decay more quickly.
- In the base system, there is an overcurrent in the DC current due to the inverter failing commutation. There is no such event in the cases with filters.

- In the system with a variable Q filter, the system recovery (Fig. 7 .2 d) is better the that of the other two cases with filter (conventional filter Fig. 7 .2 b or ER–filter Fig. 7 .2 c)

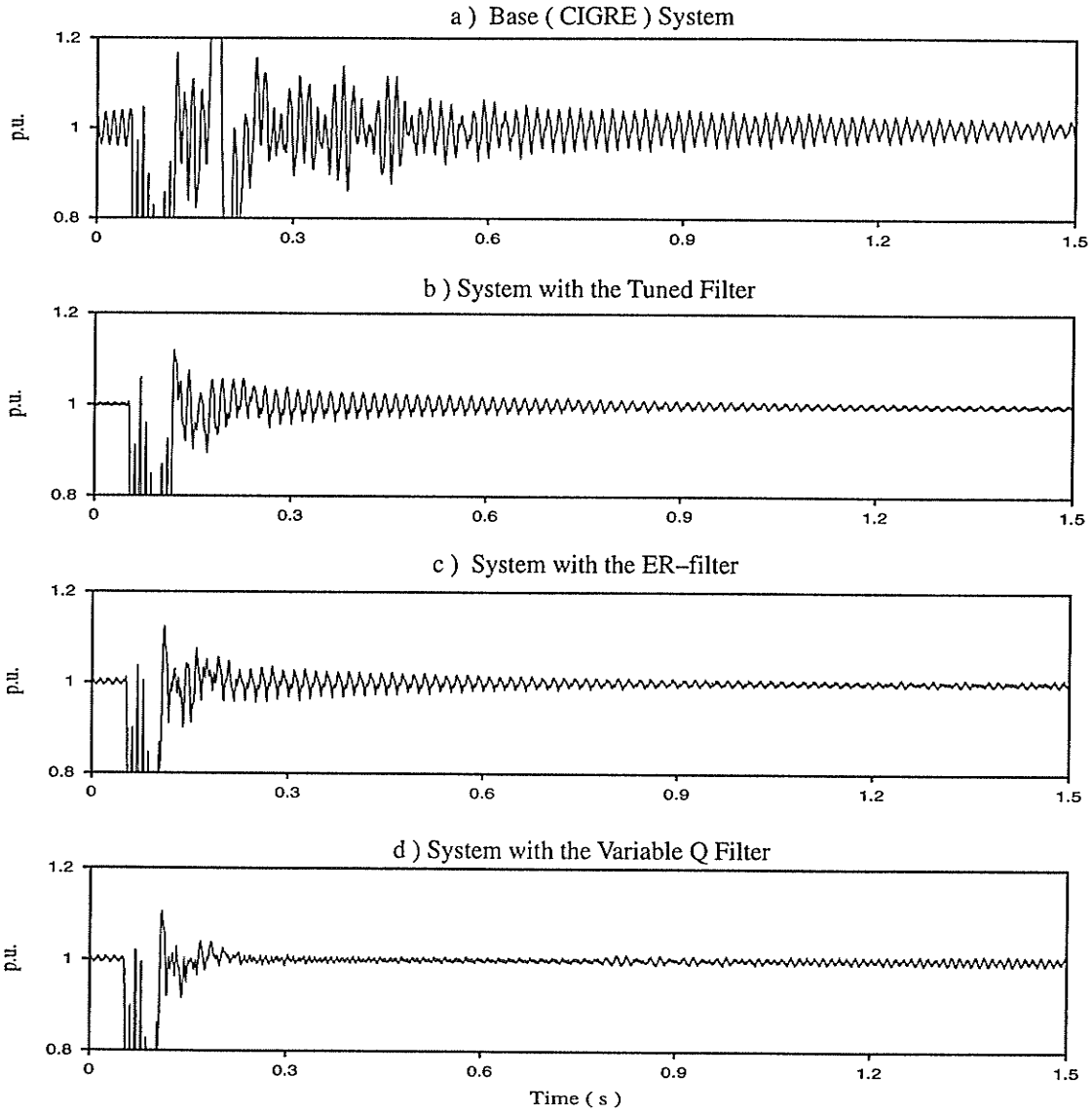

Figure 7 .2 : The DC Currents during Single Line–to–Ground Fault Recovery

7 .3 .3 COMPARISON OF THREE LINE–TO–GROUND FAULT RECOVERY

Similar phenomena are observed in the system recovery from a rectifier AC bus three line–to–ground fault recovery.

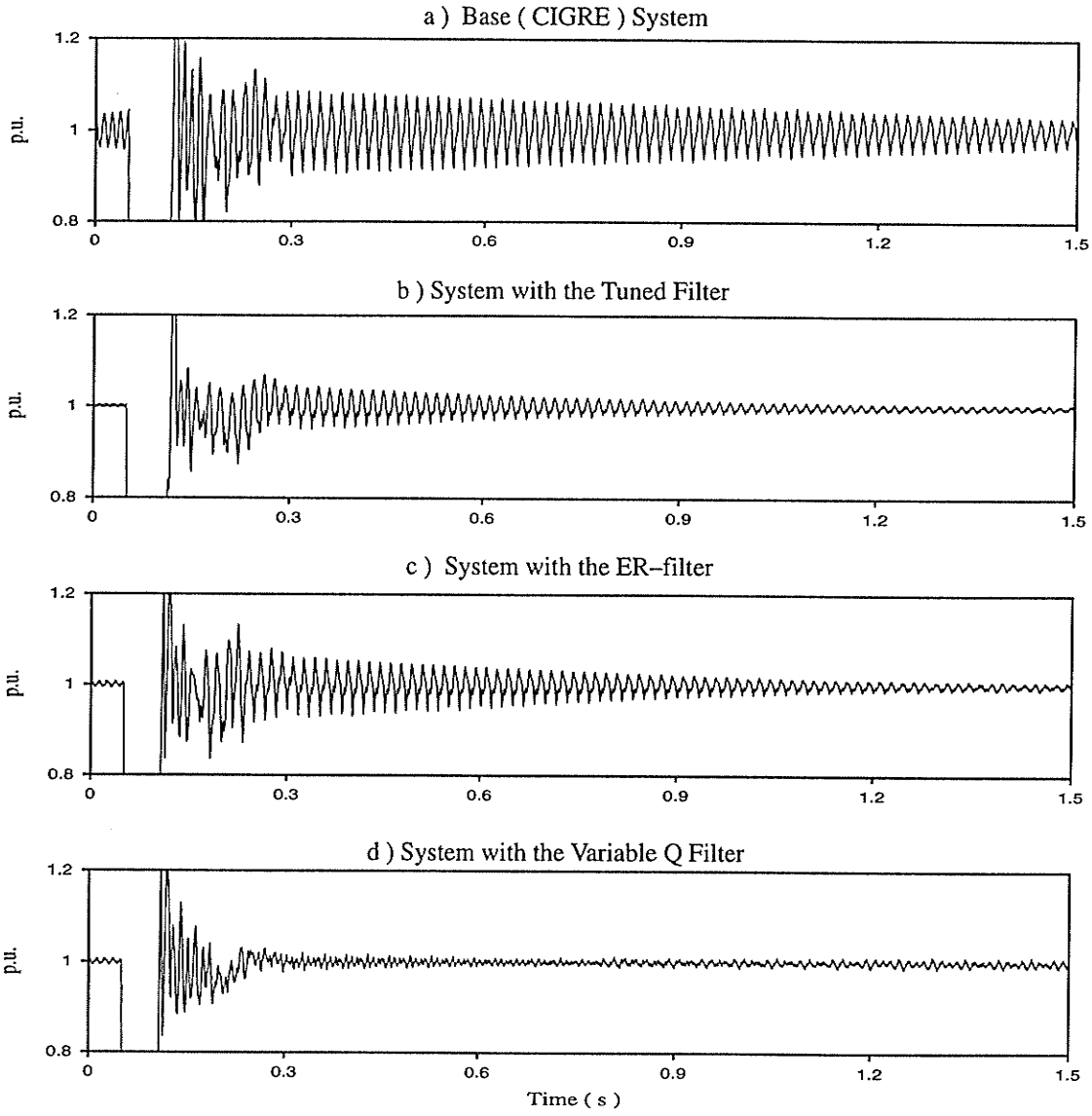

Figure 7 .3 : The DC Currents during Three Line–to–Ground Fault Recovery

7 .4 CONCLUSIONS

The simulation results in this thesis verify that an Energy Recovery type filter effectively emulates the conventional tuned filter. Installing the ER–filter (or Variable Q filter) solves the harmonic instabilities in the CIGRE system with significantly reduced power losses.

7 .5 FUTURE DIRECTIONS

The concept of Energy Recovery (or Variable quality factor) type filter may be extended to other filter topologies (such as high pass filter, C–type filter etc.) to recover the power losses in their resistors. Also, it may be possible to convert the ER damping type filter discussed here into one that also tunable. To achieve this, we may have to vary the complex part of the impedance (as opposed to merely the real part). This could be achieved by using thyristor or GTO devices in the rectifier. Adding firing angle control to the rectifier, we may change the phase difference between voltage and current and thus the equivalent impedance.

REFERENCES

[1] "Guide for Planning DC links Terminating at AC Locations Having Low Short–Circuit Capacities Part I : AC/DC Interaction Phenomena" CIGRE document, Dec., 1991.

[2] CIGRE working group 03 of study committee 14 , "A.C. Harmonic Filter and Reactive Compensation for HVDC" , Electra, Vol. 63, December 1979, pp 65 – 102.

[3] CIGRE working group 03 of study committee 14 , "A.C. Harmonic Filter and Reactive Compensation for HVDC with Particular Reference to Non–characteristic Harmonics", CIGRE Technical Brochure

[4] A. Gavrilovic, "AC/DC System Strength as Indicated by Short Circuit Ratios", IEE Fifth International Conference on AC and DC Power Transmission, London, September 1991, pp 27 – 32.

[5] J.D. Ainsworth, "Harmonic Instability between Controlled Static Convertors and A.C. Network", Proc. IEE, Vol. 114, No. 7, 1967, pp 949–957

[6] A.G. Phadke and J.H. Harlow, "Generation of Abnormal Harmonics in High–Voltage AC–DC Power Systems", IEEE Trans. on Power Apparatus and Systems, Vol. PAS–87, No. 3, Mar. 1968, pp 873–883

[7] J. Reeve, and P.C.S. Krishnayya, "Unusual Current Harmonics Arising from High–Voltage DC Transmission", IEEE Trans. on Power Apparatus and Systems, Vol. PAS–87, No. 3, Mar. 1968, pp 883–890

[8] J. Reeve, J. A. Baron and P.C.S. Krishnayya, "A General Approach to Harmonic Current Generation by HVDC Converters", IEEE Trans. on Power Apparatus and Systems, Vol. PAS–88, No. 7, July 1969, pp 989–995

[9] J.D. Ainsworth, "The Phase–Locked Oscillator – A New Control System for Controlled Stratic Convretors", IEEE Trans. on Power Apparatus and Systems, Vol. PAS–87, No. 3, March 1968, pp 859–865

[10] P.S. Bodger, G.D. Irwin and D.A. Woodford, "Controlling Harmonic Instablity of HVDC Links Connected to Weak Systems" , IEEE Trans. on Power Delivery, Vol. 5, No. 4, November 1990, pp 2039–2046

[11] N. Kaul and R.M. Mathur, "Solution to the Problem of Low Order Harmoniic Resonance fron HVDC Converters", IEEE Trans. on Power Delivery, Vol. 5, No. 4, November 1990, pp 1160–1167

[12] N. Kaul and etc."Low Order Harmonic Resonance from HVDC Concerters", Proc. of 6th National Conference, India, June, 1990, pp 17–24

[13] J.P. Bowles, "Overvoltages in HVDC Transmission Systems Caused by Transformer Magnetizing Inrush Currents" IEEE Trans. on Power Apparatus and Systems, Vol. PAS–93, No. 2, pp 487–495, Mar./April 1974.

[14] J.P. Bowles,"Alternative Techniques and Optimization of Voltage and Reactive Power Control at HVDC Converter stations", IEEE Conference on "Overvoltage and Compensation on Integrated AC–DC Systems", Winnipeg, 1980, pp 5a–5i

[15] C.V. Thio and etc.,"Switching Overvoltages on the Nelson River HVDC System – Studies, Experence and Field Tests", IEEE Conference on "Overvoltage and Compensation on Integrated AC–DC Systems", Winnipeg, 1980, pp 15–26

[16] F.A. Farret and L.L. Freris, "Minimisation of uncharacteristic harmonics in HVDC convertors through firing angle modulation", IEE Proc, Vol. 137, Pt. C, No. 1, Jan. 1990

[17] J. Reeve and J.A. Baron,"Harmonic Interaction between HVDC Converters and AC Power Systems", IEEE Trans. on Power Apparatus and Systems, Vol. PAS–90, No. 3, March 1971, pp 2785–2793

[18] D.B. Giesner and J. Arrillaga, "Behaviour of h.v.d.c. links under Balanced–a.c.–fault Conditions", Proc. IEE, Vol. 118, No. 3/4, Mar./April 1971, pp 591–599

[19] D.B. Giesner and J. Arrillaga, "Behaviour of h.v.d.c. links under Unbalanced–a.c.–fault Conditions", Proc. IEE, Vol. 119, No. 2, Feb. 1972, pp 209–215

[20] R. Yacamini and J.C. de Oliveira, "Instability in h.v.d.c. Schemes at Low–order integer Harmonics", IEE Proc., Vol. 127, Pt. C, No. 3, May 1980, pp 179–188

[21] A.E. Hammad, "Analysis of Second harmonic Instability for Chateauguay HVDC/SVC Scheme", IEEE Trans. on Power Delivery, Vol. 7, No. 1, Jan., 1992

[22] C. Wong and etc.,"Feasibility Study of AC– and DC–Side Active Filters for HVDC Converter Terminals", IEEE Trans. on Power Delivery, Vol. 4, No. 4, October 1990, pp 2067–2075

[23] X. Jiang and A. Gole," Mitigating Harmonic Instabilities in HVDC System with Energy Recovery Filter ", Accepted by the International Conference on Power System Technology, October 18–21, 1994, Beijing, China.

[24] X. Jiang and A. Gole," An Energy Recovery Filter for HVDC Systems ", IEEE Trans. on Power Delivery, Vol. 9, No. 1, January 1994, pp 119–127.

[25] X. Jiang and A. Gole," Energy Recovery Filter for Damping AC System Resonance ", International Power Engineering Conference 1993, Mar. 18–19 1993, Singapore, pp 55–60.

[26] X. Jiang and A. Gole," Energy Recovery Filter with Variable Quality Factor ", 1994 IEEE PES Winter Meeting (94 WM 063–8 PWRD), Jan. 30–Feb. 4, 1994, New York, New York, U.S.A, to be published in IEEE PES Transaction.

[27] "CIGRE Benchmark Model for DC Controls", Electra, Vol. 135, April 1991, pp 54 – 73.

[28] E.W. Kimbark" *Direct Current Transmission* ", Volume 1, John Wiley & Sons, 1971.

[29] "*EMTDC User's Manual*", Version 3, Manitoba HVDC Research Centre, Winnipeg, Canada, 1988.

Appendix

PSCAD/EMTDC draft files for CIGRE benchmark Model

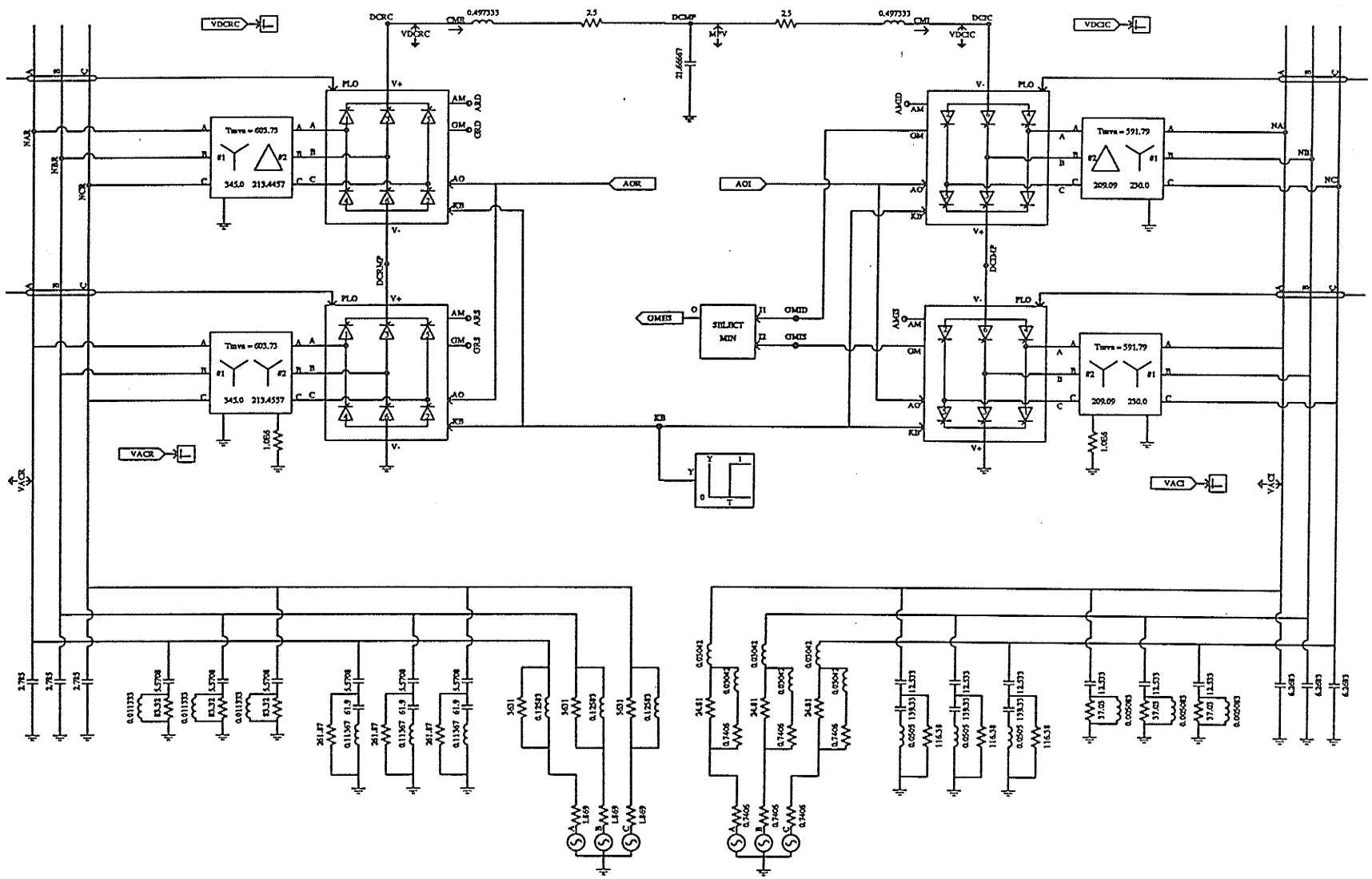

University of Manitoba, EE Dept. *Cigre Benchmark Model*	Last Modified: March 24, 1994 (xjiang) Printed On: March 24, 1994 (xjiang)	*Main System* Subsystem #1 of 3

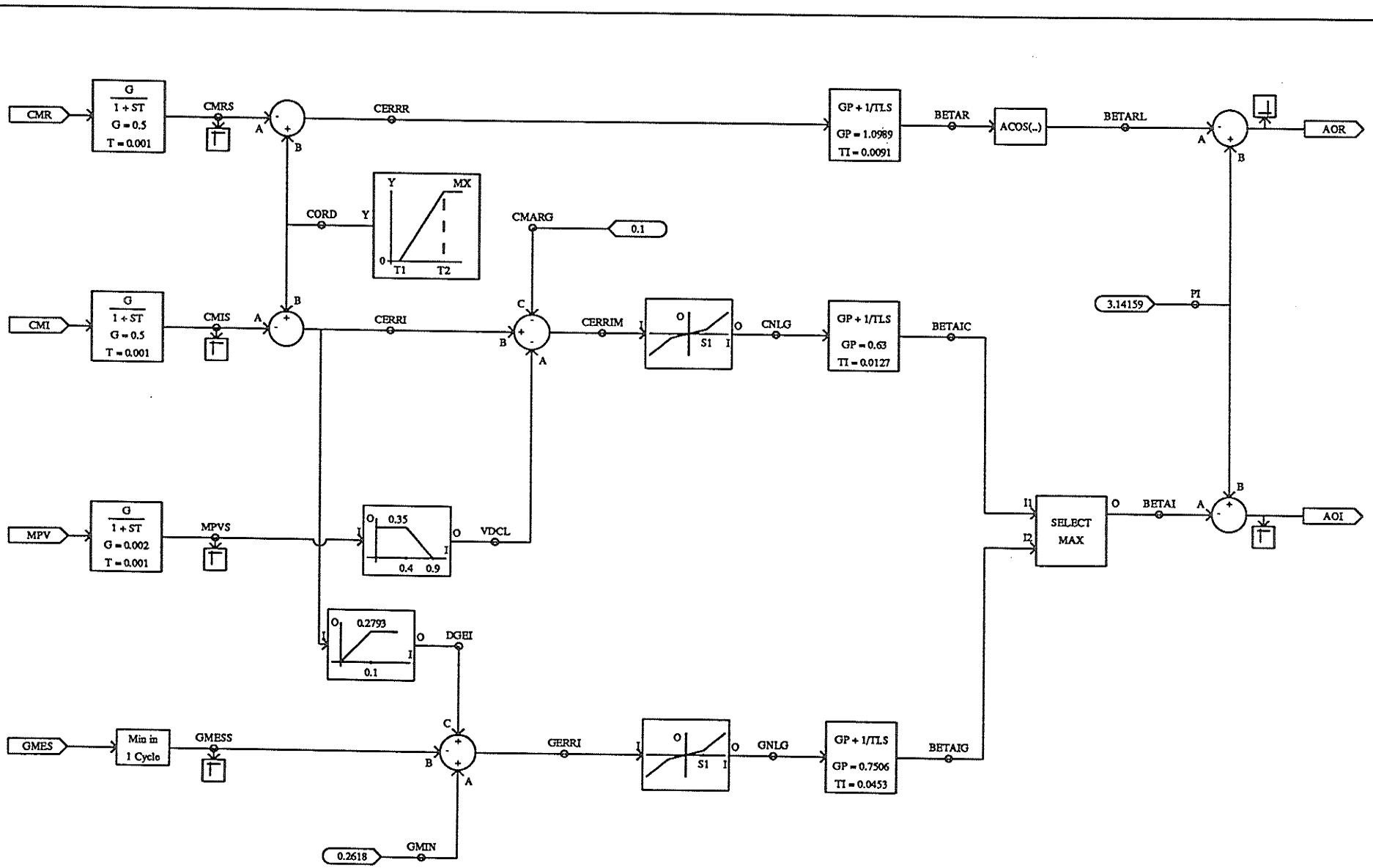

University of Manitoba, EE Dept. *Cigre Benchmark Model*	Last Modified: March 23, 1994 (xjiang) Printed On: March 29, 1994 (xjiang)	*Controls for Main System* Subsystem #2 of 3

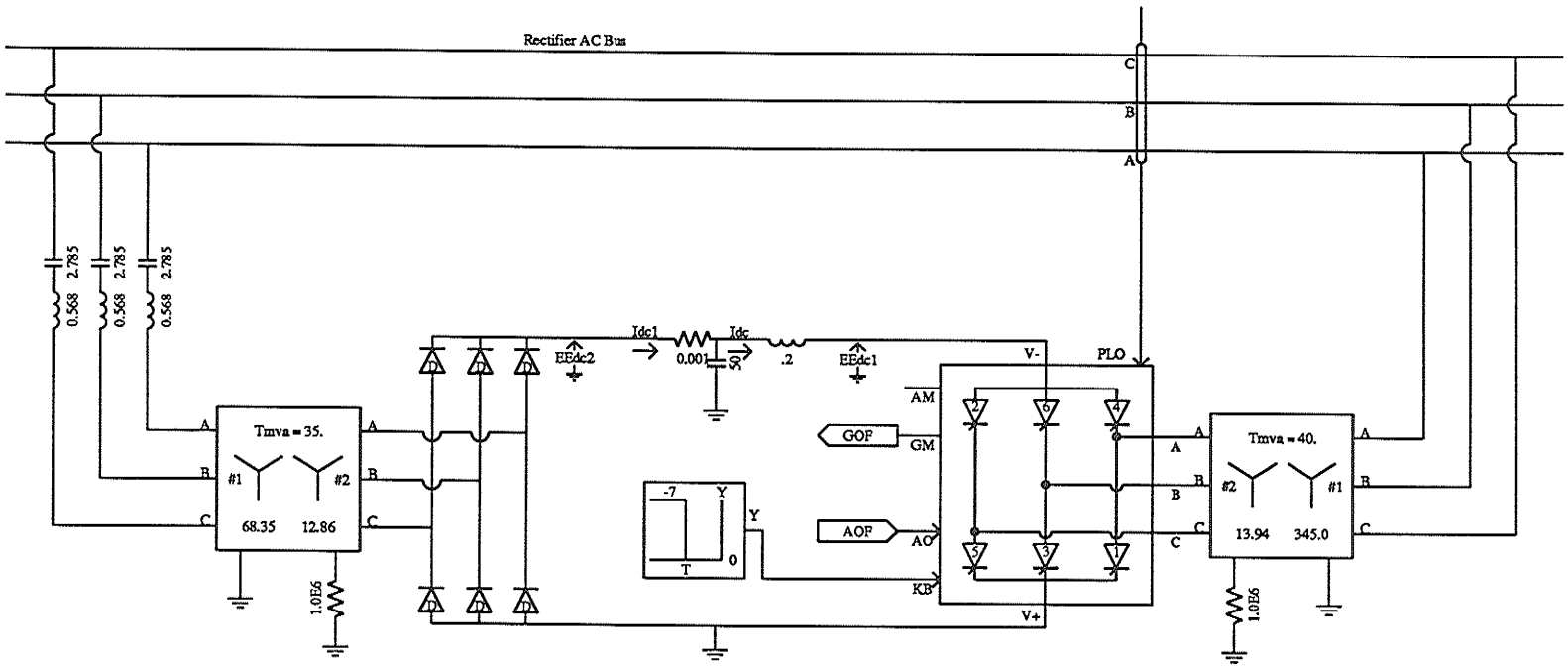

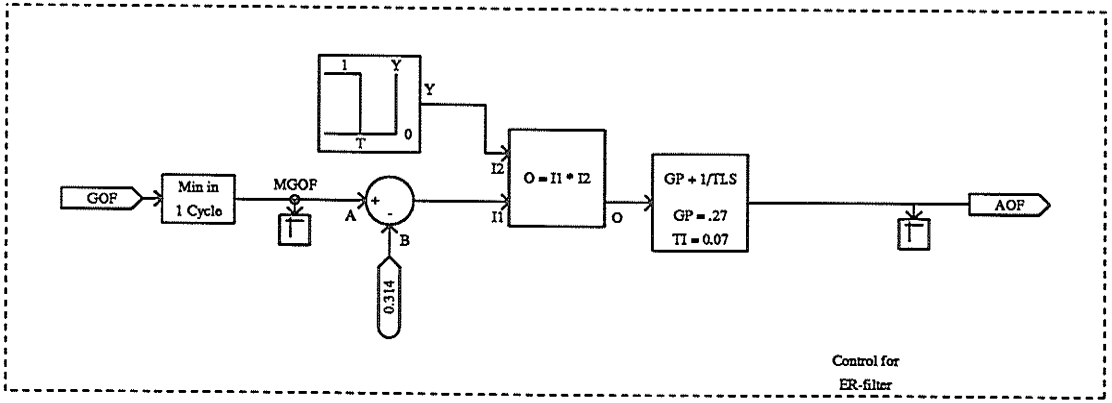

University of Manitoba, EE Dept. *Cigre Benchmark Model*	Last Modified: March 23, 1994 (xjiang) Printed On: March 29, 1994 (xjiang)	*Energy Recovery Filter* Subsystem #3 of 3